Published January 23, 2012

The Ras protein superfamily: Evolutionary tree and role of conserved amino acids

Ana Maria Rojas, Gloria Fuentes, Antonio Rausell, and Alfonso Valencia

Vol. 196 No. 2, January 23, 2012. Pages 189–201.

In this Review the bibliographic information for Valencia et al. (1991) was incorrectly listed by the authors. The correct information for Valencia et al. (1991) appears below.

The html and pdf versions of this article have been corrected. The error remains only in the print version.

Valencia, A., P. Chardin, A. Wittinghofer, and C. Sander. 1991. The ras protein family: evolutionary tree and role of conserved amino acids. *Biochemistry*. 30:4637–4648. http://dx.doi.org/10.1021/bi00233a001

Evolution

The Ras protein superfamily: Evolutionary tree and role of conserved amino acids

Ana Maria Rojas,[1] Gloria Fuentes,[2] Antonio Rausell,[3] and Alfonso Valencia[3]

[1]Computational Cell Biology Group, Institute for Predictive and Personalized Medicine of Cancer, 08916 Badalona, Barcelona, Spain
[2]Biomolecular Modelling and Design Division, Bioinformatics Institute A*STAR, 138671 Singapore
[3]Structural Biology and Biocomputing Programme, Spanish National Cancer Research Centre (CNIO), 28029 Madrid, Spain

The Ras superfamily is a fascinating example of functional diversification in the context of a preserved structural framework and a prototypic GTP binding site. Thanks to the availability of complete genome sequences of species representing important evolutionary branch points, we have analyzed the composition and organization of this superfamily at a greater level than was previously possible. Phylogenetic analysis of gene families at the organism and sequence level revealed complex relationships between the evolution of this protein superfamily sequence and the acquisition of distinct cellular functions. Together with advances in computational methods and structural studies, the sequence information has helped to identify features important for the recognition of molecular partners and the functional specialization of different members of the Ras superfamily.

Introduction

Both unicellular and multicellular organisms respond to cues expressed by other cells. In metazoans, studies of intercellular signaling during development have revealed the existence of highly conserved signaling pathways. Cellular organization and signaling is heavily influenced by the Ras superfamily of small GTP-binding proteins, which maintain a structurally and mechanistically preserved GTP-binding core despite considerable divergence in sequence and function. These GTP-binding proteins share a common enzymatic activity, producing GDP by the hydrolysis of GTP.

Ras superfamily signaling is dependent on the binding of specific effectors. Thus, minor modifications in sequence, structure, and/or cellular regulation of members of the superfamily will affect binding to regulators and consequently cell signaling. Accordingly, an important goal in studies of Ras superfamily signaling is to identify the determinants of these specific associations. The relationships between Ras superfamily proteins and their effectors have been analyzed using distinct phylogenetic approaches (Li et al., 2004; Jiang and Ramachandran, 2006; Boureux et al., 2007; Langsley et al., 2008; Mackiewicz and Wyroba, 2009; van Dam et al., 2009). To elucidate the influence of sequence evolution on Ras superfamily signaling, we have analyzed complete (or almost complete) genomes representing crucial evolutionary time points, focusing on the phylogenetic inferences gained from both species and protein trees. Using this information, we have generated a representative tree reflecting the evolutionary history of the Ras superfamily, from which we can classify the human Ras sequences. By adopting this approach to study the functional specificity of different superfamily members, we have been able to integrate the mechanistic information derived from these species and protein trees within a structural framework.

To facilitate the reading of this work we have used the following nomenclature: Ras superfamily refers to the highest organizational level that includes different protein families. Ran, Ras, Rab, Rho, and Arf refer to the specific protein families. RAS, RHO, etc. (capitalized) denote specific proteins. The G-domain refers to the structural domain common to proteins of the Ras superfamily.

The Ras superfamily

The Ras superfamily is divided into five major families: Ras, Rho, Arf/Sar, Ran, and Rab. Members of the Ras family function as signaling nodes that are activated by diverse extracellular stimuli and that regulate intracellular signaling. This signaling ultimately controls gene transcription, which in turn influences fundamental processes such as cell growth and differentiation. The human oncogenic members of the Ras family have been reviewed extensively (Karnoub and Weinberg, 2008), and in

Correspondence to Ana Maria Rojas: arojas@imppc.org; or Alfonso Valencia: valencia@cnio.es

Abbreviations used in this paper: MSA, multiple sequence alignment; SDP, specificity-determining position; SRPRB, signal recognition particle receptor subunit β.

The Rockefeller University Press
J. Cell Biol. Vol. 196 No. 2 189–201
www.jcb.org/cgi/doi/10.1083/jcb.201103008

general they regulate cell proliferation, differentiation, morphology, and apoptosis. The Rho family is involved in signaling networks that regulate actin, cell cycle progression, and gene expression. In addition to cytoskeletal organization (Heasman and Ridley, 2008) and cell polarity (Park and Bi, 2007), members of the Rho family have recently been implicated in hematopoiesis (Mulloy et al., 2010), particularly the RAC protein that is involved in both canonical and noncanonical *wnt* signaling (Schlessinger et al., 2009). The Rab family participates in vesicular cargo trafficking and it is by far the largest family of the Ras superfamily. Gene duplication has resulted in a large expansion of this protein family, as witnessed by the presence of duplicates in all vertebrate genomes. Rab family proteins regulate intracellular vesicular transport and the trafficking of proteins between different organelles via endocytotic and secretory pathways (Zerial and McBride, 2001). These proteins facilitate budding from the donor compartment, transport to acceptors, vesicle fusion, and cargo release. A key feature of the Rab family is the distinct intracellular distribution of its different members (Stenmark, 2009). By contrast, only one member of the Ran family is found in all eukaryotic lineages, with the exception of plants, which contain several copies. RAN proteins are the most abundant in the cell and they are involved in nuclear transport. Finally, the Arf family of proteins comprises the most divergent proteins, which, like Rab family proteins, are involved in vesicle trafficking (Wennerberg et al., 2005). These proteins signal through a wide range of effectors, including coat complexes (COP, AP-1, and AP-3) and lipid-modifying enzymes (PLD1, phosphatidylinositol 4,5-kinase, and phosphatidylinositol 4-kinase).

Phylogeny of Ras superfamily proteins

The most recent phylogenetic reconstruction of the Ras superfamily was based on sequences obtained from the complete draft of the human genome (Wennerberg et al., 2005). The resulting tree confirmed the general organization of five families (Ras, Rab, Rho, Arf/Sar, and Ran) and pointed to the Ras family as the root of the superfamily. Previous comparisons between human, fly, yeast (Garcia-Ranea and Valencia, 1998), and plant species revealed a similar organizational structure (Li et al., 2004; Jiang and Ramachandran, 2006). However, the recent sequencing of the complete genomes of additional species now enables us to reanalyze the Ras superfamily over a broader phylogenetic range, thereby increasing the likelihood of tracing the origin of the superfamily and correctly classifying sequences that are otherwise difficult to handle. Indeed, analyzing large sets of orthologous sequences is commonly recognized as the best strategy to improve the quality of phylogenetic analysis (Nei and Kumar, 2000).

The second important reason to reassess the organization of the Ras superfamily is the recent availability of novel techniques to build multiple sequence alignments (MSAs) and trees (Kemena and Notredame, 2009), key elements in phylogenetic reconstruction (Phillips et al., 2000).

The procedure. The generation of accurate MSAs is a key step in the tree-building process, which is based on estimating the similarities between sequences. The quality of multiple alignments is highly dependent upon the degree of similarity of the sequences to be aligned. Although standard methods work reasonably well when the sequence similarity is high (over 40%), very divergent sequences are difficult to align and the MSAs often contain errors (Kemena and Notredame, 2009). Thus, we used a well-established method to construct MSAs and corroborated the results using two additional independent approaches. The main alignment of 919 G-domains (Table S1) was built using the most recent version of HMMER (HMMERV3.0; Eddy, 2009) and it underwent detailed manual curation to detect incorrectly aligned regions. A profile was constructed that contained the statistical features of the amino acids occupying each position in a G-domain seed alignment that was derived from several Ras superfamily proteins obtained from the PFAM database (identifier PF00071; Finn et al., 2010). This profile was used as a template to align the other Ras superfamily sequences, optimizing their correspondence through the probability of each amino acid type being located at each position in the profile. The resulting alignment was compared with alignments obtained using two other methods known to perform reliably in cases of poor sequence similarity (MAFFT: Katoh et al., 2009; and T-COFFEE: Notredame, 2010). These methods confirmed the essential aspects of the alignment (unpublished data).

It should be noted that although various members of the Ras superfamily contain additional protein domains (e.g., BTB domains, N-terminal anchoring regions; see Figs. S2 and S5), our phylogenetic analysis corresponded exclusively to the G-domain, which contains the basic functional and historical core that is common to the superfamily.

The MSA was used as the basis for the phylogenetic analysis. Phylogenetic reconstruction based on protein sequences presents significant challenges that remain to be fully solved (Cavalli-Sforza and Edwards, 1967; Page and Holmes, 1999). Currently, the best approach involves the integration of thousands of trees using an appropriate statistical framework capable of handling the associated probabilities (based on Bayesian statistics and inference; Holder and Lewis, 2003; Ronquist and Huelsenbeck, 2003; Lartillot et al., 2007). The final tree represents the consensus of thousands of carefully chosen independent trees obtained after detailed matching of the probabilities of multiple combinations of branches. This final tree is the most probable representation of the evolutionary history from a statistical viewpoint (Holder and Lewis, 2003).

The statistical properties derived from evaluating thousands of alternative trees are reflected in the values associated with the tree branches. These values represent the statistical confidence in the grouping of the sequences under that branch point, i.e., the probability of that particular grouping of sequences being correct.

The trees presented were generated with MrBAYES3, the most recent implementation of tree-building methods based on Bayesian statistics (Ronquist and Huelsenbeck, 2003) and that which is considered to be the best in the field (Hall, 2005; Gaucher et al., 2010). The downside of the increased accuracy of these new methods is their high computational demands. In the case of the Ras superfamily in particular, building trees from a starting alignment of more than 900 divergent sequences is not feasible, even for large supercomputers (Wang et al., 2011).

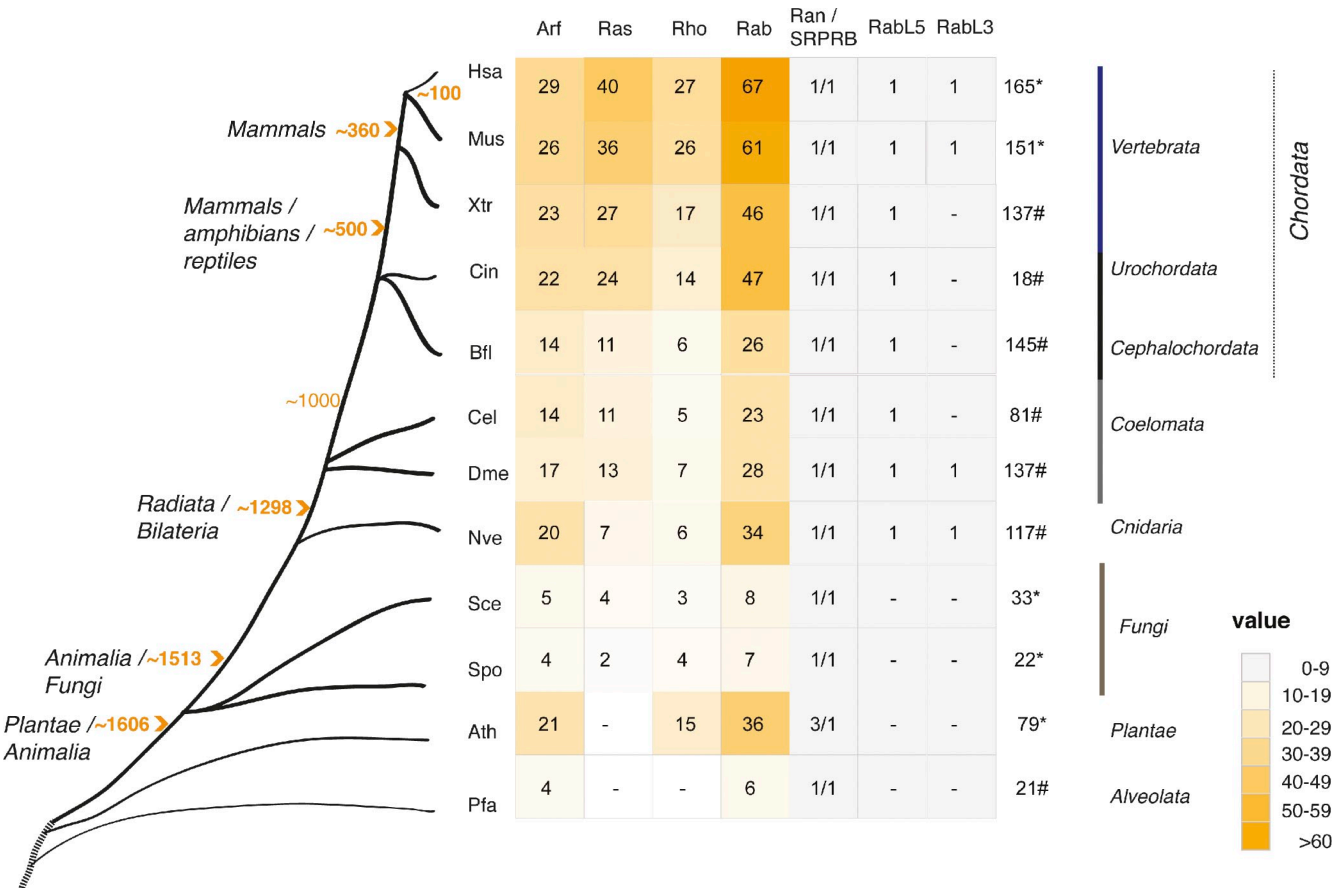

Figure 1. **The orthologues of the human Ras superfamily members in 11 proteomes.** Heat map colors indicate the number of the orthologues corresponding to human sequences in a particular species. Numbers inside the boxes indicate the number of orthologous human sequences in the Ras superfamily. Dashes inside the boxes indicate the absence of proteins. Orange numbers in the tree indicate millions of years according to a recently revised scale (Hedges et al., 2004) and the time line is an approximate scale for the purposes of illustration. Arrowheads point to important splits that occurred in the course of evolution. The classical families are represented and for the purpose of clarity, the Ran family and the "unclassified" sequences including SRPRBs, RABL5, and RABL3 proteins are shown independently. The MIRO and RAYL proteins are included in the Rho family and the RABL2 proteins (one per organism) in the Rab family. Numbers on the right of the table indicate G-domain–containing proteins extracted from the PFAM database, therefore some discrepancies are expected due to variability in the synchronization of PFAM and Uniprot databases. Asterisk indicates well-annotated sequences in complete genomes and the associated number reflects the Ras superfamily sequences obtained from PFAM. "#" indicates the presence of the RAS domain in either draft genomes or complete but poorly annotated sequences, and the associated number represents the sequences (fragments have been removed) extracted from PFAM (Finn et al., 2010) in which the G-domain has been identified. Plants: Ath (Arabidopsis *thaliana*); *Alveolata*: Pfa (*Plasmodium falciparum*); Fungi: Spo (*Schizosaccharomyces pombe*); Yeast: Sce (*Saccharomyces cerevisiae*); Radiate: Nve (*Nematostella vectensis*); Worm: Cel (*Caenorhabditis elegans*); Fly: Dme (*Drosophila melanogaster*); Lanceolet: Bfl (*Brachiostoma floridae, protochordata*); Ascidian: Cin (*Ciona intestinalis, urochordata*); Xtr (*Xenopus tropicalis*); Human: Hsa (*Homo sapiens*); and Mouse: Mus (*Mus musculus*).

Thus, we used an alternative procedure that selects key organisms and representative sequences to build independent trees for each of the five distinct families of the Ras superfamily (Ras, Rho, Rab, Ran, and Arf).

Compiling the Ras superfamily. The current study is based on Ras superfamily proteins directly related to the human Ras proteins, as compiled by Wennerberg et al. (2005). The updated human Ras superfamily contains 167 human proteins: 39 Ras proteins, 30 Arfs, 22 Rhos, 65 Rabs, and 1 Ran family sequence (Table S2). This list includes 10 "unclassified" sequences and for 5 of these sequences, there is only evidence that they exist at the transcriptional level (Table S2, listed as "Unclassified").

Orthologous sequences correspond to genes separated by species divergence, as opposed to paralogous sequences that are generated by gene duplication. Using the dedicated InParanoid resource (v.4.0; Ostlund et al., 2010), we identified a total of 766 sequences from 11 organisms (excluding human sequences) that correspond to orthologues of the 167 human proteins in the Ras proteins superfamily (orthologues were obtained from various databases, the correspondence between identifiers is given in Tables S3 and S4). These 11 species were selected based on their correspondence to relevant moments in eukaryotic evolution (Fig. 1). Important speciation events were represented by the inclusion of Ras superfamily sequences from the corresponding genomes (*Plantae-Animalia* and *Radiata-Bilateria* by *A. thaliana* and *N. vectensis*, respectively), or the different *Chordata* lineages, represented by ascidians (*C. intestinalis*) and lancelets (*B. floridae*). Well-annotated genomes are available for some of the species included (e.g., *H. sapiens*, *M. musculus*, *S. cerevisiae*, *S. pombe*, *A. thaliana*, *D. melanogaster*, and *C. elegans*), whereas for others the genome remains poorly

annotated (e.g., *P. falciparum*) or is only available in a draft format (e.g., *N. vectensis*, *C. intestinalis*, *B. floridae*, and *X. tropicalis*).

The set of orthologous sequences, along with the estimated point in evolution at which they have diverged, is depicted in Fig. 1. The Ras family is entirely absent from plants (*A. thaliana*), in which the remaining subfamilies are the signaling members of the superfamily (Yang, 2002), while no Rho family orthologues are found in alveolates (*P. falciparum*). Because our study of the Ras superfamily uses human sequences to retrieve the corresponding orthologues in other species, sequences from these species that are not present in humans may not have been included. Although ascidians would be expected to have a similar number of RAS proteins as humans, based on phylogenetic estimates, there is a noticeable decrease in the number of Ras superfamily orthologues for this organism, probably due to the loss of ancestral genes (Hughes and Friedman, 2005). Similar findings are obtained in coelomates and cnidarians as fewer orthologues are found than in the sea anemone and *N. vectensis*, although more orthologues are detected for the cnidarian than in the coelomate species. This finding is not unexpected, as gene content and genomic structure has been preserved between *N. vectensis* and vertebrates (Putnam et al., 2007), whereas extensive gene loss has occurred in the fruit fly and nematodes (Technau et al., 2005).

In some species additional gene-duplication events have produced an accumulation of paralogous sequences, which results in variation between species in terms of the numbers of each Ras superfamily member, as evident in the corresponding family trees (see Figs. S1–S5). For example, three copies of the Ran family sequences were detected in *A. thaliana* whereas only one was found in the other species analyzed (Figs. 1 and 2; Fig. S1).

Rho family proteins expanded extraordinarily in plants (Yang, 2002), and although plant RACs are homologues of RAC, RHO, and CDC42 (Fig. S2), the expansion of RAC in plants after speciation has resulted in the generation of a larger number of RAC proteins (RAC1–RAC11) than in other organisms. The ancestral duplications of RAC in fungi/metazoans led to the appearance of CDC42, which controls cell polarity, and RHO, which is implicated in cytokinesis (Jaffe and Hall, 2005). The CDC42 protein, which promotes the formation of actin microspikes and filopodia, is conserved in all the lineages except plants. Interestingly, the absence of Rho genes in alveolates suggests that other proteins fulfill its role in cell polarity and cytokinesis.

The gene duplication that generated the Ras family proteins in vertebrate genomes (H-Ras, K-Ras; group 7a in Fig. S3) is another example of how variation in the number of Ras superfamily proteins arises (Fig. S3). Indeed, although they are present in *Xenopus*, the evolutionarily more ancestral genomes only contain one copy (LET60 in *C. elegans* and RAS1 in *D. melanogaster*) that is involved in embryogenesis (Ezer et al., 1994). Fungal orthologous sequences (Fig. S3) are only found for RHEB (group 12), RAP (group 4), and RRAS (group 8). Further duplications of these sequences after speciation yielded the MRAS and KRAS groups. Together, these data are consistent with major gene duplication in vertebrates (Kondrashov et al., 2002).

The vertebrate branch of the Rab protein family has expanded considerably (Fig. S4; see also Mackiewicz and Wyroba, 2009) and significantly. We found representatives of each of the different groups of Rab proteins in all lineages, indicating that the appearance of this family was an important evolutionary event. The implication of Rab genes in a complex network of vesicular trafficking events suggests a relationship with multi-cellularity that merits further investigation. The Arf family of proteins (Kahn et al., 2006) is the most divergent member of the superfamily and it is associated with recurrent duplication events (Fig. S5).

Representative phylogenetic tree of the Ras superfamily. As it was not feasible to generate a full tree with all the sequences orthologous to the proteins of the human Ras superfamily, we generated independent trees for each of the protein families using the sequences from the 12 proteomes (see Figs. S1–S5) and for each of the species. This information was then used to select the sequences that best represented the diversity of species and branches in the tree.

Specific criteria for sequence inclusion were applied to select stable and representative groups from each tree. Thus, information regarding the function of the sequences selected was necessary, as well as that related to any clear orthologues in each of the species analyzed. The selection aimed to respect the variability of the sequences included in each tree (see Figs. S1–S5, which show the groups selected to build the representative tree). For instance, as the Ras family is not represented in plants and alveolates, we selected groups with at least a yeast homologue. Moreover, because the RHEB proteins (Fig. S3, group 12) constitute the most basal branch present in all the organisms of interest, and RAP1 proteins (Fig. S3, group 4) correspond to the most basal group with a yeast orthologue, these two groups were chosen to represent the Ras family in the representative tree.

Given the large number of sequences in the Rab family, we selected two stable groups that covered the phylogeny of the whole family (Fig. S4, stars). RAB7 was chosen on the basis of its well-characterized involvement in Golgi late endosomal transport. RAB7 lineages emerged before the divergence of plants (Mackiewicz and Wyroba, 2009) and this protein is present in amebozoans and ciliates. Analogously, RAB1 (Fig. S4, stars) was selected due to its position in the tree in all species. All the Ran family sequences were included. For the Arf family (Fig. S5, stars) we included the ARD-1 (also known as TRIM23, an Arf-related protein involved in ubiquitination; Mishima et al., 1993) and SRPRB (signal recognition particle receptor subunit β) proteins. These groups cover the phylogenetic range of this family.

Difficult sequences (i.e., those not classified by Wennerberg et al., 2005) were also included for those species in which orthologues corresponding to human sequences could be identified. In addition, we included sequences from the elongation factor Tu (EFTU) family, a distant relative with a G-domain that was used as a guide to situate the root of the Ras superfamily tree. The inclusion of distant sequences (known as outgroups) to define the tree is an accepted procedure to trace the origin of protein families (Nei and Kumar, 2000).

The superfamily tree (Fig. 2) includes 165 sequences, of which 22 are human (Fig. 2, underlined sequences). The remaining

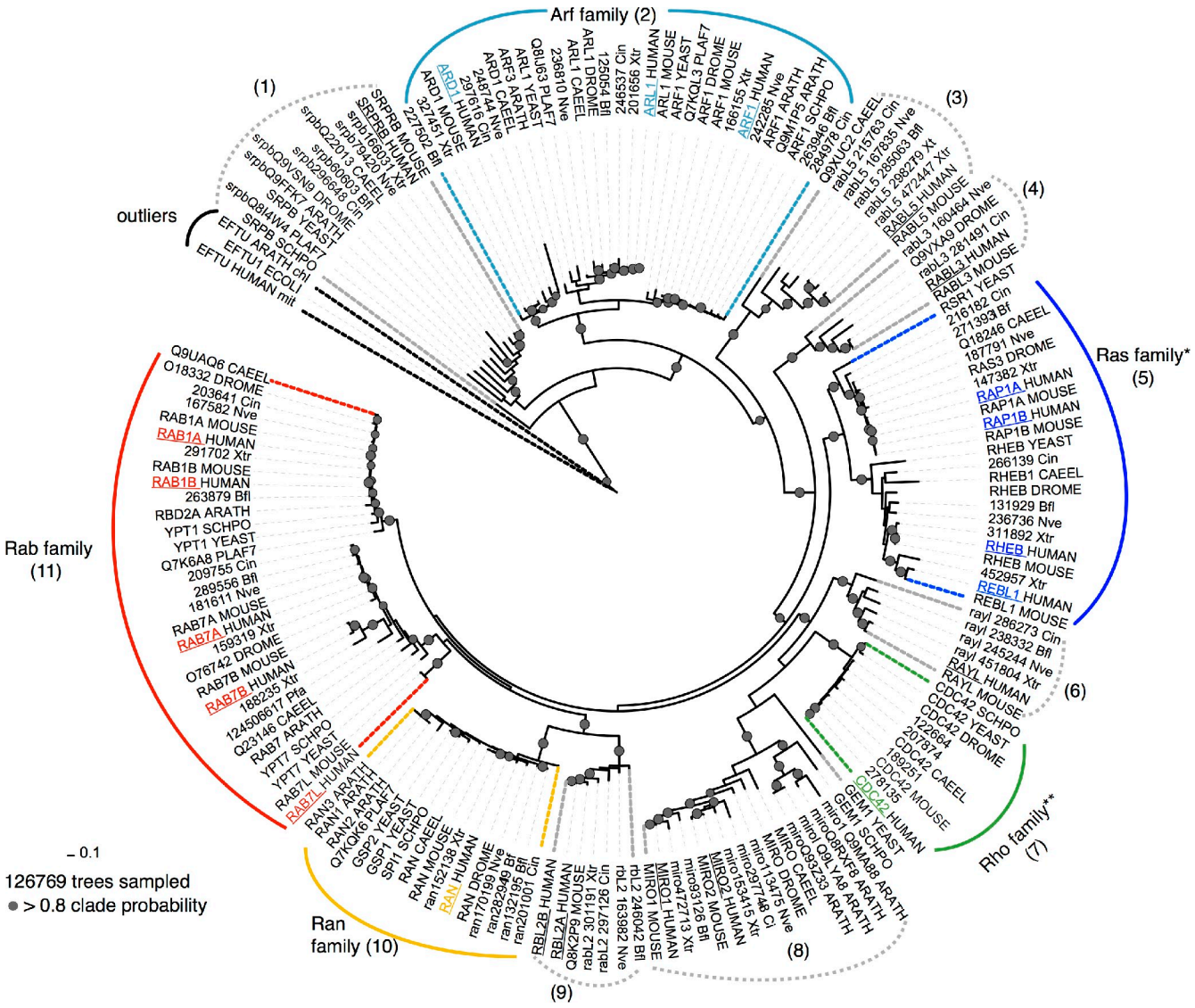

Figure 2. **Consensus phylogenetic tree of selected Ras superfamily members rooted with outliers.** The 165 proteins selected after careful individual analyses (see Figs. S1–S5) of species-trees and gene-trees covering the Ras superfamily sequences, plus three sequences (human mitochondrial, plant chloroplast, and bacterial) of representative Elongation factor Tu (a remote homologue of Ras superfamily) used to root the tree, were aligned to the G-domain (see main text). The tree is a consensus of more than 126,769 sampled trees with their associated probabilities. The numbers in brackets indicate stable groups; *, absent in Plants and alveolates; **, absent in alveolates. The founder members are the SRPRB group (1) and the Arf family (2). RABL5 (3; Wu et al., 2002) and RABL3 (4) appear at the basal branches of the Ras family (most likely as founders). This phylogeny proposes SRPRB and the Arf family to be the founder members of the classical Ras superfamily. Underlined names indicate the 22 human sequences. Plants: ARATH (Arabidopsis *thaliana*); *Alveolata*: PLAF7 (*Plasmodium falciparum*); Fungi: SCHPO (*Schizosaccharomyces pombe*); Yeast: Sce (*Saccharomyces cerevisiae*); Radiate: Nve (*Nematostella vectensis*); Worm: CAEEL (*Caenorhabditis elegans*); Fly: DROME (*Drosophila melanogaster*); Lanceolet: Bfl (*Brachiostoma floridae, protochordata*); Ascidian: Cin (*Ciona intestinalis, urochordata*); Xtr (*Xenopus tropicalis*); Human (*Homo sapiens*); and Mouse (*Mus musculus*).

sequences belong to 11 species, and 3 additional non-Ras superfamily sequences are included. The first observation is the clear separation of the five main families, which group together with a high degree of confidence. Indeed, of the thousands of independent trees constructed using this procedure, over 80% exhibited the same general tree structure. The clear separation between families is a distinctive feature of the Ras superfamily that is not commonly observed in other large superfamilies, such as protein kinases.

The inclusion of an outgroup (in our case, the EFTU proteins) appears to clarify the overall topology of the superfamily. This new phylogeny places the SRPRBs (Fig. 2, group 1) as the founder members of the Ras superfamily. There is significant support for this structure, even though it differs from that described in previous analyses based on human Ras superfamily sequences alone (Wennerberg et al., 2005). The SRPRB protein is located at membranes and it is an essential component of the signal recognition receptor, which ensures that nascent secretory proteins are targeted to the endoplasmic reticulum (ER) membrane system. This suggests that the original function of the superfamily is related to specific signaling events involving membrane structures.

The human-only Ras superfamily phylogenetic tree. Our most up-to-date representation of the human sequences tree is shown in Fig. 3. As discussed in the previous

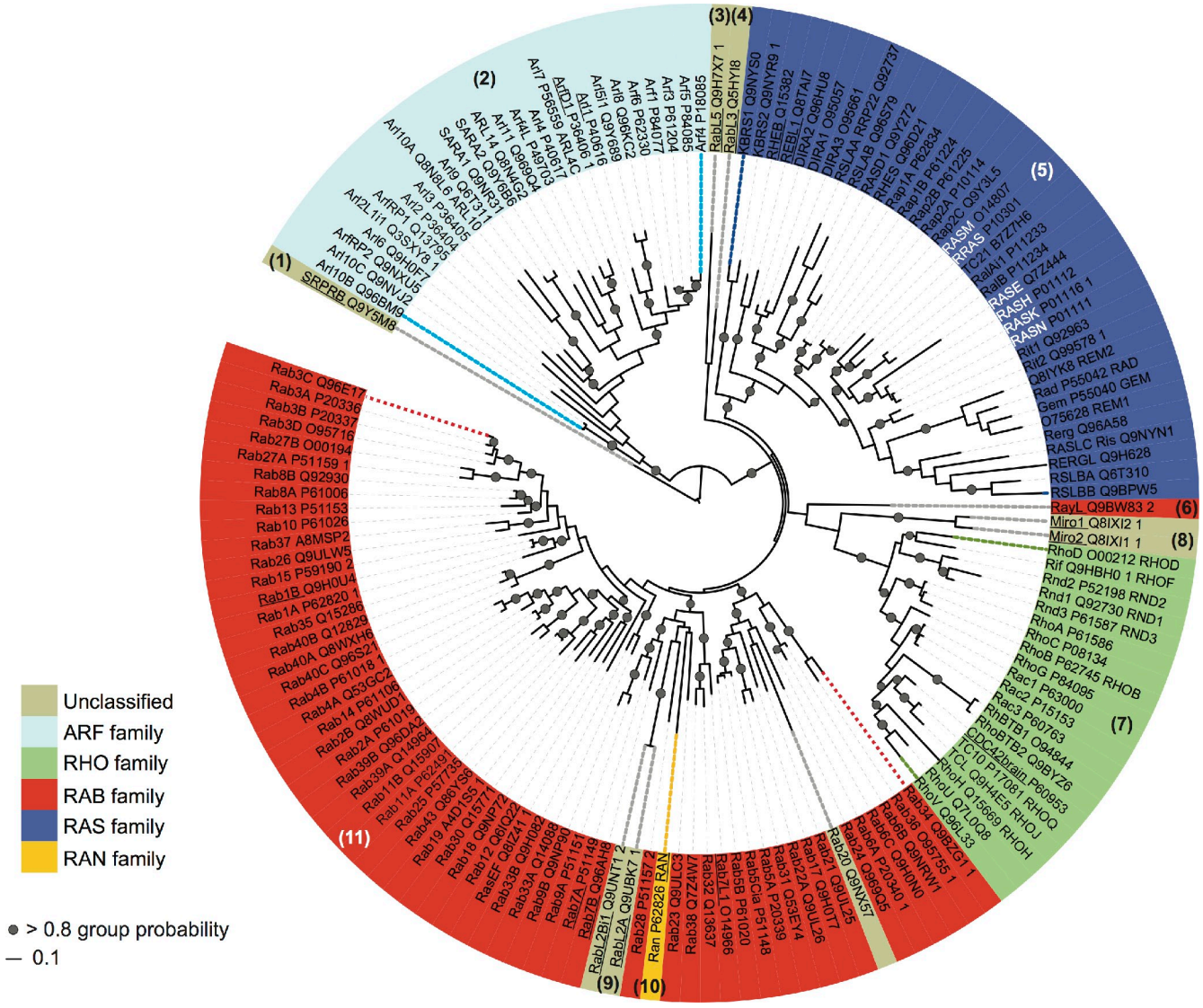

Figure 3. **Phylogenetic tree of the human Ras superfamily.** Of the 167 sequences defined (Table S2), some proteins are identical in the G-domain while exhibiting differences in other regions of the protein. Thus, identical sequences were removed before performing the alignments. The tree contains 151 sequences that correspond to bona fide unique protein sequences (Table S2) that were aligned with the G-domain profile (PF00071, also RAS) to define the domain boundaries. The alignment was used as the input to generate the probabilistic phylogeny using a Bayesian inference (Ronquist and Huelsenbeck, 2003). Thus, 29,340 trees were sampled and the associated confidence values (group probability values) were obtained for each group. The numbers in brackets indicate the equivalent group numbering, as in Fig. 2. The background colors indicate the original classification (Wennerberg et al., 2005): blue, Ras family; green, Rho; red, Rab; cyan, Arf; and yellow, Ran. Unclassified members are shown in beige. Gray circles indicate group probabilities >80% (confidence value assigned to a group and expressed as a percentage). The white font indicates the archetypal Ras family proteins and the names underlined indicate the human sequences from Fig. 2. The tree was visualized with iTOL (Letunic and Bork, 2007).

paragraph, generating an accurate tree of the human sequences requires that their relationship with sequences from other species be taken into account. Thus, we used the topology of the complete species tree represented in Fig. 2 to organize the rest of the human sequences. Additionally, SRPRBs were used to root the human tree based on the information from the representative tree.

Of the 167 defined sequences (Table S2), some genes present alternative splice variants with identical sequences in their G-domains. As we only compared the precise G-domain region, these identical sequences were removed before alignment. The remaining 151 human Ras superfamily sequences were aligned and a phylogenetic analysis was performed following the procedure described in the previous section. The main families were divided into stable groups, as evident by the high confidence values (Fig. 3, gray dots). It is clear that this superfamily has experienced extensive gene duplication, with the Rab family representing the most abundant family in humans (Fig. 3, red background). Previous phylogenetic analyses (Schwartz et al., 2007) divided the Rab family into eight functional groups (Pereira-Leal and Seabra, 2001), whereas a more recent study proposed nine groups (Stenmark, 2009). Incorporating our data with the corresponding subcellular localization described previously (Stenmark, 2009), we can generate a phylogenetic distribution of the Rab repertoire, as shown in Fig. S4. The colored branches represent the functional family to which

each particular protein belongs (Stenmark, 2009), and the numbers in brackets represents the previous groupings (Schwartz et al., 2007), in which 14 divisions were established. We found some discrepancies (Fig. S4, group numbers labeled with an asterisk) with the earlier phylogeny proposed (Schwartz et al., 2007), probably due to the inclusion of additional species in our analysis. For instance, group number 10 (Fig. S4, beige branches) contains RAB18, which is traditionally assigned to an independent family (Stenmark, 2009). However, in our analyses RAB18 was grouped within Stenmark's "RAB3" group (Fig. S4, red branches). A similar situation occurred with "RAB1" (dark brown) and "Rab 28" (dark orange).

A previous phylogenetic analysis of the Arf family described 11 groups: the Arfs, ARL1-6, ARL-8, ARL10/11, ARFRP, and SAR (Li et al., 2004). However, this study included none of the ARD proteins (Arf-like proteins also known as the TRIM23 group; Kahn et al., 2006). We expanded the phylogenetic analysis to include the ARD (TRIM23) proteins, which in our analysis had a high probability of grouping with the ARF proteins (a significant confidence value of the corresponding tree branches). Interestingly, this group contains multidomain proteins with a Ring domain (SMART), a protein interaction domain that shows E3 ubiquitin–protein ligase activity, Zf_boxes that are also protein interaction domains at the N-terminal region (PFAM PF00643), and an ARF domain similarity region in the C-terminal region. The presence of these domains may point to specific functions related to ubiquitination and binding to targets such as DNA, RNA, and proteins.

The analysis of sequences from species not previously included in other studies allowed us to reassess the earlier classifications. For instance, although the NKIRAS (KBRAS) protein (Fig. S3, group 1) was believed to be human specific (Jiang and Ramachandran, 2006), our results indicate that this protein is present in all the eukaryotic lineages except fungi and *Plasmodium*.

Difficult-to-classify sequences. The overall classification of the family including information from divergent species may help to elucidate the role of some of the less well-known sequences in the superfamily. For example, the analysis reveals a putative relationship between the MIRO and RAYL sequences within the Rho family, despite the fact that MIRO proteins are considered to be an independent family as they regulate mitochondrial rather than cytoskeletal dynamics (Colicelli, 2004). The position of these proteins within the Rho family (Fig. 2, group 8) suggests that some functional diversification (sub-functionalization) has occurred, although this may also point to a common original mode of action that was later co-opted to perform distinct cellular roles.

The present findings provide some insight into the potential functions of some of the superfamily proteins, for instance Rab-like proteins (named "like" because they are similar to Rab) that lack the conventional C-terminal modification site. Although the role of the RABL5 protein remains a mystery, RAYL protein is thought to be a cell cycle–related protein (Qin et al., 2007), consistent with its phylogenic placement with CDC42 proteins (Fig. 2, group 6). RABL2A/B (Kramer et al., 2010) are Rab-like proteins mapping to the subtelomeric region of chromosome 22q13 (Wong et al., 1999), suggesting that in humans at least, duplicate genes actively express proteins of as yet unknown function in telomeric regions. Curiously, in our phylogeny these proteins grouped with the Ran protein family (Fig. 2, groups 10 and 9). Because the RABL2 proteins are metazoan specific, they may have originated from duplications of Ran proteins after speciation events. The function of RABL3 is also unknown, although it was recently implicated in regulating the proliferation and motility of human cancer cells (Li et al., 2010). Future analysis of additional sequences may clarify certain aspects of this classification.

A particularly interesting case is that of RAG proteins (Sekiguchi et al., 2001) that are believed to be part of the Ras superfamily based on the presence of a GTP domain. Although their structure and overall sequence similarity shows that they contain a G-domain, we found that the lack of conservation and the unusual composition of the GTP-binding sites, otherwise conserved in the superfamily, sheds doubt on their classification as a family of the Ras superfamily. Future studies of this group of proteins using a larger set of sequences from new complete genomes will be required to confirm their classification.

Functional specificity of the proteins in the Ras superfamily

The large functional diversity of the Ras superfamily is perplexing. The conserved 3D structure of the G-domain that is common to the entire superfamily allows these proteins to preserve large structural similarity and common biochemical properties while they recognize their individual binding partners with remarkable affinity and specificity (Colicelli, 2004; Wennerberg et al., 2005). The promiscuity and diversity in this superfamily is illustrated by the multiple upstream (regulators) and downstream proteins to which Ras superfamily proteins bind (Bishop and Hall, 2000; Karnoub and Weinberg, 2008: Table S5). The list of these interacting proteins is continually growing and a plethora of functions have been attributed to both effectors and regulators. Moreover, some GTPases share effectors despite performing distinct functions, leading to another level of regulation within this family (Kiel et al., 2007; Barnekow et al., 2009).

The GTP-binding site is made up of a core of essential residues that also participate in the conformational changes linking GTPase activity to effector binding. The specific distribution of these residues and the differential sequence conservation within families determines the specificity of the association between Ras superfamily proteins and their effectors, interactions that ultimately determine the biological activity of the protein. It is important to note that although structural and sequence-specific features are clearly correlated with function, other factors work together to influence the network of Ras superfamily interactions, like gene expression of the proteins, and the regulation and acquisition of domains that determine subcellular localization (Rodriguez-Viciana et al., 2004; Goldfinger, 2008).

We compared and contrasted the families in the Ras superfamily to identify the residues in the G-domain and to determine any differences that may underlie their specific interactions

Table 1. **The position of SDP residues in the structures of the five Ras superfamily members, and their possible biological and functional implications**

Family PDB chain	Arf 1hurA,B	Ras (Fig. 5) 121pA	Rho 1a2bA	Rab 2folA	Ran 1l2MA
Residues in the proximity of the GTP/GDP binding pocket	Ala28, Pro47, Gly69	Ala11, Val14, Pro34, Thr58, Ala59	Asp13, Cys16, Pro36	Asp16, Val19, Leu25, Ser39	Thr21, Asp18, Ala41, Ala67
Residues involved in protein–protein interactions	Pro47, Phe51, Trp66, Val68, Gly69	Pro34, Glu37, Leu56, Ala59, Arg68	Asp13, Cys16, Leu22, Pro36, Phe39, Thr58, Thr60, Ala61, Asp67, Arg70, Arg122	Val43, Trp62, Ala65, Arg71	Asp18, Val45, Trp64, Ala67, Gly73, Arg76, Asp91 Lys127
Residues coordinating communication between different lobes	Arg75, Val91, Asp93, Pro131	Ala65, Val81, Ala83, Ala121	Asp67, Cys83, Ser85, Arg122	Arg71, Ala81, Val87, Leu89, Ala126	Gly73, Met89, Asp91, Lys127
Conserved SDP residues with unknown function	Leu25, Leu34, Trp78, Thr85	Gly75, Thr20	Thr77	Thr64, Thr74	Val27, Thr66, Ala83

Numbers correspond to positions in the PDB structures (see Table S5).

with effectors. These positions are considered specificity-determining positions (SDPs), as they provide information regarding the branching of the phylogenetic tree (del Sol et al., 2003), also known as tree determinants, and they are associated with ligand-binding sites and protein interaction regions (Rausell et al., 2010). We analyzed the Ras superfamily to identify family-specific residues, using the complete sequence alignment of 919 G-domains, including representatives from each family of the 12 genomes. This analysis was performed using a recently described unsupervised approach (Rausell et al., 2010) that is based on multiple correspondence analysis. This technique represents the sequences of the alignment as vectors (Fig. S6), and their organization is optimized into groups according to their similarities and differences. The groups of sequences resulting from the association of similar vectors with a k-means algorithm are equivalent to the branches of the phylogenetic tree. The advantage of this procedure is that it allows the characteristic residues (SDPs) that dictate the organization of the sequences into groups to be extracted directly. In this way the MSA is transformed into a catalog of groups of sequences with their associated characteristic amino acid and positions.

For example, the sequences corresponding to the Rho, Rab, and Ran families have a characteristic conserved Asp residue within the G1 motif (position 7 in the alignment, corresponding to residues 13, 16, and 18 for the Rho, Rab, and Ran structures indicated in Table 1, respectively). By contrast, the Arf family has a Leu residue in this motif (position 25 for Arf PDB:1HUR), whereas Ras family sequences are not highly conserved (position 11 for RAS PDB:121P). Completely conserved residues (i.e., those binding GTP) cannot be assigned to any particular group of sequences (for more details on this method, see Rausell et al. [2010]).

The summary of sequence features is presented in Table 1 and Fig. 4. The analysis of SDPs provided independent evidence for the classification of RABL3, RABL5, RAYL, MIRO, and SRPRB proteins (Tables S7 and S8). Significantly, the SDP pattern of these proteins did not correspond well with the characteristic amino acids in the classical families (Table S8). In particular, the conservation of the RABL3, RABL5, and SRPRB sequences reflects important differences at key positions within the groups to which they are assigned, and this is more consistent with their organization as independent groups and it is in agreement with the rooted phylogenetic tree. By contrast, the low intensity SDP signal in the RAYL and MIRO groups (Fig. S7) suggests that they constitute a peculiar group within the Rho family. Additional genomic information will be required to further study this group.

To further advance our analysis, we focused on the interaction of these SDP residue proteins with the nucleotide-binding pocket, their association with specific binding partners, and their role in communicating between the GTP-binding site and other functional areas of the Ras superfamily (Fig. 5).

SDPs involved in GTP/GDP hydrolysis. Ras superfamily proteins generally undergo an enzymatic cycle that involves the so-called loaded-spring mechanism, whereby the switch regions relax after release of the hydrolyzed γ-phosphate in the active state, adopting an open-inactive GDP conformation (Vetter and Wittinghofer, 2001). In terms of their 3D structure, the G1–G5 loops form the nucleotide-binding site, with an interface that is responsible for nucleotide specificity and affinity, and that regulates GTP hydrolysis. The SDP residue Val14 reportedly forms hydrogen bonds with the phosphate groups of the nucleotides (Tong et al., 1991). This residue, together with Ala11 and Pro34, is located in regions characterized as hinges that act in the conformational transition between GTP and GDP forms (Díaz et al., 1995, 1997; Futatsugi and Tsuda, 2001), thereby modulating GTP hydrolysis (see Table 1 for the equivalence of these residues in the various families). The residues in switch II (Thr58 and Ala59) may influence nucleotide cycling, in which the movement of neighboring side chains plays a key role, as demonstrated by x-ray diffraction, NMR, spectroscopy, and MD studies (Noé et al., 2005; Gorfe et al., 2008; Lukman et al., 2010). Thus, mutating these residues may alter the structure or dynamics of the system, favoring either active or inactive states, as occurs with oncogenic mutations such as G12V (Gorfe et al., 2008).

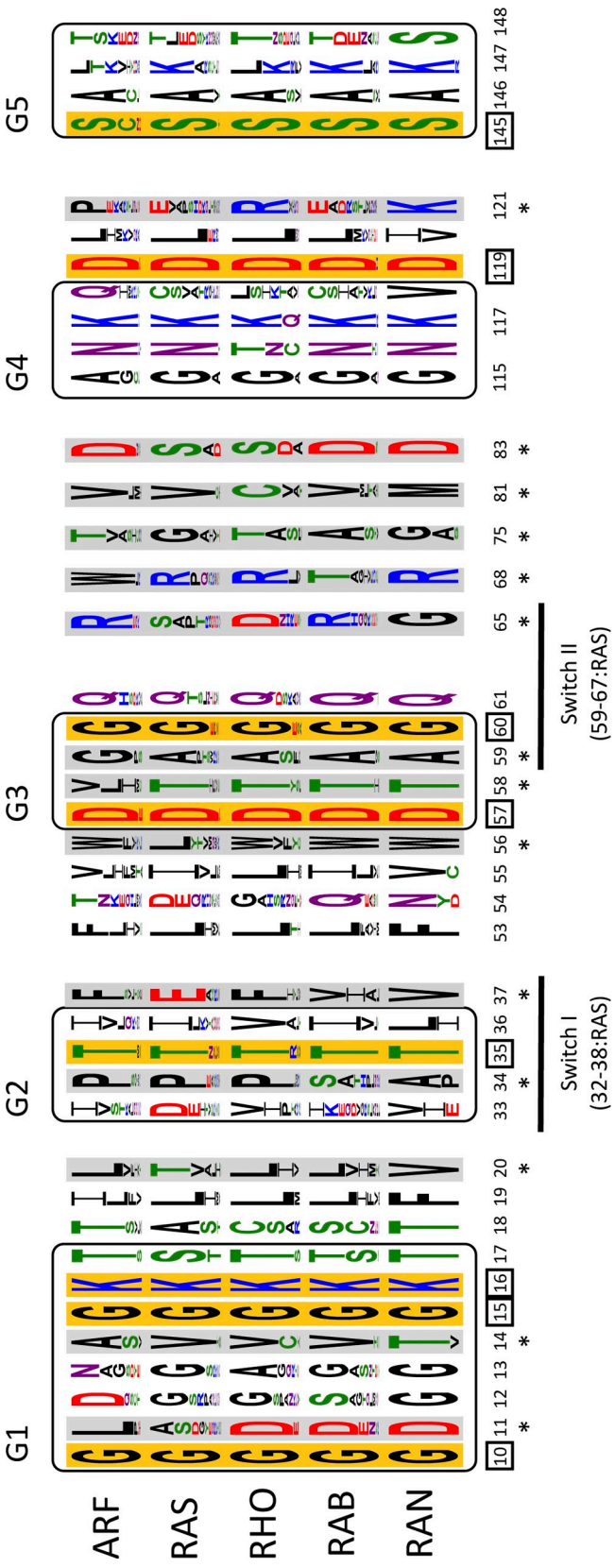

Figure 4. **Specificity-determining positions (SDPs).** These residues are displayed in sequence logos corresponding to the different Ras superfamily members and represented in the context of the characteristic G-boxes. The positions are numbered according to the corresponding residue in PDB 121P (H-Ras-1). The SDPs detected according to the classical scenario (the distribution in the classical five subfamilies, Ras, Rab, Ran, Rho, and Arf) are indicated by an asterisk and highlighted against a gray background. The conserved positions are marked with a square and shown on an orange background. The relative size of the amino acid letters in the logos represents the raw frequency for the alignment of the 919 sequences (Table S1), colored as follows: green (polar: S,T,Y,C,Q,N); blue (basic: K,R,H); red (acidic: D,E) and black: G and hydrophobic (A,V,L,I,P,W,F,M). Logos were generated using Weblogo3 (http://weblogo.threeplusone.com; Crooks et al., 2004) and the switch regions are indicated below in the G-boxes.

SDPs involved in interactions with different binding partners. Ras superfamily proteins are very specific when transmitting signals to their partners, as illustrated by the extent to which single amino acid changes can alter their individual specificities (Stenmark et al., 1994; Azuma et al., 1999; Bauer et al., 1999; Karnoub et al., 2001). As a general rule, conformational changes induced by nucleotide states are transmitted to the switch I and switch II regions, where they are recognized by the corresponding effectors (Vetter and Wittinghofer, 2001). In addition, the interacting interface is typically comprised of other residues outside the canonical switch regions (Heo and Meyer, 2003; Fuentes and Valencia, 2009), as confirmed by the structures of the Ras–effector complexes (Corbett and Alber, 2001).

To define the SDP residues involved in protein–protein interactions, we inspected the interacting surfaces of a set of complexes within the Ras superfamily using a previously described method (Corbett and Alber, 2001; Biou and Cherfils, 2004; Dvorsky and Ahmadian, 2004; see Table S5 and Fig. S8). It should be noted that the information pertaining to binding surfaces is necessarily incomplete, due to the limited structural characterization of Ras superfamily protein-interacting partner complexes. We considered the static features of the structures, as well as the potential plasticity of neighboring residues (Sprang, 2000). This plasticity of interacting and neighboring residues is important for the binding of Ras superfamily proteins to different partners, and in distinguishing related members within a family (Cherfils et al., 1997).

We analyzed the distribution of SDP residues (Table 1) at the interfaces that interact with both GEF and GAP proteins (Fig. S9). In the case of GAPs, most Ras superfamily proteins interact by means of at least one residue at switch I, which occupies position 85 in the full sequence alignment (Table S6). However, the Rab protein family is an exception as it uses a completely different set of interacting residues, possibly related to other interactions in the context of larger complexes (Goldberg, 1998). Both Rho and Ran families selectively use residues located in their G1 box (residues 13 and 18, respectively), in switch I (residue 39 of RHO), and the β-sheet adjacent to switch II (residue 91 of RAN; Fig. S9).

In the case of binding to GEFs, the binding surface forms an extended patch at the surface and the interactions differ for each family. Residues at position 94 in the full sequence alignment (Table S6) are located at the C terminus of switch I, and they are common to the Arf and Ras families (residues 51 and 37, respectively). Residues at the N terminus of switch II (residue 64 in RAN and 65 in RAB for the PDB entries 1I2M and 2FOL, respectively) form part of the recognition site. The residue

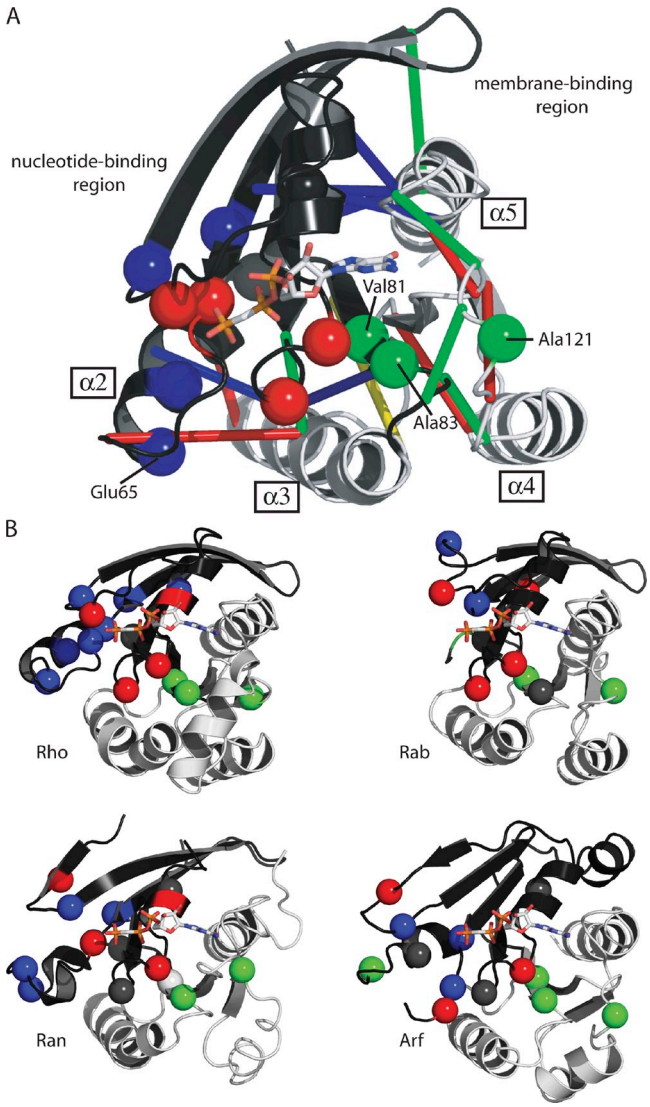

Figure 5. **Location of the SDPs for the different Ras superfamily proteins.** (A) SDP residues in the RAS subfamily. The SDPs (Table 1) are shown as spheres. In the RAS protein the three different isoform-specific contacts are indicated by red, blue, and green lines for NRAS, KRAS, and HRAS, respectively. The proposed routes of communication between lobes 1 and 2 linking the nucleotide-binding region with the membrane-binding region are shown in dark gray and pale gray cartoon. (B) SDP residues for the different Ras subfamilies. The SDPs (Table 1) are mapped onto the structure of representative members (Rho, Rab, Ran, and Arf in the four panels). In both panels the colored spheres indicate SDPs mapped into structures. Red: residues in the proximity of the GTP/GDP-binding pocket. Blue: residues involved in protein–protein interaction. Green: SDP residues coordinating the communication between lobes (see explanation in the text). Gray: residues with no identified biological function. Equivalent regions potentially involved in communication between lobes 1 and 2 linking the nucleotide-binding region with the membrane-binding region are shown in dark gray and pale gray cartoon.

at position 85 in the alignment corresponding to residues 47, 34, 36, 39, and 41 for the Arf, Ras, Rho, Rab, and Ran structures, respectively (as indicated in Table 1), and which corresponds to G2 and switch I, is found in the sequences of both Ras and Rho families. The residue at position 219 in the C terminus of the switch II region is shared by proteins of the Ras and Ran families (position 219 in the alignment, corresponding to residues 68 and 76 in Ras and Ran structures, respectively, as indicated in Table 1).

SDPs involved in communication between GTP and membrane-binding regions. The extension of Arf, Arl, and Sar proteins at the N terminus is required for membrane anchoring (Pasqualato et al., 2002), also serving as a family-specific switch (Goldberg, 1998). Interestingly, recent studies highlighted a more general switch mechanism, involving communication between the membrane-binding domain and the GTP-binding site (Abankwa et al., 2008; Gorfe et al., 2008). Based on sequence variation, two different lobes have been defined in the canonical RAS structure: lobe 1 (comprising the first 86 conserved residues), which lines up the GTP/GDP pocket; and lobe 2 (residues 87–171), which exhibits significant sequence variability and that is associated with Ras anchoring to the membrane (the lobes are shown in dark gray and pale gray in Fig. 5 A). In the 3D structure, different routes of communication between these two regions have been proposed for different isoforms (Gorfe et al., 2008). To characterize residues that mediate the communication between the two lobes, we mapped the proposed GTP–membrane communication routes for the three RAS isoforms onto the canonical G-domain, based on the specific pairwise contacts for each isoform and the location of the SDP residues (Fig. 5 A). Three specific SDP residues may transfer the conformational changes required for the correct transmission of the biological signal. In the 3D structure of RAS, residues Val81 and Ala83 are located in a buried β-sheet, which is sandwiched between the two lobes that coordinate the conformational changes involved in this back-to-front communication mechanism. By contrast, Ala121 is found in a loop that is thought to weave different spatial motifs into the structure, such as the preceding α3 and α5 loops (Fig. 5 A). Although no data are available for the members of other families, the similarity of the SDP patterns suggests that similar routes connect the two regions (see Table 1 for the equivalent residues in the other families).

Based on the location and biological implications of the SDP residues, we conclude that the specificity of the small G protein structural module is characterized by a "canonical" nucleotide switch, multiple specific interactions, and communication with the nucleotide–membrane region. A precise balance between a rigid, high-affinity conformation and conformational flexibility is required to create such an efficient and stringent molecular switch, which may involve residues specific to individual proteins as well as distinct families.

Overview

New genomic information and the improvements to phylogenetic tools have further advanced our understanding of the structure and organization of the Ras protein superfamily. These advances are evident when comparing the current superfamily tree with that initially proposed 20 years ago (Valencia et al., 1991). It is now clear that the separation of the five main families (Ras, Rho, Arf/Sar, Ran, and Rab) was an early evolutionary event that predated the expansion of eukaryotes. Although it was believed that the founding members belonged to the Ras family, our comprehensive phylogenetic analyses of selected, well-defined members of each family in representative species, using EFTU sequences as an outgroup, points to the SRPRB

proteins and the Arf family as possible founding members. This implies that the original function of these proteins may have been related to the regulation of membrane trafficking in eukaryotic cells (Munro, 2005), a process potentially linked to the emergence of complex intracellular structures. The presence of representative sequences of each family in the selected genomes indicates that divergence occurred before the emergence of eukaryotes, and strongly suggests that this superfamily expanded very early to generate the functionally distinct families. It is tempting to propose that this ancestral diversification is related to the increasing complexity of intracellular eukaryotic structures. This hypothesis merits further investigation and such studies will require additional information from genomes of more distant species, more precise functional data, and possibly new computational methods.

The general phylogenetic reconstruction proposed here fits well with the known functional properties of the individual families. In some cases, early functional divergence may be related to divisions such as that of the Ran family sequences, which represent a sub-functionalization of Rab to properly achieve nuclear transport capabilities. A number of other observations relating to specific groups in some species, such as the absence of the entire Ras family in *A. thaliana*, or the loss of genes in coelomates (Technau et al., 2005) and their ascidian vertebrate sisters (Hughes and Friedman, 2005), illustrate the complex gene loss and gain in different lineages (Kondrashov et al., 2002). More functional studies will be necessary to marry the details of functional and evolutionary divergence.

Our review of the phylogenetic classification of the Ras superfamily has provided useful data relating to the classification of a set of more divergent members. According to our analyses, some of these members may be placed in the traditional families, as seen in our reassigning of RAYL and MIRO proteins to the Rho family, and the RAB20 and RABL2A/B proteins to the Rab family. Based on the information available, other sequences such SRPRBs and RABL5/3 can be tentatively classified as independent families.

Phylogenetic approaches such as those described here can further our understanding of the relationships between proteins and protein groups. However, the assignment of function based on orthologous relationships should be approached with caution, and ultimately such facets should be confirmed experimentally.

The protein functions proposed here based on experimental data and phylogenetic inference can be complemented by a combination of structural analyses, and by determining the key residues in functional regions and in the mechanisms adopted by the distinct families (see Pymol Scripts in the Online supplemental material for the mapping of SPDs to structures). Within this new framework, such an approach could identify molecular landmarks that underlie the specific functional differences between families (i.e., the presence of residues such as Val81 and Ala83 in the core of the protein [PDB entry 121P]; or the presence of residues correlated with functional movement, such as Ala121 in the loop regions). These residues may be implicated in signal transmission between GTP-binding sites associated with the GTP state of the protein and the membrane-anchoring regions (N terminus of ARF, ARL, and SAR proteins in the Arf family, and the C terminus in the Ras and Ran families). Similarly, positions 156, 164, and 219 (numbered according to the full sequence alignment and mapping to the switch II region; see Table S6 for correspondence with the representative structures of each family) may be responsible for the recognition of family-specific binding partners (e.g., Arg68 and Arg76 mediate the association of RAS and RAN with GEFs, respectively; Table 1). Positions around the GTP-binding site, such as residues 13 and 18 in Rho and Ran members, respectively, appear to determine the specificity toward GAPs, and to influence the dynamic features of the GTP/GDP-binding pocket. Accordingly, these residues regulate the GTP hydrolysis/exchange mechanisms in each of these families.

Our understanding of the Ras superfamily will be enhanced by future developments in this field, including the incorporation of new complete genomes, elucidation of the structures of Ras superfamily protein–effector complexes, and biophysical studies of signal transmission between GTPase and effector binding sites in individual families. Similarly, a new generation of phylogenetic methods that can accurately organize larger numbers of sequences and refined bioinformatics approaches for the study of structure–sequence relationships will advance our understanding of protein evolution and function.

Online supplemental material

Supplemental figures, tables, and a .zip file that contains pymol scripts are available at http://www.jcb.org/cgi/content/full/jcb.201103008/DC1.

We are indebted to Fred Wittinghofer and Anne Spang for their critical reading of the manuscript.

This work was supported by two grants from the Spanish Ministerio de Ciencia e Innovación: BIO2007-66855-E.00408 and FIS PS09/02111.

Submitted: 2 March 2011
Accepted: 30 December 2011

References

Abankwa, D., M. Hanzal-Bayer, N. Ariotti, S.J. Plowman, A.A. Gorfe, R.G. Parton, J.A. McCammon, and J.F. Hancock. 2008. A novel switch region regulates H-ras membrane orientation and signal output. *EMBO J.* 27:727–735. http://dx.doi.org/10.1038/emboj.2008.10

Azuma, Y., L. Renault, J.A. García-Ranea, A. Valencia, T. Nishimoto, and A. Wittinghofer. 1999. Model of the ran-RCC1 interaction using biochemical and docking experiments. *J. Mol. Biol.* 289:1119–1130. http://dx.doi.org/10.1006/jmbi.1999.2820

Barnekow, A., A. Thyrock, and D. Kessler. 2009. Chapter 5: rab proteins and their interaction partners. *Int Rev Cell Mol Biol*. 274:235–274. http://dx.doi.org/10.1016/S1937-6448(08)02005-4

Bauer, B., G. Mirey, I.R. Vetter, J.A. García-Ranea, A. Valencia, A. Wittinghofer, J.H. Camonis, and R.H. Cool. 1999. Effector recognition by the small GTP-binding proteins Ras and Ral. *J. Biol. Chem.* 274:17763–17770. http://dx.doi.org/10.1074/jbc.274.25.17763

Biou, V., and J. Cherfils. 2004. Structural principles for the multispecificity of small GTP-binding proteins. *Biochemistry*. 43:6833–6840. http://dx.doi.org/10.1021/bi049630u

Bishop, A.L., and A. Hall. 2000. Rho GTPases and their effector proteins. *Biochem. J.* 348:241–255. http://dx.doi.org/10.1042/0264-6021:3480241

Boureux, A., E. Vignal, S. Faure, and P. Fort. 2007. Evolution of the Rho family of ras-like GTPases in eukaryotes. *Mol. Biol. Evol.* 24:203–216. http://dx.doi.org/10.1093/molbev/msl145

Cavalli-Sforza, L.L., and A.W. Edwards. 1967. Phylogenetic analysis. Models and estimation procedures. *Am. J. Hum. Genet.* 19:233–257.

Cherfils, J., J. Ménétrey, G. Le Bras, I. Janoueix-Lerosey, J. de Gunzburg, J.R. Garel, and I. Auzat. 1997. Crystal structures of the small G protein Rap2A

in complex with its substrate GTP, with GDP and with GTPgammaS. *EMBO J.* 16:5582–5591. http://dx.doi.org/10.1093/emboj/16.18.5582

Colicelli, J. 2004. Human RAS superfamily proteins and related GTPases. *Sci. STKE.* 2004:RE13. http://dx.doi.org/10.1126/stke.2502004re13

Corbett, K.D., and T. Alber. 2001. The many faces of Ras: recognition of small GTP-binding proteins. *Trends Biochem. Sci.* 26:710–716. http://dx.doi.org/10.1016/S0968-0004(01)01974-0

Crooks, G.E., G. Hon, J.M. Chandonia, and S.E. Brenner. 2004. WebLogo: a sequence logo generator. *Genome Res.* 14:1188–1190. http://dx.doi.org/10.1101/gr.849004

del Sol, A., F. Pazos, and A. Valencia. 2003. Automatic methods for predicting functionally important residues. *J. Mol. Biol.* 326:1289–1302. http://dx.doi.org/10.1016/S0022-2836(02)01451-1

Díaz, J.F., B. Wroblowski, and Y. Engelborghs. 1995. Molecular dynamics simulation of the solution structures of Ha-ras-p21 GDP and GTP complexes: flexibility, possible hinges, and levers of the conformational transition. *Biochemistry*. 34:12038–12047. http://dx.doi.org/10.1021/bi00037a047

Díaz, J.F., B. Wroblowski, J. Schlitter, and Y. Engelborghs. 1997. Calculation of pathways for the conformational transition between the GTP- and GDP-bound states of the Ha-ras-p21 protein: calculations with explicit solvent simulations and comparison with calculations in vacuum. *Proteins*. 28:434–451. http://dx.doi.org/10.1002/(SICI)1097-0134(199707)28:3<434::AID-PROT12>3.0.CO;2-I

Dvorsky, R., and M.R. Ahmadian. 2004. Always look on the bright site of Rho: structural implications for a conserved intermolecular interface. *EMBO Rep.* 5:1130–1136. http://dx.doi.org/10.1038/sj.embor.7400293

Eddy, S.R. 2009. A new generation of homology search tools based on probabilistic inference. *Genome Inform.* 23:205–211. http://dx.doi.org/10.1142/9781848165632_0019

Ezer, S.T., D. Sahar, A. Salzberg, and Z. Lev. 1994. Differential expression during embryogenesis of three genes clustered in the Ras1 region of *Drosophila melanogaster*. *Dev. Dyn.* 201:179–190. http://dx.doi.org/10.1002/aja.1002010208

Finn, R.D., J. Mistry, J. Tate, P. Coggill, A. Heger, J.E. Pollington, O.L. Gavin, P. Gunasekaran, G. Ceric, K. Forslund, et al. 2010. The Pfam protein families database. *Nucleic Acids Res.* 38(Database issue):D211–D222. http://dx.doi.org/10.1093/nar/gkp985

Fuentes, G., and A. Valencia. 2009. Ras classical effectors: new tales from in silico complexes. *Trends Biochem. Sci.* 34:533–539. http://dx.doi.org/10.1016/j.tibs.2009.07.001

Futatsugi, N., and M. Tsuda. 2001. Molecular dynamics simulations of Gly-12—>Val mutant of p21(ras): dynamic inhibition mechanism. *Biophys. J.* 81:3483–3488. http://dx.doi.org/10.1016/S0006-3495(01)75979-6

Garcia-Ranea, J.A., and A. Valencia. 1998. Distribution and functional diversification of the ras superfamily in *Saccharomyces cerevisiae*. *FEBS Lett.* 434:219–225. http://dx.doi.org/10.1016/S0014-5793(98)00967-3

Gaucher, E.A., J.T. Kratzer, and R.N. Randall. 2010. Deep phylogeny—how a tree can help characterize early life on Earth. *Cold Spring Harb. Perspect. Biol.* 2:a002238. http://dx.doi.org/10.1101/cshperspect.a002238

Goldberg, J. 1998. Structural basis for activation of ARF GTPase: mechanisms of guanine nucleotide exchange and GTP-myristoyl switching. *Cell*. 95:237–248. http://dx.doi.org/10.1016/S0092-8674(00)81754-7

Goldfinger, L.E. 2008. Choose your own path: specificity in Ras GTPase signaling. *Mol. Biosyst.* 4:293–299. http://dx.doi.org/10.1039/b716887j

Gorfe, A.A., B.J. Grant, and J.A. McCammon. 2008. Mapping the nucleotide and isoform-dependent structural and dynamical features of Ras proteins. *Structure*. 16:885–896. http://dx.doi.org/10.1016/j.str.2008.03.009

Hall, B.G. 2005. Comparison of the accuracies of several phylogenetic methods using protein and DNA sequences. *Mol. Biol. Evol.* 22:792–802. http://dx.doi.org/10.1093/molbev/msi066

Heasman, S.J., and A.J. Ridley. 2008. Mammalian Rho GTPases: new insights into their functions from in vivo studies. *Nat. Rev. Mol. Cell Biol.* 9:690–701. http://dx.doi.org/10.1038/nrm2476

Hedges, S.B., J.E. Blair, M.L. Venturi, and J.L. Shoe. 2004. A molecular timescale of eukaryote evolution and the rise of complex multicellular life. *BMC Evol. Biol.* 4:2. http://dx.doi.org/10.1186/1471-2148-4-2

Heo, W.D., and T. Meyer. 2003. Switch-of-function mutants based on morphology classification of Ras superfamily small GTPases. *Cell*. 113:315–328. http://dx.doi.org/10.1016/S0092-8674(03)00315-5

Holder, M., and P.O. Lewis. 2003. Phylogeny estimation: traditional and Bayesian approaches. *Nat. Rev. Genet.* 4:275–284. http://dx.doi.org/10.1038/nrg1044

Hughes, A.L., and R. Friedman. 2005. Loss of ancestral genes in the genomic evolution of Ciona intestinalis. *Evol. Dev.* 7:196–200. http://dx.doi.org/10.1111/j.1525-142X.2005.05022.x

Jaffe, A.B., and A. Hall. 2005. Rho GTPases: biochemistry and biology. *Annu. Rev. Cell Dev. Biol.* 21:247–269. http://dx.doi.org/10.1146/annurev.cellbio.21.020604.150721

Jiang, S.Y., and S. Ramachandran. 2006. Comparative and evolutionary analysis of genes encoding small GTPases and their activating proteins in eukaryotic genomes. *Physiol. Genomics*. 24:235–251.

Kahn, R.A., J. Cherfils, M. Elias, R.C. Lovering, S. Munro, and A. Schurmann. 2006. Nomenclature for the human Arf family of GTP-binding proteins: ARF, ARL, and SAR proteins. *J. Cell Biol.* 172:645–650. http://dx.doi.org/10.1083/jcb.200512057

Karnoub, A.E., and R.A. Weinberg. 2008. Ras oncogenes: split personalities. *Nat. Rev. Mol. Cell Biol.* 9:517–531. http://dx.doi.org/10.1038/nrm2438

Karnoub, A.E., D.K. Worthylake, K.L. Rossman, W.M. Pruitt, S.L. Campbell, J. Sondek, and C.J. Der. 2001. Molecular basis for Rac1 recognition by guanine nucleotide exchange factors. *Nat. Struct. Biol.* 8:1037–1041. http://dx.doi.org/10.1038/nsb719

Katoh, K., G. Asimenos, and H. Toh. 2009. Multiple alignment of DNA sequences with MAFFT. *Methods Mol. Biol.* 537:39–64. http://dx.doi.org/10.1007/978-1-59745-251-9_3

Kemena, C., and C. Notredame. 2009. Upcoming challenges for multiple sequence alignment methods in the high-throughput era. *Bioinformatics*. 25:2455–2465. http://dx.doi.org/10.1093/bioinformatics/btp452

Kiel, C., M. Foglierini, N. Kuemmerer, P. Beltrao, and L. Serrano. 2007. A genome-wide Ras-effector interaction network. *J. Mol. Biol.* 370:1020–1032. http://dx.doi.org/10.1016/j.jmb.2007.05.015

Kondrashov, F.A., I.B. Rogozin, Y.I. Wolf, and E.V. Koonin. 2002. Selection in the evolution of gene duplications. *Genome Biol.* 3:RESEARCH0008. http://dx.doi.org/10.1186/gb-2002-3-2-research0008

Kramer, M., O. Backhaus, P. Rosenstiel, D. Horn, E. Klopocki, G. Birkenmeier, S. Schreiber, M. Platzer, J. Hampe, and K. Huse. 2010. Analysis of relative gene dosage and expression differences of the paralogs RABL2A and RABL2B by Pyrosequencing. *Gene*. 455:1–7. http://dx.doi.org/10.1016/j.gene.2010.01.005

Langsley, G., V. van Noort, C. Carret, M. Meissner, E.P. de Villiers, R. Bishop, and A. Pain. 2008. Comparative genomics of the Rab protein family in Apicomplexan parasites. *Microbes Infect.* 10:462–470. http://dx.doi.org/10.1016/j.micinf.2008.01.017

Lartillot, N., H. Brinkmann, and H. Philippe. 2007. Suppression of long-branch attraction artefacts in the animal phylogeny using a site-heterogeneous model. *BMC Evol. Biol.* 7:S4. http://dx.doi.org/10.1186/1471-2148-7-S1-S4

Letunic, I., and P. Bork. 2007. Interactive Tree Of Life (iTOL): an online tool for phylogenetic tree display and annotation. *Bioinformatics*. 23:127–128. http://dx.doi.org/10.1093/bioinformatics/btl529

Li, Y., W.G. Kelly, J.M. Logsdon Jr., A.M. Schurko, B.D. Harfe, K.L. Hill-Harfe, and R.A. Kahn. 2004. Functional genomic analysis of the ADP-ribosylation factor family of GTPases: phylogeny among diverse eukaryotes and function in *C. elegans*. *FASEB J.* 18:1834–1850. http://dx.doi.org/10.1096/fj.04-2273com

Li, Q., L. Wang, L. Zeng, Y. Zhang, K. Li, P. Jin, B. Su, and L. Wang. 2010. Evaluation of the novel gene Rabl3 in the regulation of proliferation and motility in human cancer cells. *Oncol. Rep.* 24:433–440.

Lukman, S., B.J. Grant, A.A. Gorfe, G.H. Grant, and J.A. McCammon. 2010. The distinct conformational dynamics of K-Ras and H-Ras A59G. *PLOS Comput. Biol.* 6. http://dx.doi.org/10.1371/journal.pcbi.1000922

Mackiewicz, P., and E. Wyroba. 2009. Phylogeny and evolution of Rab7 and Rab9 proteins. *BMC Evol. Biol.* 9:101. http://dx.doi.org/10.1186/1471-2148-9-101

Mishima, K., M. Tsuchiya, M.S. Nightingale, J. Moss, and M. Vaughan. 1993. ARD 1, a 64-kDa guanine nucleotide-binding protein with a carboxyl-terminal ADP-ribosylation factor domain. *J. Biol. Chem.* 268:8801–8807.

Mulloy, J.C., J.A. Cancelas, M.D. Filippi, T.A. Kalfa, F. Guo, and Y. Zheng. 2010. Rho GTPases in hematopoiesis and hemopathies. *Blood*. 115:936–947. http://dx.doi.org/10.1182/blood-2009-09-198127

Munro, S. 2005. The Arf-like GTPase Arl1 and its role in membrane traffic. *Biochem. Soc. Trans.* 33:601–605. http://dx.doi.org/10.1042/BST0330601

Nei, M., and S. Kumar. 2000. Molecular Evolution and Phylogenetics. Oxford University Press.

Noé, F., F. Ille, J.C. Smith, and S. Fischer. 2005. Automated computation of low-energy pathways for complex rearrangements in proteins: application to the conformational switch of Ras p21. *Proteins*. 59:534–544. http://dx.doi.org/10.1002/prot.20422

Notredame, C. 2010. Computing multiple sequence/structure alignments with the T-coffee package. *Curr. Protoc. Bioinformatics*. Chapter 3:Unit 3.8 1–25.

Ostlund, G., T. Schmitt, K. Forslund, T. Köstler, D.N. Messina, S. Roopra, O. Frings, and E.L. Sonnhammer. 2010. InParanoid 7: new algorithms and

tools for eukaryotic orthology analysis. *Nucleic Acids Res.* 38(Database issue):D196–D203. http://dx.doi.org/10.1093/nar/gkp931

Page, R.D.M., and E.C. Holmes. 1999. Molecular Evolution: A Phylogenetic Approach. Blackwell Sciences Ltd., Oxford.

Park, H.O., and E. Bi. 2007. Central roles of small GTPases in the development of cell polarity in yeast and beyond. *Microbiol. Mol. Biol. Rev.* 71:48–96. http://dx.doi.org/10.1128/MMBR.00028-06

Pasqualato, S., L. Renault, and J. Cherfils. 2002. Arf, Arl, Arp and Sar proteins: a family of GTP-binding proteins with a structural device for 'front-back' communication. *EMBO Rep.* 3:1035–1041. http://dx.doi.org/10.1093/embo-reports/kvf221

Pereira-Leal, J.B., and M.C. Seabra. 2001. Evolution of the Rab family of small GTP-binding proteins. *J. Mol. Biol.* 313:889–901. http://dx.doi.org/10.1006/jmbi.2001.5072

Phillips, A., D. Janies, and W. Wheeler. 2000. Multiple sequence alignment in phylogenetic analysis. *Mol. Phylogenet. Evol.* 16:317–330. http://dx.doi.org/10.1006/mpev.2000.0785

Putnam, N.H., M. Srivastava, U. Hellsten, B. Dirks, J. Chapman, A. Salamov, A. Terry, H. Shapiro, E. Lindquist, V.V. Kapitonov, et al. 2007. Sea anemone genome reveals ancestral eumetazoan gene repertoire and genomic organization. *Science*. 317:86–94. http://dx.doi.org/10.1126/science.1139158

Qin, H., Z. Wang, D. Diener, and J. Rosenbaum. 2007. Intraflagellar transport protein 27 is a small G protein involved in cell-cycle control. *Curr. Biol.* 17:193–202. http://dx.doi.org/10.1016/j.cub.2006.12.040

Rausell, A., D. Juan, F. Pazos, and A. Valencia. 2010. Protein interactions and ligand binding: from protein subfamilies to functional specificity. *Proc. Natl. Acad. Sci. USA*. 107:1995–2000. http://dx.doi.org/10.1073/pnas.0908044107

Rodriguez-Viciana, P., C. Sabatier, and F. McCormick. 2004. Signaling specificity by Ras family GTPases is determined by the full spectrum of effectors they regulate. *Mol. Cell. Biol.* 24:4943–4954. http://dx.doi.org/10.1128/MCB.24.11.4943-4954.2004

Ronquist, F., and J.P. Huelsenbeck. 2003. MrBayes 3: Bayesian phylogenetic inference under mixed models. *Bioinformatics*. 19:1572–1574. http://dx.doi.org/10.1093/bioinformatics/btg180

Schlessinger, K., A. Hall, and N. Tolwinski. 2009. Wnt signaling pathways meet Rho GTPases. *Genes Dev.* 23:265–277. http://dx.doi.org/10.1101/gad.1760809

Schwartz, S.L., C. Cao, O. Pylypenko, A. Rak, and A. Wandinger-Ness. 2007. Rab GTPases at a glance. *J. Cell Sci.* 120:3905–3910. http://dx.doi.org/10.1242/jcs.015909

Sekiguchi, T., E. Hirose, N. Nakashima, M. Ii, and T. Nishimoto. 2001. Novel G proteins, Rag C and Rag D, interact with GTP-binding proteins, Rag A and Rag B. *J. Biol. Chem.* 276:7246–7257. http://dx.doi.org/10.1074/jbc.M004389200

Sprang, S.R. 2000. Conformational display: a role for switch polymorphism in the superfamily of regulatory GTPases. *Sci. STKE*. 2000:pe1. http://dx.doi.org/10.1126/stke.2000.50.pe1

Stenmark, H. 2009. Rab GTPases as coordinators of vesicle traffic. *Nat. Rev. Mol. Cell Biol.* 10:513–525. http://dx.doi.org/10.1038/nrm2728

Stenmark, H., A. Valencia, O. Martinez, O. Ullrich, B. Goud, and M. Zerial. 1994. Distinct structural elements of rab5 define its functional specificity. *EMBO J.* 13:575–583.

Technau, U., S. Rudd, P. Maxwell, P.M. Gordon, M. Saina, L.C. Grasso, D.C. Hayward, C.W. Sensen, R. Saint, T.W. Holstein, et al. 2005. Maintenance of ancestral complexity and non-metazoan genes in two basal cnidarians. *Trends Genet.* 21:633–639. http://dx.doi.org/10.1016/j.tig.2005.09.007

Tong, L.A., A.M. de Vos, M.V. Milburn, and S.H. Kim. 1991. Crystal structures at 2.2 A resolution of the catalytic domains of normal ras protein and an oncogenic mutant complexed with GDP. *J. Mol. Biol.* 217:503–516. http://dx.doi.org/10.1016/0022-2836(91)90753-S

Valencia, A., P. Chardin, A. Wittinghofer, and C. Sander. 1991. The ras protein family: evolutionary tree and role of conserved amino acids. *Biochemistry*. 30:4637–4648. http://dx.doi.org/10.1021/bi00233a001

van Dam, T.J., H. Rehmann, J.L. Bos, and B. Snel. 2009. Phylogeny of the CDC25 homology domain reveals rapid differentiation of Ras pathways between early animals and fungi. *Cell. Signal.* 21:1579–1585. http://dx.doi.org/10.1016/j.cellsig.2009.06.004

Vetter, I.R., and A. Wittinghofer. 2001. The guanine nucleotide-binding switch in three dimensions. *Science*. 294:1299–1304. http://dx.doi.org/10.1126/science.1062023

Wang, L.S., J. Leebens-Mack, P. Kerr Wall, K. Beckmann, C.W. dePamphilis, and T. Warnow. 2011. The impact of multiple protein sequence alignment on phylogenetic estimation. *IEEE/ACM Trans. Comput. Biol. Bioinformatics*. 8:1108–1119. http://dx.doi.org/10.1109/TCBB.2009.68

Wennerberg, K., K.L. Rossman, and C.J. Der. 2005. The Ras superfamily at a glance. *J. Cell Sci.* 118:843–846. http://dx.doi.org/10.1242/jcs.01660

Wong, A.C., D. Shkolny, A. Dorman, D. Willingham, B.A. Roe, and H.E. McDermid. 1999. Two novel human RAB genes with near identical sequence each map to a telomere-associated region: the subtelomeric region of 22q13.3 and the ancestral telomere band 2q13. *Genomics*. 59:326–334. http://dx.doi.org/10.1006/geno.1999.5889

Wu, X.S., K. Rao, H. Zhang, F. Wang, J.R. Sellers, L.E. Matesic, N.G. Copeland, N.A. Jenkins, and J.A. Hammer III. 2002. Identification of an organelle receptor for myosin-Va. *Nat. Cell Biol.* 4:271–278. http://dx.doi.org/10.1038/ncb760

Yang, Z. 2002. Small GTPases: versatile signaling switches in plants. *Plant Cell*. 14(Suppl):S375–S388.

Zerial, M., and H. McBride. 2001. Rab proteins as membrane organizers. *Nat. Rev. Mol. Cell Biol.* 2:107–117. http://dx.doi.org/10.1038/35052055

Rojas et al., http://www.jcb.org/cgi/content/full/jcb.201103008/DC1

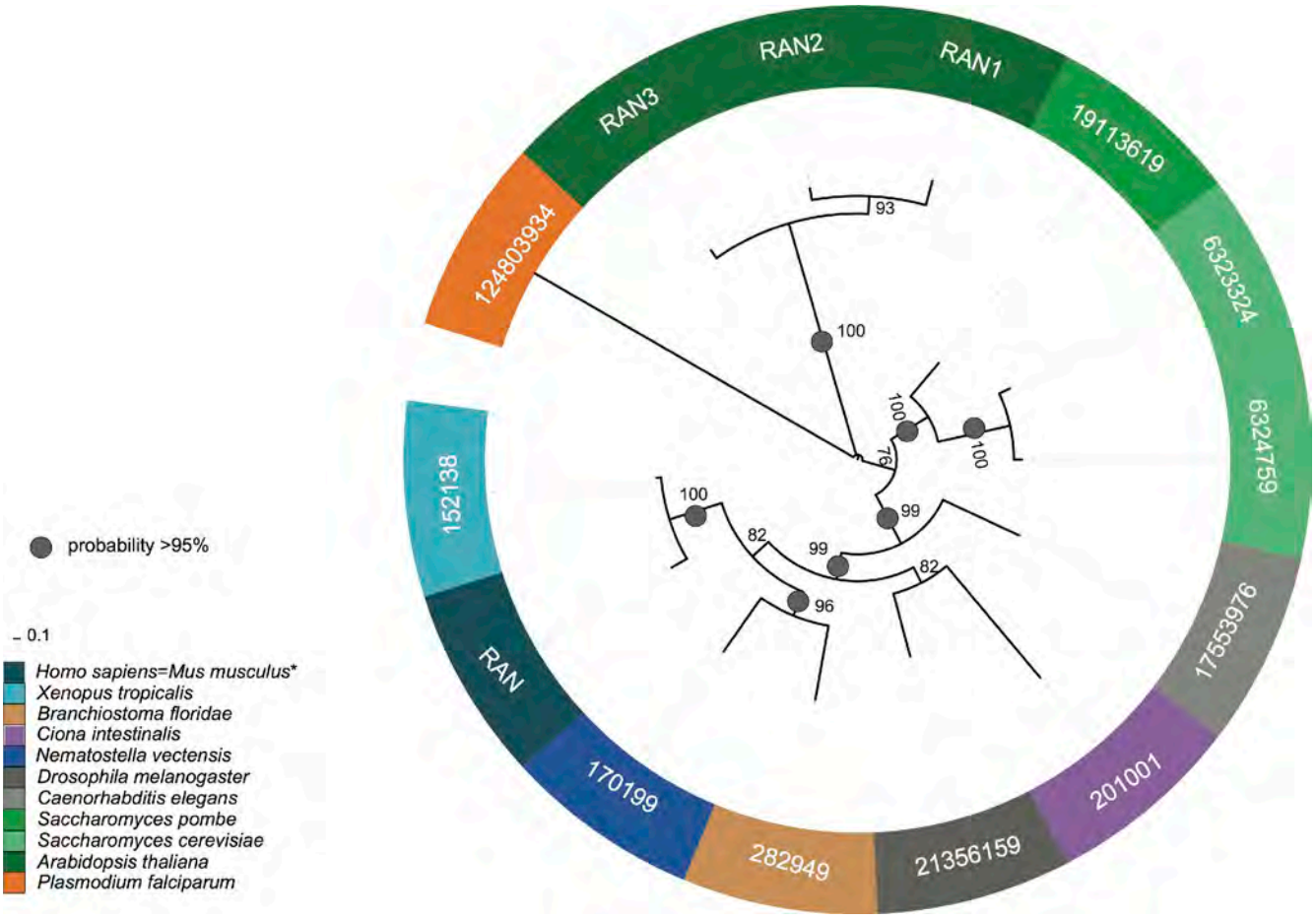

Figure S1. **Ran family phylogenetic tree.** The alignment of the whole protein for 14 orthologues of the human Ran family sequences was used to construct the phylogenies. From the 390 RAS sequences, identical sequences were removed for the sake of clarity. Analyses were performed in 6 chains and 100,000 generations. Trees were sampled after convergence was reached. Color ranges indicate each of the 12 species. Gray circles indicate group probabilities higher than 95%. All the sequences were included in the representative tree (Fig. 2).

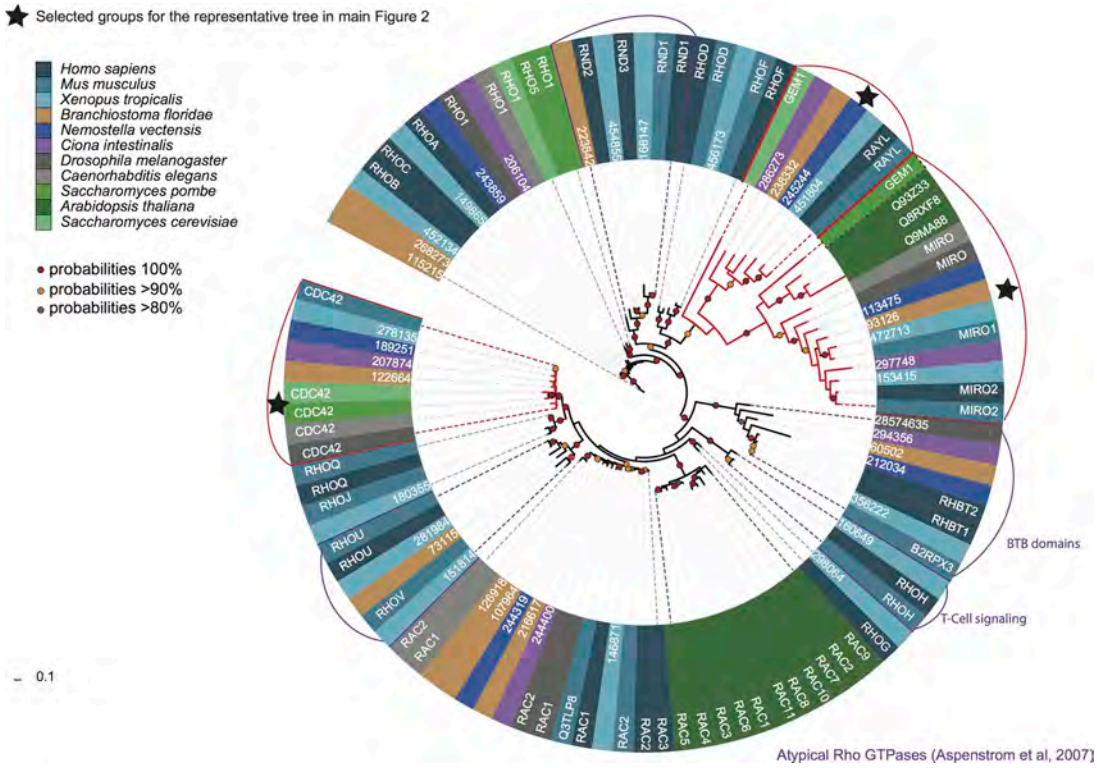

Figure S2. **Rho family phylogenetic tree.** The alignment of the G-domain from 105 orthologues of the human Rho family was used to construct the phylogenies. Analyses were performed in 4 chains and 5,000,000 generations. Trees were sampled after convergence was reached. Color ranges indicate each of the 12 species. Red branches indicate atypical RHO according to Aspenstrom et al. (2007). Red circles indicate group probabilities of 100%. Orange circles indicate probabilities of 90–100%. Gray circles indicate group probabilities of 80–90%. In cases where mouse and human sequences are identical, only the mouse sequence is represented in the tree. Stars indicate selected groups used to build the representative phylogenetic tree (Fig. 2).

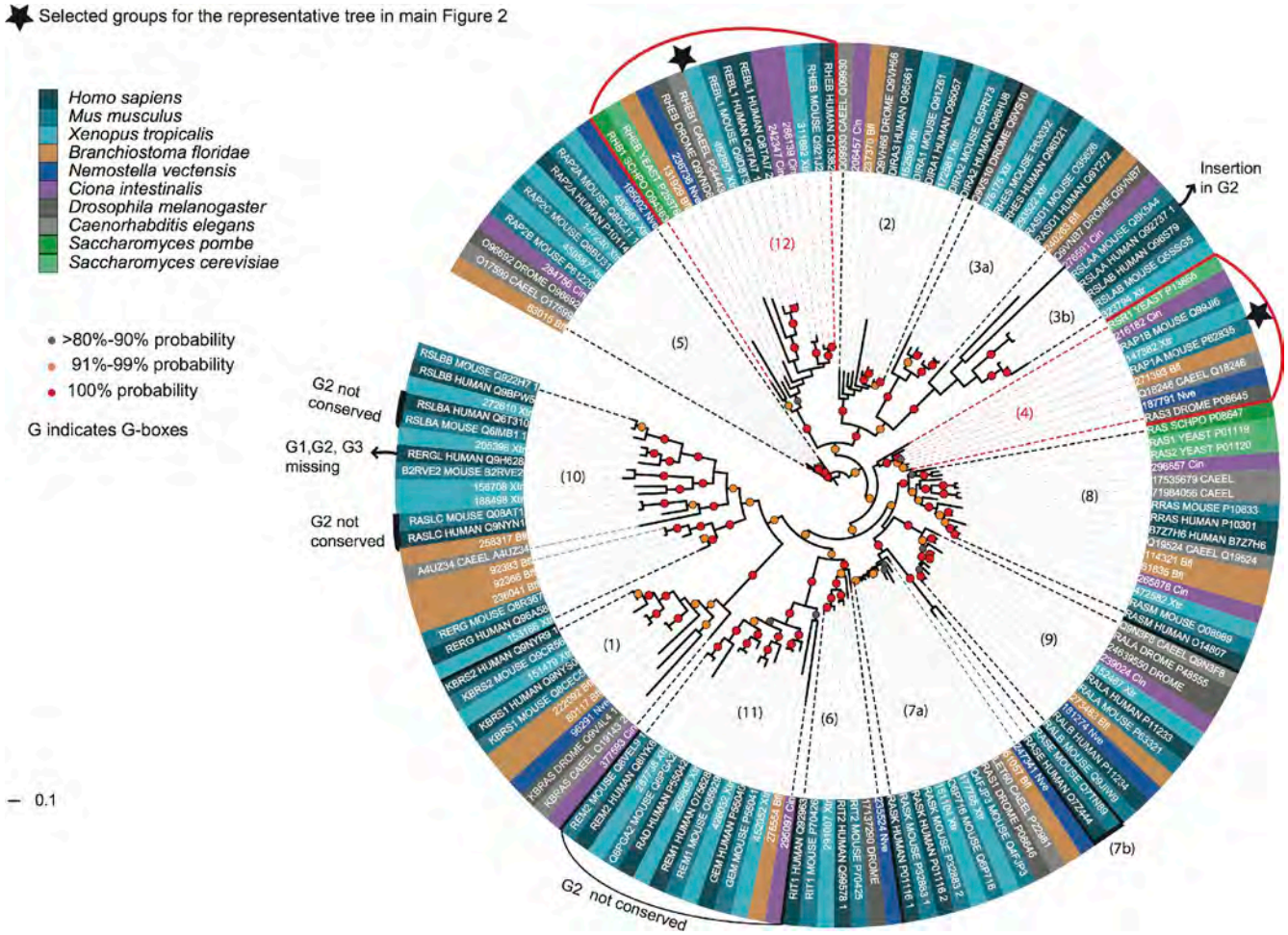

Figure S3. **Ras family phylogenetic tree.** The alignment of the G-domain from 155 orthologues of the human Ras family was used to construct the phylogenies. From the 172 sequences, identical sequences at the G-domain were removed for the sake of clarity. Analyses were performed in 4 chains and 1,000,000 generations, and trees were sampled after convergence was reached. Color ranges indicate each of the species. Red circles indicate group probabilities of 100%. Orange circles indicate probabilities of 90–99%. Gray circles indicate group probabilities of 80–89%. Stars indicate selected groups used to build the representative phylogenetic tree (Fig. 2).

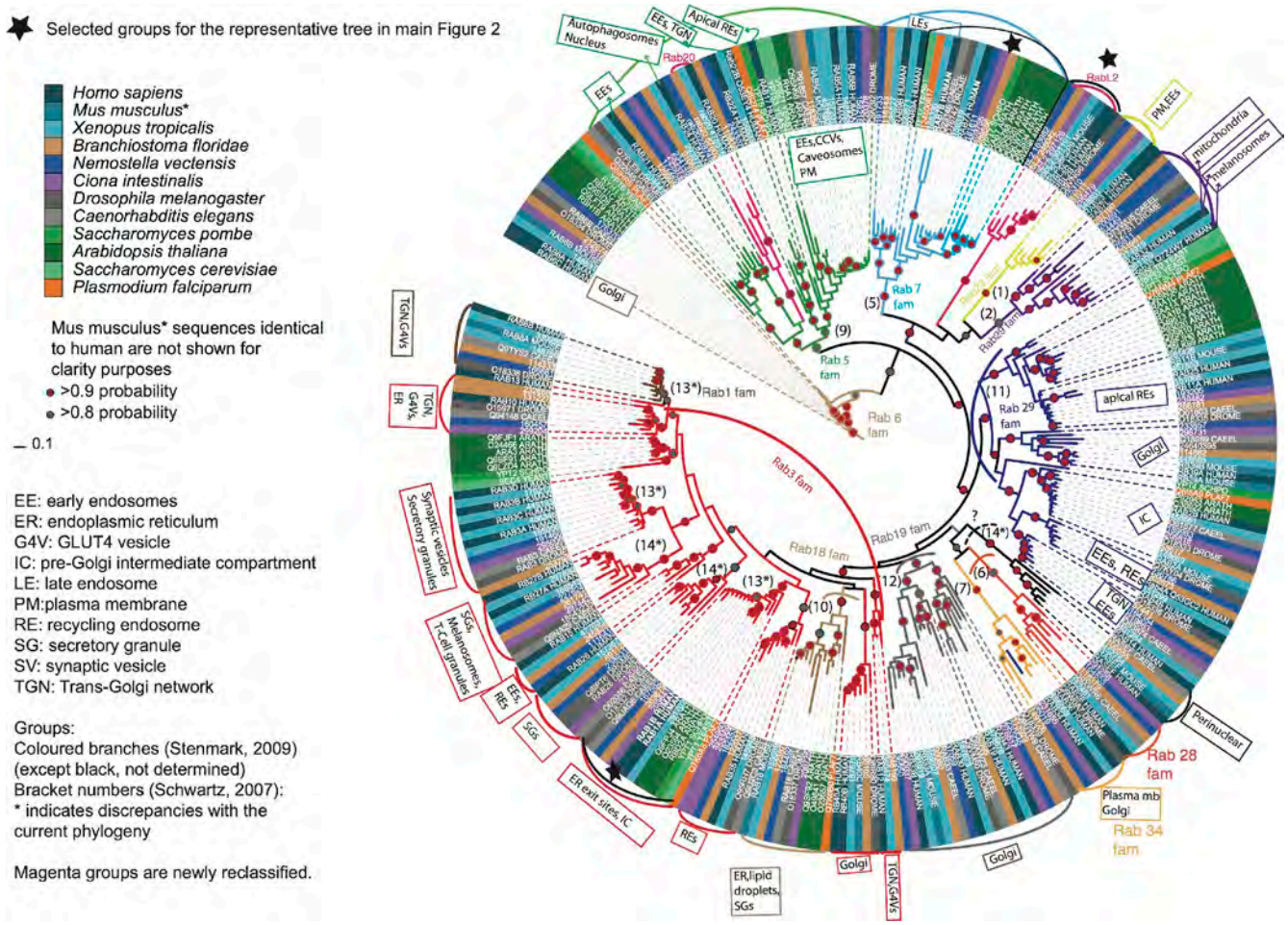

Figure S4. **Rab family phylogenetic tree.** The alignment of the G-domain from 301 orthologues of the human Rab family was used to construct phylogenies. From the 390 RAS sequences, identical sequences were removed for the sake of clarity. Analyses were performed in 4 chains and 5,000,000 generations, and the trees were sampled after convergence was reached. Color ranges indicate each of the 12 species and the subcellular locations are: EE, early endosome; ER, endoplasmic reticulum; G4V, GLUT4 vesicle; IC, preGolgi intermediate compartment; LE, late endosome; PM, plasma membrane; RE, recycling endosome; SG, secretory granule; SV, synaptic vesicle; TGN, trans-Golgi network. Colored branches are in accordance with Stenmark (2009), black branches are not determined. The numbers in brackets indicate the clustering described by Schwartz et al. (2007). Asterisk indicates discrepancies with the aforementioned phylogenies. Newly classified groups are shown in magenta. Red circles indicate group probabilities higher than 90%. Gray circles indicate group probabilities of 80–90%. When the mouse and human sequences are identical, only the mouse sequence is represented in the tree. Stars indicate selected groups used to build the representative phylogenetic tree (Fig. 2).

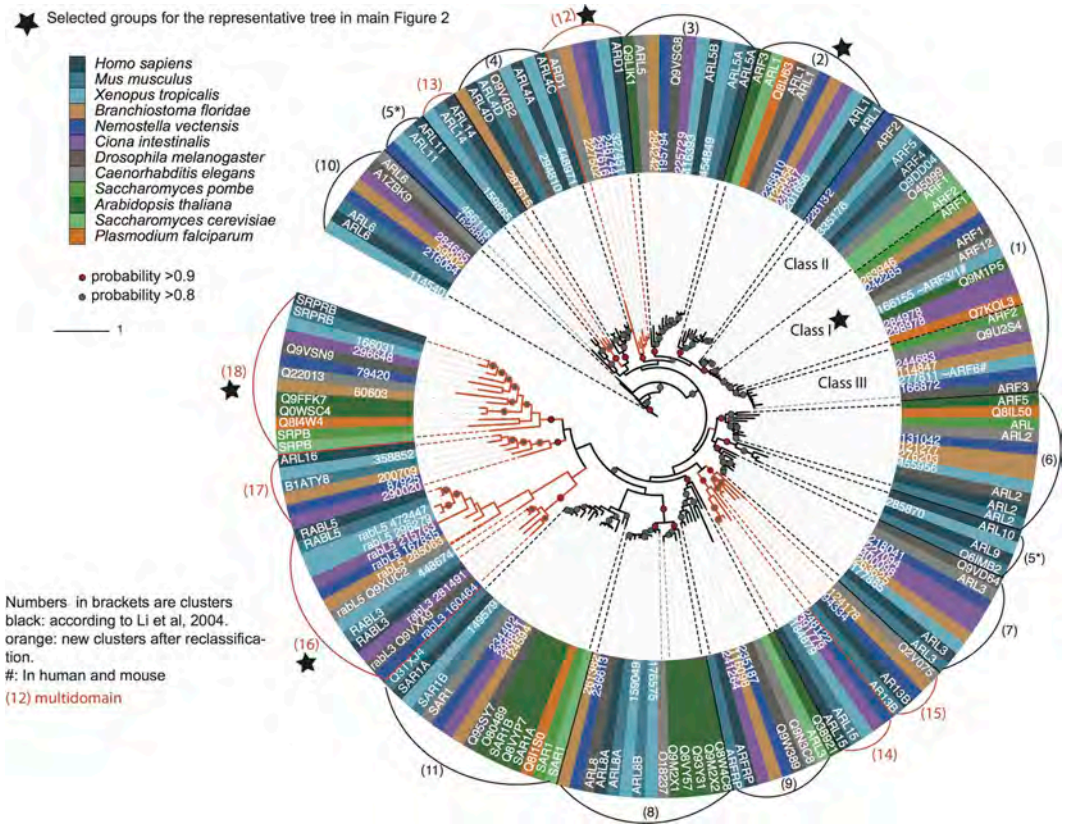

Figure S5. **Arf family phylogenetic tree.** The alignment of the G-domain from 183 orthologues of the human Arf family was used to construct the phylogenies. Analyses were performed in 4 chains and 5,000,000 generations, and the trees were sampled after convergence was reached. Color ranges indicate each of the 12 species and the numbers in brackets indicate clustering according to Li et al. (2004). Orange clusters are newly introduced families. "#" indicates identical sequences for human, frog, and mouse, and thus only one is represented. Red circles indicate group probabilities higher than 90%. Gray circles indicate group probabilities of 80–90%. Stars indicate selected groups used to build the representative phylogenetic tree (Fig. 2).

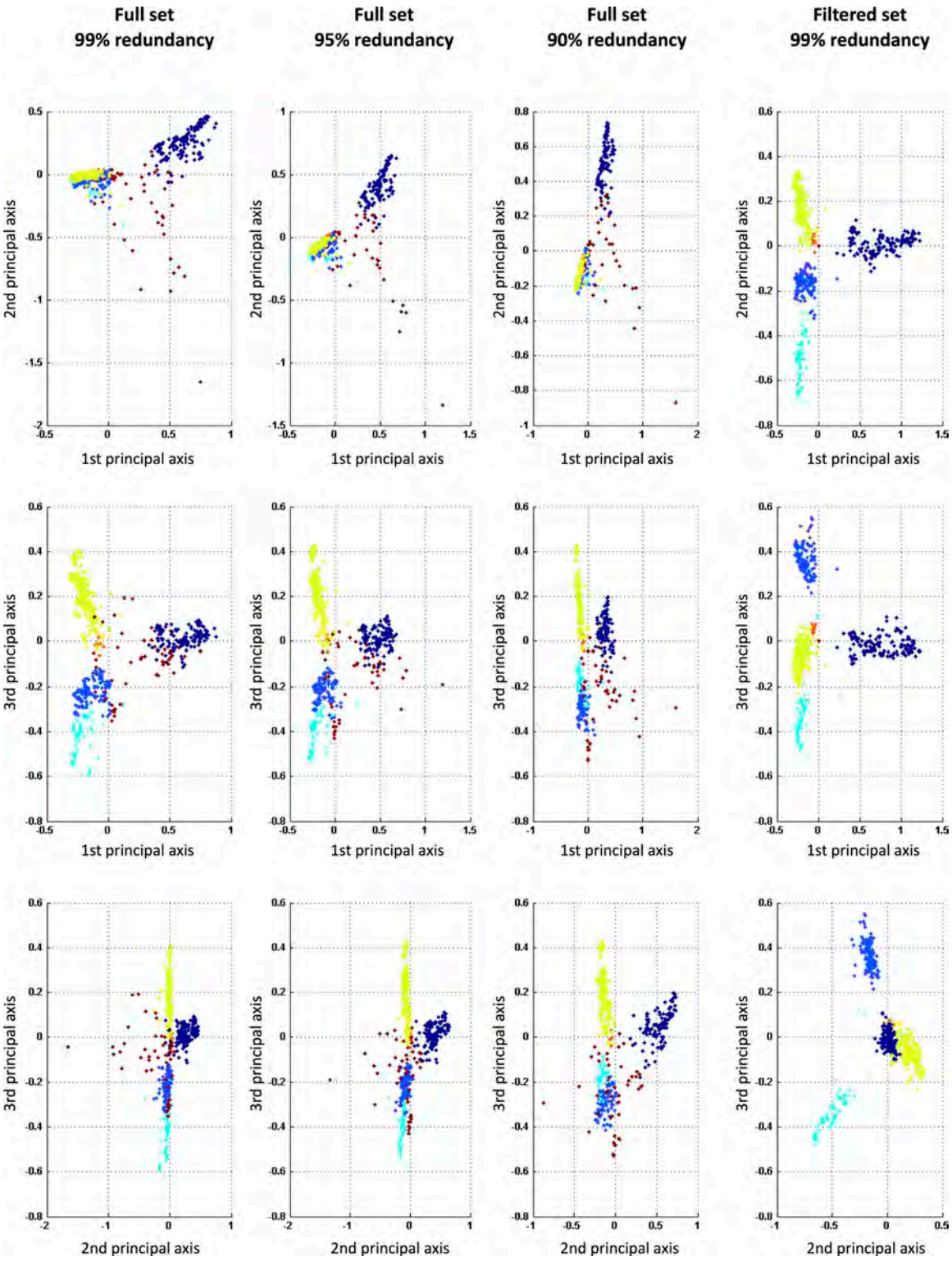

Figure S6. **Vectorial representation of G-domain sequences in the first three principal axes resulting from the multiple correspondence analysis (Rausell et al., 2010) of the alignment.** Sequences are represented in dots and colored according to the phylogenetic classification (main text); dark blue (Arf), blue (Ras), light blue (Rho), yellow (Rab), and orange (Ran), with the exception of the set of noisy sequences (Table S7), which is colored in red. Results are displayed for different levels of nonredundancy (99, 95, and 90%) of the initial alignment of 919 sequences (Table S1) and for the alignment in which the 53 sequences within the noisy set (Table S7) were filtered out. The 53 sequences are dispersed among the main families, intertwining the groups and distorting the principal axes with variable consequences at different levels of nonredundancy. Based on these results, we performed an unsupervised analysis of the SDPs on the filtered set of 866 sequences corresponding to the classical group to study functional specificity within the G-domain family. Redundancy was filtered out using Belvu software.

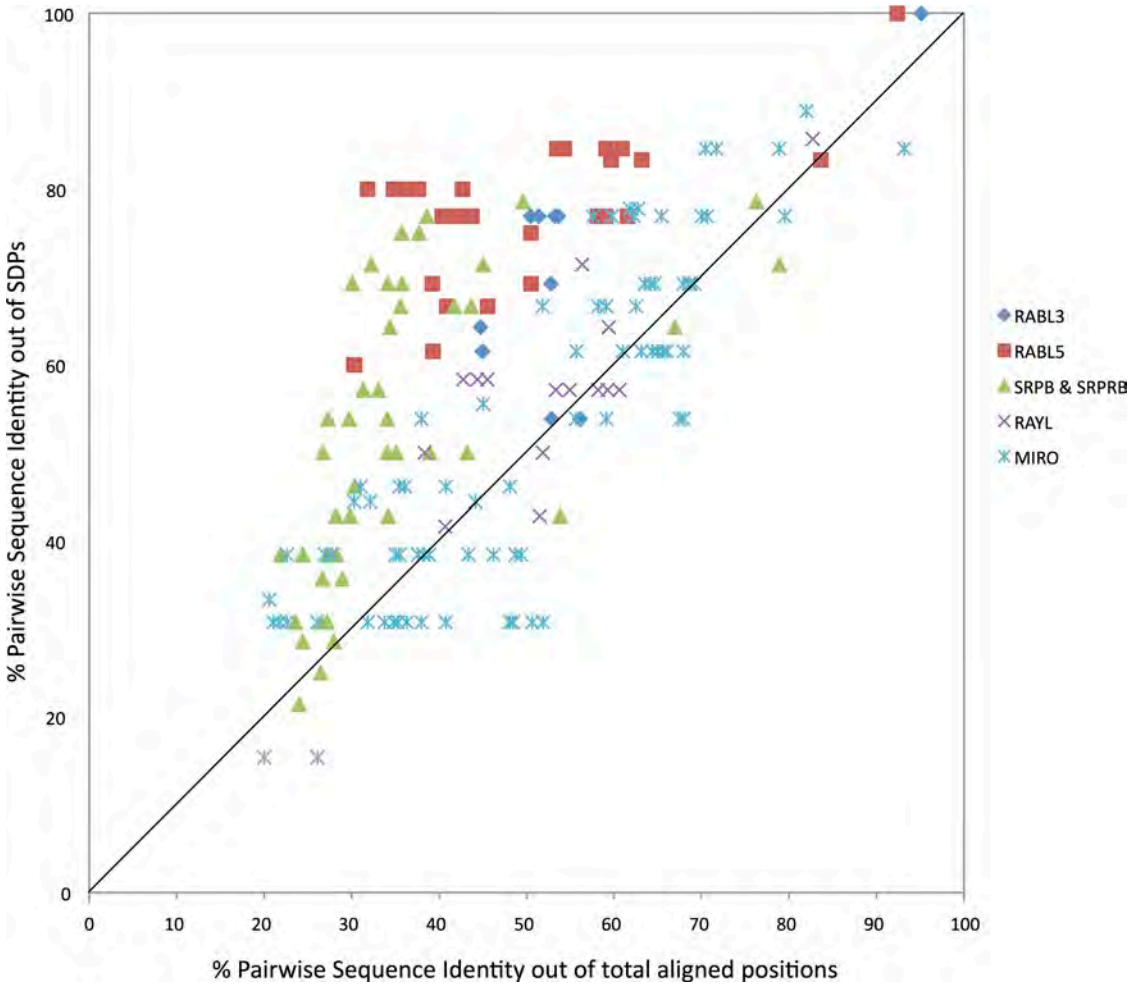

Figure S7. **Pairwise sequence identities calculated from the SDPs (see main text, Fig. 4, and Table S8) plotted against the pairwise sequence identities from the total aligned positions among the proteins of the main classes within the 53 noisy sequences: RABL3, RABL5, RAYL, MIRO, and SRPB.** Note the low intensity of the SDP signal in the RAYL and Miro groups, indicating that the sequences available do not confirm an evolutionary restriction at the positions corresponding to SDPs in the Ras superfamily. These results could be interpreted as supporting their classification in the Rho family (Fig. 2) and suggest that the peculiar features of RAYL and MIRO proteins are determined by a particular set of residues located at positions that differ from those of other members of the family. By contrast, the intensity of the SDP conservation in RABL3, RABL5, and SRPB/SRPRB (together with the clear differences at these positions with the characteristic amino acid types of the classical families; Table S8) can be interpreted as additional evidence of their differences in key functional regions. This provides further support for their classification into three potentially independent groups, as proposed by analysis of the phylogenetic tree (see main text, Fig. 2).

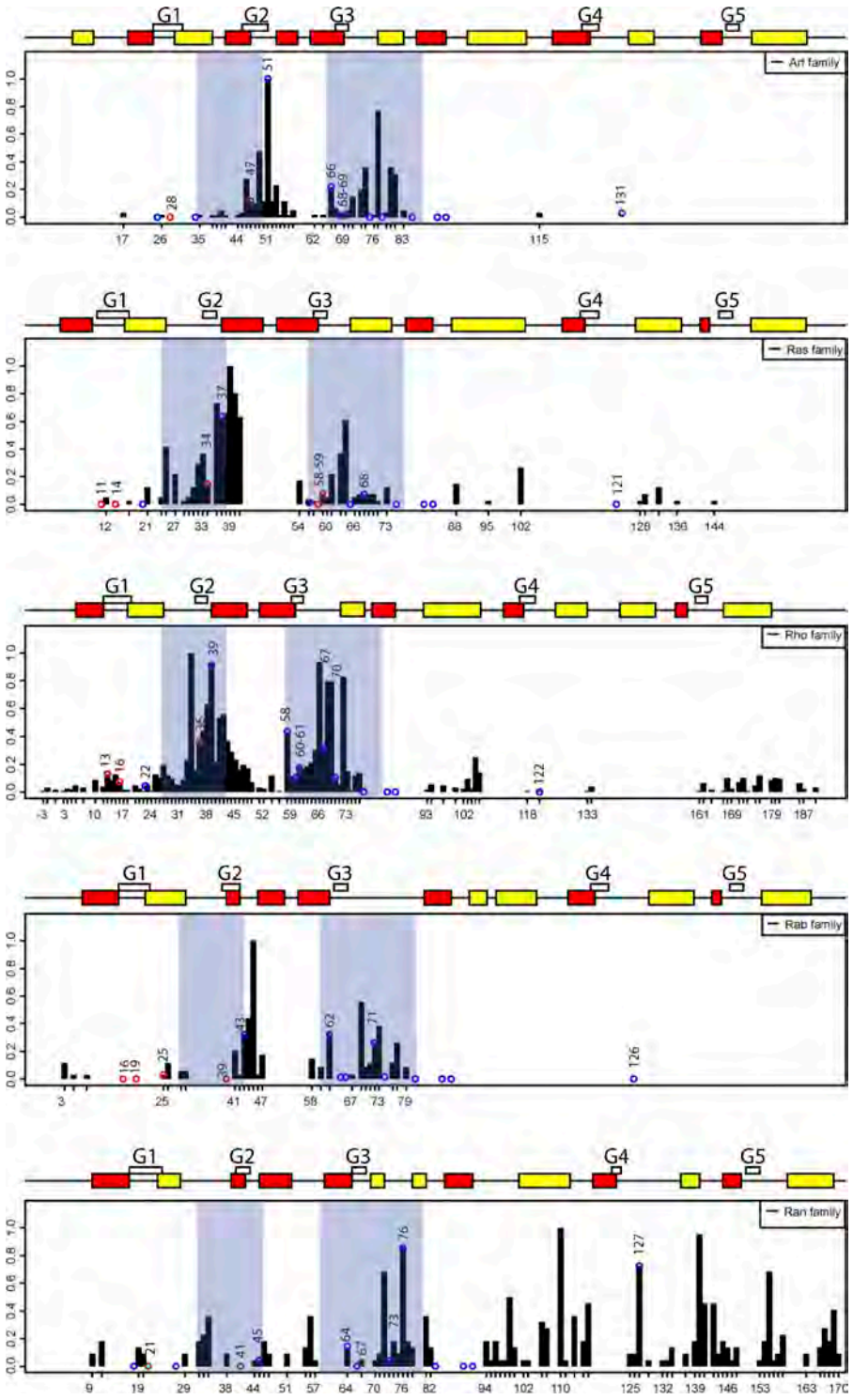

Figure S8. **Secondary structural motifs, guanine nucleotide-binding peptide loops (G1–G5), location of the switch regions I and II, and the frequency of interacting residues in different members of the Ras family.** Structural elements: α-helices are shown in yellow and β-strands in red; G1–G5 loops are sequentially marked above the secondary structure elements with white boxes; regions comprising switch I and switch II are highlighted in a transparent blue box. The frequency of intermolecular contacts of Ras proteins with different interacting partners (Table S5) are shown as histograms, and normalized by accounting for the number of contacts between the partners divided by the higher number of contacts found in a complex for the particular family. The residues involved in nucleotide binding, either GTP and/or GDP, and the SDP residues, are marked with red and blue circles, respectively.

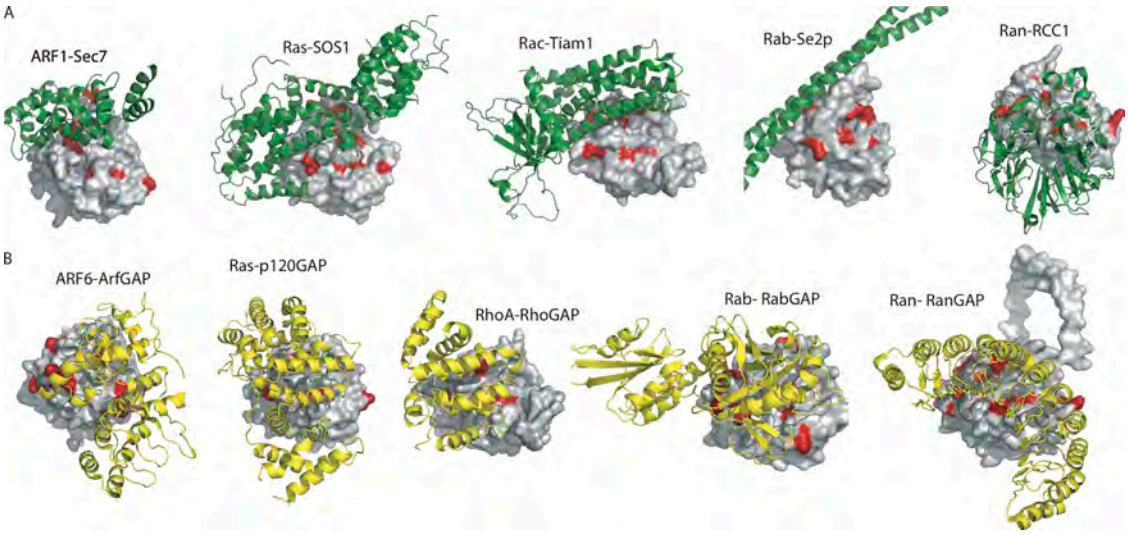

Figure S9. **Distinct modes by which the different members of the Ras superfamily bind to their guanine nucleotide exchange factor proteins (GEFs) and GTPase-activating proteins (GAPs).** Ras proteins are shown as surface representations with the respective SDP residues shown in red; the GEFs and GAPs are shown as ribbon diagrams and in green and yellow, respectively. The residues of the Ras superfamily members implicated in binding via hydrogen bonds, salt bridges, and hydrophobic interactions with the corresponding partners in the different complexes are shown. (A) The ARF1–SEC7 interaction is based on the PDB entry 1r8s and involves the following ARF1 residues (using the UNIPROT numbering, see Table S7): 94, 161, 164, and 156. The RAS–SOS1 interaction is based on PDB entry 1bkd, and involves the following RAS-interacting residues: 85, 94, 164, 219, and 156. The RAC–TIAM1 interaction is based on 1foe and involves the following RAC residues: 164, 204, 85, and 156. The RAB–SEC7 interaction is based on 2ocy and involves RAB residues 204 and 156. The RAN–RCC1 interaction is based on 1i2m and involves RAN residues 164, 204, and 219. (B) The ARF6–ARFGAP interaction is based on the PDB entry 3lvq with the interacting residue at UNIPROT position 85 for ARF6. The RAS–p120GAP interaction is based on 1wq1 and involves residue 85 of RAS. The RHOA–RHOGAP interaction is based on 1tx4 and involves corresponding RHOA residues at positions 7, 85, and 94. The RAP–RAPGAP interaction is based on 3brw and involves Rap residues 261 and 156. The RAN–RANGAP interaction is based on 1k5g and involves residues 7, 85, and 272.

Table S1 is provided as a .txt file

Tables S7 and S8 are provided as Excel files

A .zip file is also provided that contains pymol scripts

Table S2. **Updated 167 human RAS sequences**

Family	Primary	Uniprot_name	Name/synonyms	GenBank	G-domain amino acids
RAB	P61026	RAB10_HUMAN	Rab10	NP_057215	6–170
RAB	P62491	RB11A_HUMAN	Rab11A, YL8	NP_004654	8–172
RAB	Q15907	RB11B_HUMAN	Rab11B, H-YPT3	NP_004209	8–172
RAB	Q6IQ22	RAB12_HUMAN	Rab12	XP_113967 NP_001020471	39–204
RAB	P51153	RAB13_HUMAN	Rab13	NP_002861	5–169
RAB	P61106	RAB14_HUMAN	Rab14, FBP	NP_057406	8–172
RAB	P59190-2	RAB15_HUMAN	Rab15	NP_941959	5–168
RAB	Q9H0T7	RAB17_HUMAN	Rab17	NP_071894	16–180
RAB	Q6PJZ0	Q6PJZ0	Rab17	NP_071894	16–180
RAB	Q9NP72	RAB18_HUMAN	Rab18	NP_067075	5–169
RAB	A4D1S5-1	RAB19_HUMAN	Rab19, Rab19B	XP_379935, NP_001008749	14–179
RAB	C9JJQ5	C9JJQ5	Rab19, Rab19B	XP_379935, NP_001008749	14–179
RAB	P62820-1	RAB1A_HUMAN	Rab1A	NP_004152	8–172
RAB	Q9H0U4	RAB1B_HUMAN	Rab1B	NP_112243	5–169
RAB	Q6FIG4	Q6FIG4	Rab1B	NP_112243	5–169
RAB	Q9UL25	RAB21_HUMAN	Rab21	NP_055814	16–180
RAB	Q9UL26	RB22A_HUMAN	Rab22A	NP_065724	2–166
RAB	Q53EY4	Q53EY4	Rab22B, Rab31	NP_006859	3–167
RAB	Q9ULC3	RAB23_HUMAN	Rab23, HSPC137	NP_057361	6–169
RAB	Q969Q5	RAB24_HUMAN	Rab24	AAH21263	4–172
RAB	P57735	RAB25_HUMAN	Rab25, CATX-8	AAH33322	9–173
RAB	Q9ULW5	RAB26_HUMAN	Rab26	NP_055168	60–225
RAB	P51159-1	RB27A_HUMAN	Rab27A, Ram	NP_899059	6–181
RAB	O00194	RB27B_HUMAN	Rab27B	NP_004154	6–181
RAB	P51157-2	RAB28_HUMAN	Rab28	NP_004240	9–177
RAB	P61019	RAB2A_HUMAN	Rab2A	NP_002856	3–167
RAB	Q8WUD1	RAB2B_HUMAN	Rab2B	NP_116235	3–167
RAB	Q15771	RAB30_HUMAN	Rab30	NP_055303	6–170
RAB	Q13637	RAB32_HUMAN	Rab32	NP_006825	22–192
RAB	Q14088	RB33A_HUMAN	Rab33A, RabS10	NP_004785	33–202
RAB	Q9H082	RB33B_HUMAN	Rab33B	NP_112586	30–199
RAB	Q9BZG1-1	RAB34_HUMAN	Rab34, Rah, Rab39	NP_114140	49–216
RAB	Q15286	RAB35_HUMAN	Rab35, Ray_, H-ray, Rab1C	NP_006852	5–168
RAB	O95755-1	RAB36_HUMAN	Rab36	NP_004905	120–287
RAB	A8MSP2	A8MSP2	Rab37	NP_783865	19–184
RAB	Q7Z4W7	Q7Z4W7	Rab38, NY-MEL-1	NP_071732	6–177
RAB	Q14964	RB39A_HUMAN	Rab39A	NP_059986	5–175
RAB	Q96DA2	RB39B_HUMAN	Rab39B	NP_741995	5–171
RAB	P20336	RAB3A_HUMAN	Rab3A	NP_002857	19–183
RAB	P20337	RAB3B_HUMAN	Rab3B	NP_002858	19–183
RAB	Q96E17	RAB3C_HUMAN	Rab3C	NP_612462	27–191
RAB	O95716	RAB3D_HUMAN	Rab3D, GOV_D2-2, Rab16, Rad3D	NP_004274	19–183
RAB	Q8WXH6	RB40A_HUMAN	Rab40A, Rar2A, Rar-2	NP_543155	11–174
RAB	Q12829	RB40B_HUMAN	Rab40B, Rar, SEC4L	NP_006813	11–174
RAB	Q96S21	RB40C_HUMAN	Rab40C, Rar3, RarL, RasL8C	NP_066991	11–174
RAB	Q86YS6	RAB43_HUMAN	Rab41, Rab43	NP_940892	15–180
RAB	Q53GC2	Q53GC2	Rab4A	NP_004569	10–174
RAB	P61018-1	RAB4B_HUMAN	Rab4B	NP_057238	5–169
RAB	P20339	RAB5A_HUMAN	Rab5A	NP_004153	17–181
RAB	P61020	RAB5B_HUMAN	Rab5B	NP_002859	17–181
RAB	P51148	RAB5C_HUMAN	Rab5Cisofa, RabL, ab5CL	NP_958842	18–182
RAB	P51148	RAB5C_HUMAN	Rab5Cisofb	NP_004574	18–182
RAB	P20340-2	RAB6A_HUMAN	Rab6Aisofa	NP_002860	10–174
RAB	P20340-1	RAB6A_HUMAN	Rab6Aisofb	NP_942599	10–174
RAB	Q9NRW1	RAB6B_HUMAN	Rab6B	NP_057661	10–174
RAB	Q9H0N0	RAB6C_HUMAN	Rab6C, WTH3	NP_115520	10–174
RAB	P51149	RAB7A_HUMAN	Rab7A	NP_004628	5–173
RAB	Q96AH8	RAB7B_HUMAN	Rab7B	NP_796377	5–171

RAB	O14966	RAB7L_HUMAN	Rab7L1, Rab29(rat)	NP_003920	4–173
RAB	P61006	RAB8A_HUMAN	Rab8A, MEL	NP_005361	5–169
RAB	Q92930	RAB8B_HUMAN	Rab8B	NP_057614	5–169
RAB	P51151	RAB9A_HUMAN	Rab9A	NP_004242	4–172
RAB	Q9NP90	RAB9B_HUMAN	Rab9B, Rab9L	NP_057454	4–172
RAB	Q9BW83-2	RAYL_HUMAN	RabL4, RayL	NP_006851	1–170
RAB	Q8IZ41-1	RASEF_HUMAN	RasEF, Rab45	NP_689786	538–708
ARF	Q6T311	–	Arl9	AAS07576	13–187
ARF	P40616	–	Arl1	NP_001168	12–178
ARF	P36406-1	–	Ard1isofa, ArfD1, Trim23, RNF46	NP_001647	399–571
ARF	P84077	–	Arf1	NP_001649	12–178
ARF	P61204	–	Arf3	NP_001650	12–178
ARF	P18085	–	Arf4	NP_001651	12–178
ARF	NotUP	–	Arf4L	NP_001652	16–188
ARF	P84085	–	Arf5	NP_001653	12–178
ARF	P62330	–	Arf6	NP_001654	8–174
ARF	P36404	–	Arl2	NP_001658	11–177
ARF	Q13795	–	ArfRP1, Arp	NP_003215	12–188
ARF	P36405	–	Arl3	NP_004302	12–178
ARF	–	–	Arl7, LAK	NP_005728	8–180
ARF	Q9Y689	–	Arl5isof1	NP_036229	11–177
ARF	Q9Y6B6	–	Sar1b, SARA2, Sar1a, homolog_2, CMRD	NP_057187	20–198
ARF	Q9NVJ2	–	Arl10C, Gie1	NP_060654	15–182
ARF	Q9NXU5	–	ArfRP2	NP_061960	27–195
ARF	Q9NR31	–	Sar1a, SARA1, Masra2	NP_064535	20–198
ARF	Q8N4G2	–	ARL14_HUMAN, FLJ22595	NP_079323	8–176
ARF	P36406-2	–	Ard1isofa	NP_150230	399–568
ARF	P36406-3	–	Ard1isofb	NP_150231	399–545
ARF	Q969Q4	–	Arl11, ArlTS1	NP_612459	7–174
ARF	Q96BM9	–	Arl10B, Gie2	NP_620150	15–182
ARF	NotUP	–	Arl10A	NP_775935	72–244
ARF	Q9H0F7	–	Arl6, BBS3	NP_816931	12–182
ARF	Q9Y689	–	Arl5isof2	NP_817114	1–140
ARF	Q96KC2	–	Arl8	NP_848930	11–177
ARF	Q3SXY8-1	–	Arl2L1isof1	NP_878899	16–196
ARF	P40617	–	Arl4	NP_997625	15–187
ARF	Q0P5N6	–	Arf-like16	XP_290777, NP_001035114	18–194
RAS	P11233	RALA_HUMAN	RalAisoform_2	AAA36542	16–181
RAS	Q8IYK8	REM2_HUMAN	Rem2	AAH35663	103–270
RAS	P01111	RASN_HUMAN	N-Ras	NP_002515	2–166
RAS	P11234	RALB_HUMAN	RalB	NP_002872	13–179
RAS	P62834	RAP1A_HUMAN	Rap1A, Krev-1, Smgp21	NP_002875	2–168
RAS	P61225	RAP2B_HUMAN	Rap2B	NP_002877	2–167
RAS	Q99578-1	RIT2_HUMAN	Rit2, Rin, Roc2, RibA	NP_002921	19–184
RAS	P55042	RAD_HUMAN	Rad_R, Rad, Rem3	NP_004156	90–254
RAS	O95661	DIRA3_HUMAN	Noey2, ARHI, RhoI	NP_004666	36–202
RAS	P01116-2	RASK_HUMAN	K-Ras2B	NP_004976	2–166
RAS	P01112	RASH_HUMAN	H-Rasisof1	NP_005334	2–166
RAS	P11233	RALA_HUMAN	RalAisof1	NP_005393	13–178
RAS	Q15382	RHEB_HUMAN	Rheb1, Rheb2	NP_005605	5–170
RAS	P10301	RRAS_HUMAN	R-Ras	NP_006261	28–193
RAS	Q92737-1	RSLAA_HUMAN	RRP22, RasL10A	NP_006468	3–181
RAS	Q92963	RIT1_HUMAN	Rit1, Roc1, RibB	NP_008843	20–185
RAS	O14807	RASM_HUMAN	M-Ras, R-Ras3	NP_036351	12–178
RAS	B7Z7H6	B7Z7H6_HUMAN	TC21, R-Ras2	NP_036382	13–178
RAS	O75628	REM1_HUMAN	Rem1, Ges	NP_054731	79–246
RAS	Q96D21	RHES_HUMAN	RasD2, Rhes, Tem2	NP_055125	18–193
RAS	P61224	RAP1B_HUMAN	Rap1B	NP_056461	2–168
RAS	Q9Y272	RASD1_HUMAN	RasD1, DexRas, Ags1	NP_057168	23–198
RAS	Q9NYN1	RASLC_HUMAN	Ris, RasL12	NP_057647	19–186
RAS	Q96HU8	DIRA2_HUMAN	Di-Ras2	NP_060064	6–172
RAS	Q9NYR9-1	KBRS2_HUMAN	NKIRas2a, Ras2	NP_060065	3–171
RAS	Q9NYS0	KBRS1_HUMAN	NKIRas1b, Ras1	NP_065078	3–171
RAS	P10114	RAP2A_HUMAN	Rap2A	NP_066361	2–167

RAS	Q9Y3L5	RAP2C_HUMAN	Rap2C	NP_067006	2–167
RAS	Q9BPW5	RSLBB_HUMAN	RasL11B	NP_076429	32–204
RAS	Q9H628	RERGL_HUMAN	FLJ22655	NP_079006	2–175
RAS	Q96A58	RERG_HUMAN	Rerg	NP_116307	5–170
RAS	Q96S79	RSLAB_HUMAN	RasL10B	NP_201572	3–180
RAS	P01116-1	RASK_HUMAN	K-Ras2A	NP_203524	2–166
RAS	Q8TAI7-1	REBL1_HUMAN	Rheb2, RhebL1	NP_653194	5–170
RAS	O95057	DIRA1_HUMAN	Di-Ras1, Rig, GBTS1	NP_660156	6–171
RAS	Q9BR65	Q9BR65_HUMAN	H-Rasisof2, H-RasIDX	NP_789765	2–155
RAS	Q7Z444	RASE_HUMAN	E-Ras, H-Ras2, H-RasP	NP_853510	40–202
RAS	P55040	GEM_HUMAN	Gem_Kir	NP_859053	74–242
RAS	Q6T310	RSLBA_HUMAN	RasL11A	NP_996563	26–199
RHO	P60953-1	CDC42_HUMAN	Cdc42_brain	NP_426359	3–186
RHO	P60953-2	CDC42_HUMAN	Cdc42_placental, G25K, Cdc42Hs	NP_001782	3–186
RHO	P63000-2	RAC1_HUMAN	Rac1_isoform_b	NP_061485	3–205
RHO	P63000-1	RAC1_HUMAN	Rac1_TC25	NP_008839	3–186
RHO	P15153	RAC2_HUMAN	Rac2	NP_002863	3–186
RHO	P60763	RAC3_HUMAN	Rac3	NP_005043	3–186
RHO	P61586	RHOA_HUMAN	RhoA, ARHA, Rho, H12	NP_001655	5–188
RHO	P62745	RHOB_HUMAN	RhoB, ARHB, Rho, H6	NP_004031	5–187
RHO	O94844	RHBT1_HUMAN	RhoBTB1	NP_055651	14–218
RHO	Q9BYZ6	RHBT2_HUMAN	RhoBTB2_DBC2	NP_055993	14–218
RHO	P08134	RHOC_HUMAN	RhoC, ARHC, Rho, H9	NP_786886	5–188
RHO	O00212	RHOD_HUMAN	RhoD, ARHD, RhoHP1	NP_055393	17–200
RHO	P84095	RHOG_HUMAN	RhoG, ARHG	NP_001656	3–186
RHO	Q15669	RHOH_HUMAN	RhoH, TTF, ARHH	NP_004301	4–180
RHO	Q9HBH0-1	RHOF_HUMAN	Rif, ARHF, RhoF	NP_061907	19–201
RHO	Q92730	RND1_HUMAN	Rnd1, ARHS, Rho6	NP_055285	13–197
RHO	P52198	RND2_HUMAN	Rnd2, ARHN, RhoN, Rho7	NP_005431	7–191
RHO	P61587	RND3_HUMAN	Rnd3, RhoE, ARHE, Rho8	NP_005159	23–207
RHO	P17081	RHOQ_HUMAN	TC10, RhoQ, ARHQ, RasL7A	NP_036381	9–192
RHO	Q9H4E5-1	RHOJ_HUMAN	TCL_TC10ia, RhoT, RhoJ, ARHJ, RasL7B	NP_065714	21–204
RHO	Q7L0Q8-1	RHOU_HUMAN	Wrch-1, RhoU, ARHU, Cdc42L1	NP_067028	49–232
RHO	Q96L33	RHOV_HUMAN	Wrch-2, Chp, RhoV, ARHV	NP_598378	31–215
Unclassified	*B4E190*	B4E190_HUMAN	LOC401884	XP_377476	3–48
Unclassified	Q8IXI2-1	MIRO1_HUMAN	Miro-1_RhoT1	NP_060777	4–223
Unclassified	Q8IXI1-1	MIRO2_HUMAN	Miro-2_RhoT2	NP_620124	4–223
Unclassified	Q9NX57	RAB20_HUMAN	Rab20	NP_060287	5–183
Unclassified	*Q9UBK7*-1	RBL2A_HUMAN	RabL2A	NP_009013	21–221
Unclassified	*Q9UNT1*-2	RBL2B_HUMAN	RabL2Bisof1	NP_001003789	21–222
Unclassified	*Q9UNT1*-1	RBL2B_HUMAN	RabL2Bisof2	NP_009012	21–221
Unclassified	Q5HYI8	RABL3_HUMAN	RabL3	NP_776186	6–233
Unclassified	*Q9H7X7*-1	RABL5_HUMAN	RabL5	NP_073614	3–185
Unclassified	Q9Y5M8	SRPRB_HUMAN	SRPRB_APMCF1	NP_067026	64–271
RAN	P62826	RAN_HUMAN	Ran	NP_006316	

Table S3. **Orthologues of the 167 human sequences**

Family	Uniprot primary accession	Uniprot other accession	Organism	Source
ARF	Q8I1S0	Q8I1S0_PLAF7	Pfa	Integr8
ARF	Q7KQL3	Q7KQL3_PLAF7	Pfa	Integr8
ARF	Q8IJ63	Q8IJ63_PLAF7	Pfa	Integr8
ARF	Q8IL50	Q8IL50_PLAF7	Pfa	Integr8
ARF	P61209	ARF1_DROME	Dme	Integr8
ARF	Q06849	ARL2_DROME	Dme	Integr8
ARF	P61209	ARF1_DROME	Dme	Integr8
ARF	Q9N3C8	Q9N3C8_CAEEL	Cel	Integr8
ARF	Q20758	ARL1_CAEEL	Cel	Integr8
ARF	O45379	ARL3_CAEEL	Cel	Integr8
ARF	Q19705	ARL2_CAEEL	Cel	Integr8
ARF	O45099	O45099_CAEEL	Cel	Integr8
ARF	Q9U2S4	Q9U2S4_CAEEL	Cel	Integr8
ARF	O18237	O18237_CAEEL	Cel	Integr8
ARF	Q23445	SAR1_CAEEL	Cel	Integr8
ARF	Q10943	ARF12_CAEEL	Cel	Integr8
ARF	P34212	ARL5_CAEEL	Cel	Integr8
ARF	Q18510	ARL6_CAEEL	Cel	Integr8
ARF	P40945	ARF2_DROME	Dme	Integr8
ARF	Q9W389	Q9W389_DROME	Dme	Integr8
ARF	P36579	ARF1_SCHPO	Spo	Integr8
ARF	Q01475	SAR1_SCHPO	Spo	Integr8
ARF	Q9Y7Z2	ARF2_SCHPO	Spo	Integr8
ARF	Q09767	ARL_SCHPO	Spo	Integr8
ARF	Q9VHV5	ARL8_DROME	Dme	Integr8
ARF	Q95SY7	Q95SY7_DROME	Dme	Integr8
ARF	Q9VD64	Q9VD64_DROME	Dme	Integr8
ARF	P61209	ARF1_DROME	Dme	Integr8
ARF	Q9V4B2	Q9V4B2_DROME	Dme	Integr8
ARF	Q95SY7	Q95SY7_DROME	Dme	Integr8
ARF	P40946	ARF3_DROME	Dme	Integr8
ARF	A1ZBK9	A1ZBK9_DROME	Dme	Integr8
ARF	Q9VSG8	Q9VSG8_DROME	Dme	Integr8
ARF	P25160	ARL1_DROME	Dme	Integr8
ARF	P61209	ARF1_DROME	Dme	Integr8
ARF	Q95SY7	Q95SY7_DROME	Dme	Integr8
ARF	P38116	ARL1_YEAST	Sce	Integr8
ARF	P11076	ARF1_YEAST	Sce	Integr8
ARF	P19146	ARF2_YEAST	Sce	Integr8
ARF	P20606	SAR1_YEAST	Sce	Integr8
ARF	Q02804	ARL3_YEAST	Sce	Integr8
ARF	Q09654	ARD1_CAEEL	Cel	Integr8
ARF	Q2V076	Q2V076_CAEEL	Cel	Integr8
ARF	Q2V075	Q2V075_CAEEL	Cel	Integr8
ARF	-	114540	Xtr	JGI
ARF	-	114847	Bfl	JGI
ARF	-	116098	Bfl	JGI
ARF	-	121277	Bfl	JGI
ARF	-	123592	Bfl	JGI
ARF	-	124178	Bfl	JGI
ARF	-	124594	Bfl	JGI
ARF	-	125054	Bfl	JGI
ARF	-	131042	Nve	JGI
ARF	-	149579	Xtr	JGI
ARF	-	159049	Xtr	JGI
ARF	-	159865	Xtr	JGI
ARF	-	162886	Nve	JGI
ARF	-	166155	Xtr	JGI
ARF	-	166872	Nve	JGI
ARF	-	176575	Xtr	JGI
ARF	-	177865	Xtr	JGI
ARF	-	184879	Xtr	JGI

ARF	-	195794	Nve	JGI
ARF	-	200709	Bfl	JGI
ARF	-	201656	Xtr	JGI
ARF	-	216064	Nve	JGI
ARF	-	218041	Nve	JGI
ARF	-	227502	Bfl	JGI
ARF	-	228132	Nve	JGI
ARF	-	234402	Nve	JGI
ARF	-	235187	Nve	JGI
ARF	-	235432	Nve	JGI
ARF	-	236613	Nve	JGI
ARF	-	236810	Nve	JGI
ARF	-	238733	Nve	JGI
ARF	-	242285	Nve	JGI
ARF	-	248122	Nve	JGI
ARF	-	248616	Nve	JGI
ARF	-	248744	Nve	JGI
ARF	-	261382	Bfl	JGI
ARF	-	263625	Bfl	JGI
ARF	-	263630	Bfl	JGI
ARF	-	263946	Bfl	JGI
ARF	-	268541	Bfl	JGI
ARF	-	276203	Bfl	JGI
ARF	-	277811	Xtr	JGI
ARF	-	283109	Xtr	JGI
ARF	-	284242	Bfl	JGI
ARF	-	285870	Xtr	JGI
ARF	-	287615	Bfl	JGI
ARF	-	294810	Xtr	JGI
ARF	-	327451	Xtr	JGI
ARF	-	335176	Xtr	JGI
ARF	-	358852	Xtr	JGI
ARF	-	416393	Xtr	JGI
ARF	-	448674	Xtr	JGI
ARF	-	448971	Xtr	JGI
ARF	-	454849	Xtr	JGI
ARF	-	455956	Xtr	JGI
ARF	-	466115	Xtr	JGI
ARF	-	59902	Bfl	JGI
ARF	-	60117	Bfl	JGI
ARF	-	63086	Bfl	JGI
ARF	-	85415	Bfl	JGI
ARF	-	87925	Nve	JGI
ARF	-	91033	Bfl	JGI
ARF	-	94334	Nve	JGI
ARF	-	96651	Nve	JGI
ARF	-	225729	Cin	JGI
ARF	-	227094	Cin	JGI
ARF	-	241264	Cin	JGI
ARF	-	244683	Cin	JGI
ARF	-	246537	Cin	JGI
ARF	-	284665	Cin	JGI
ARF	-	284978	Cin	JGI
ARF	-	290020	Cin	JGI
ARF	-	297616	Cin	JGI
ARF	-	298851	Cin	JGI
ARF	-	298978	Cin	JGI
ARF	-	391779	Cin	JGI
ARF	-	400098	Cin	JGI
ARF	O04834	SAR1A_ARATH	Ath	Integr8
ARF	O88848	ARL6_MOUSE	Mus	Integr8
ARF	P18085	ARF4_HUMAN	Hsa	Integr8
ARF	P36397	ARF1_ARATH	Ath	Integr8
ARF	P36404	ARL2_HUMAN	Hsa	Integr8
ARF	P36405	ARL3_HUMAN	Hsa	Integr8
ARF	P36406-1	ARD1_HUMAN	Hsa	Integr8

ARF	P36406-2	ARD1_HUMAN	Hsa	Integr8
ARF	P36406-3	ARD1_HUMAN	Hsa	Integr8
ARF	P40616	ARL1_HUMAN	Hsa	Integr8
ARF	P40617	ARL4A_HUMAN	Hsa	Integr8
ARF	P40940-1	ARF3_ARATH	Ath	Integr8
ARF	P40940-2	ARF3_ARATH	Ath	Integr8
ARF	P49703	ARL4D_HUMAN	Hsa	Integr8
ARF	P56559	ARL4C_HUMAN	Hsa	Integr8
ARF	P61204	ARF3_HUMAN	Hsa	Integr8
ARF	P61205	ARF3_MOUSE	Mus	Integr8
ARF	P61208	ARL4C_MOUSE	Mus	Integr8
ARF	P61211	ARL1_MOUSE	Mus	Integr8
ARF	P61213	ARL4A_MOUSE	Mus	Integr8
ARF	P62330	ARF6_HUMAN	Hsa	Integr8
ARF	P62331	ARF6_MOUSE	Mus	Integr8
ARF	P84077	ARF1_HUMAN	Hsa	Integr8
ARF	P84078	ARF1_MOUSE	Mus	Integr8
ARF	P84084	ARF5_MOUSE	Mus	Integr8
ARF	P84085	ARF5_HUMAN	Hsa	Integr8
ARF	Q01474	SAR1B_ARATH	Ath	Integr8
ARF	Q0P5N6	ARL16_HUMAN	Hsa	Integr8
ARF	Q13795	ARFRP_HUMAN	Hsa	Integr8
ARF	Q3SXC5	ARL14_MOUSE	Mus	Integr8
ARF	Q3SXY8-1	AR13B_HUMAN	Hsa	Integr8
ARF	Q640N2	AR13B_MOUSE	Mus	Integr8
ARF	Q6P3A9	ARL11_MOUSE	Mus	Integr8
ARF	Q6T311	ARL9_HUMAN	Hsa	Integr8
ARF	Q80ZU0	ARL5A_MOUSE	Mus	Integr8
ARF	Q8BGR6	ARL15_MOUSE	Mus	Integr8
ARF	Q8BGX0-1	ARD1_MOUSE	Mus	Integr8
ARF	Q8BXL7	ARFRP_MOUSE	Mus	Integr8
ARF	Q8N4G2	ARL14_HUMAN	Hsa	Integr8
ARF	Q8N8L6	ARL10_HUMAN	Hsa	Integr8
ARF	Q8VEH3	ARL8A_MOUSE	Mus	Integr8
ARF	Q969Q4	ARL11_HUMAN	Hsa	Integr8
ARF	Q96BM9	ARL8A_HUMAN	Hsa	Integr8
ARF	Q96KC2	ARL5B_HUMAN	Hsa	Integr8
ARF	Q99PE9	ARL4D_MOUSE	Mus	Integr8
ARF	Q9CQC9	SAR1B_MOUSE	Mus	Integr8
ARF	Q9CQW2	ARL8B_MOUSE	Mus	Integr8
ARF	Q9D0J4	ARL2_MOUSE	Mus	Integr8
ARF	Q9H0F7	ARL6_HUMAN	Hsa	Integr8
ARF	Q9NR31	SAR1A_HUMAN	Hsa	Integr8
ARF	Q9NVJ2	ARL8B_HUMAN	Hsa	Integr8
ARF	Q9NXU5	ARL15_HUMAN	Hsa	Integr8
ARF	Q9SRC3	ARF2_ARATH	Ath	Integr8
ARF	Q9WUL7	ARL3_MOUSE	Mus	Integr8
ARF	Q9Y689	ARL5A_HUMAN	Hsa	Integr8
ARF	Q9Y6B6	SAR1B_HUMAN	Hsa	Integr8
ARF	Q9ZPX1	ARF5_ARATH	Ath	Integr8
ARF	B1ATY8	B1ATY8_MOUSE	Mus	Integr8
ARF	O80489	O80489_ARATH	Ath	Integr8
ARF	Q38921	Q38921_ARATH	Ath	Integr8
ARF	Q3TXJ4	Q3TXJ4_MOUSE	Mus	Integr8
ARF	Q6ID97	Q6ID97_ARATH	Ath	Integr8
ARF	Q6IMB2	Q6IMB2_MOUSE	Mus	Integr8
ARF	Q6NXZ5	Q6NXZ5_MOUSE	Mus	Integr8
ARF	Q8VY57	Q8VY57_ARATH	Ath	Integr8
ARF	Q8VYP7	Q8VYP7_ARATH	Ath	Integr8
ARF	Q8W4C8	Q8W4C8_ARATH	Ath	Integr8
ARF	Q93Y31	Q93Y31_ARATH	Ath	Integr8
ARF	Q9DD04	Q9DD04_MOUSE	Mus	Integr8
ARF	Q9LIK1	Q9LIK1_ARATH	Ath	Integr8
ARF	Q9LQC8	Q9LQC8_ARATH	Ath	Integr8
ARF	Q9LYJ3	Q9LYJ3_ARATH	Ath	Integr8
ARF	Q9M1P5	Q9M1P5_ARATH	Ath	Integr8

ARF	Q9M2X1	Q9M2X1_ARATH	Ath	Integr8
ARF	Q9M2X2	Q9M2X2_ARATH	Ath	Integr8
ARF	-	160464	Nve	JGI
ARF	-	281491	Cin	JGI
ARF	Q9VXA9	Q9VXA9_DROME	Dme	Integr8
ARF	Q5HYI8	RABL3_HUMAN	Hsa	Integr8
ARF	Q9D4V7-1	RABL3_MOUSE	Mus	Integr8
ARF	-	167835	Nve	JGI
ARF	-	215763	Cin	JGI
ARF	-	285063	Bfl	JGI
ARF	-	298279	Xtr	JGI
ARF	-	472447	Xtr	JGI
ARF	Q9XUC2	Q9XUC2_CAEEL	Cel	Integr8
ARF	Q9DAI2	RABL5_MOUSE	Mus	Integr8
ARF	Q9H7X7-1	RABL5_HUMAN	Hsa	Integr8
ARF	-	166031	Xtr	JGI
ARF	-	296648	Cin	JGI
ARF	-	60603	Bfl	JGI
ARF	-	79420	Nve	JGI
ARF	Q0WSC4	Q0WSC4_ARATH	Ath	Integr8
ARF	Q9FFK7	Q9FFK7_ARATH	Ath	Integr8
ARF	Q8I4W4	Q8I4W4_PLAF7	Pfa	Integr8
ARF	Q22013	Q22013_CAEEL	Cel	Integr8
ARF	Q9VSN9	Q9VSN9_DROME	Dme	Integr8
ARF	O13950	SRPB_SCHPO	Spo	Integr8
ARF	P36057	SRPB_YEAST	Sce	Integr8
ARF	P47758	SRPRB_MOUSE	Mus	Integr8
ARF	Q9Y5M8	SRPRB_HUMAN	Hsa	Integr8
RAS	P25378	RHEB_YEAST	Sce	Integr8
RAS	P08646	RAS1_DROME	Dme	Integr8
RAS	P08645	RAS3_DROME	Dme	Integr8
RAS	-	17137290	Dme	JGI
RAS	O96692	O96692_DROME	Dme	Integr8
RAS	Q19143-2	KBRAS_CAEEL	Cel	Integr8
RAS	A4UZ34	A4UZ34_CAEEL	Cel	Integr8
RAS	Q09930	Q09930_CAEEL	Cel	Integr8
RAS	-	17535679	Cel	JGI
RAS	Q18246	Q18246_CAEEL	Cel	Integr8
RAS	P34443	RHEB1_CAEEL	Cel	Integr8
RAS	Q19524	Q19524_CAEEL	Cel	Integr8
RAS	Q9N3F8	Q9N3F8_CAEEL	Cel	Integr8
RAS	P48555	RALA_DROME	Dme	Integr8
RAS	O94363	RHB1_SCHPO	Spo	Integr8
RAS	P08647	RAS_SCHPO	Spo	Integr8
RAS	Q9V4L4-1	KBRAS_DROME	Dme	Integr8
RAS	-	24639550	Dme	JGI
RAS	P48555	RALA_DROME	Dme	Integr8
RAS	Q9VH66	Q9VH66_DROME	Dme	Integr8
RAS	Q9VS10	Q9VS10_DROME	Dme	Integr8
RAS	Q9VNB7	Q9VNB7_DROME	Dme	Integr8
RAS	Q7JMZ0	Q7JMZ0_DROME	Dme	Integr8
RAS	Q9VND8	RHEB_DROME	Dme	Integr8
RAS	P13856	RSR1_YEAST	Sce	Integr8
RAS	P01120	RAS2_YEAST	Sce	Integr8
RAS	P01119	RAS1_YEAST	Sce	Integr8
RAS	-	71984056	Cel	JGI
RAS	O17599	O17599_CAEEL	Cel	Integr8
RAS	P22981	LET60_CAEEL	Cel	Integr8
RAS	-	271393	Bfl	JGI
RAS	-	209131	Bfl	JGI
RAS	-	61057	Bfl	JGI
RAS	-	59113	Bfl	JGI
RAS	-	273483	Bfl	JGI
RAS	-	58968	Bfl	JGI
RAS	-	237370	Bfl	JGI
RAS	-	99945	Bfl	JGI

RAS	-	114321	Bfl	JGI
RAS	-	61835	Bfl	JGI
RAS	-	63015	Bfl	JGI
RAS	-	236041	Bfl	JGI
RAS	-	92366	Bfl	JGI
RAS	-	92383	Bfl	JGI
RAS	-	131929	Bfl	JGI
RAS	-	120734	Bfl	JGI
RAS	-	80117	Bfl	JGI
RAS	-	222092	Bfl	JGI
RAS	-	240263	Bfl	JGI
RAS	-	206770	Bfl	JGI
RAS	-	258317	Bfl	JGI
RAS	-	275554	Bfl	JGI
RAS	-	92501	Bfl	JGI
RAS	-	85196	Bfl	JGI
RAS	-	187791	Nve	JGI
RAS	-	247341	Nve	JGI
RAS	-	181274	Nve	JGI
RAS	-	195002	Nve	JGI
RAS	-	236736	Nve	JGI
RAS	-	235524	Nve	JGI
RAS	-	96291	Nve	JGI
RAS	Q8VEL9-1	REM2_MOUSE	Mus	Integr8
RAS	P55041	GEM_MOUSE	Mus	Integr8
RAS	Q6PGA2	Q6PGA2_MOUSE	Mus	Integr8
RAS	O35626	RASD1_MOUSE	Mus	Integr8
RAS	O35929	REM1_MOUSE	Mus	Integr8
RAS	P63032	RHES_MOUSE	Mus	Integr8
RAS	Q08AT1	RASLC_MOUSE	Mus	Integr8
RAS	Q922H7-1	RSLBB_MOUSE	Mus	Integr8
RAS	Q6IMB1-1	RSLBA_MOUSE	Mus	Integr8
RAS	P70426	RIT1_MOUSE	Mus	Integr8
RAS	P10833	RRAS_MOUSE	Mus	Integr8
RAS	Q5SSG5	RSLAB_MOUSE	Mus	Integr8
RAS	O08989	RASM_MOUSE	Mus	Integr8
RAS	P63321	RALA_MOUSE	Mus	Integr8
RAS	P70425	RIT2_MOUSE	Mus	Integr8
RAS	Q8K5A4	RSLAA_MOUSE	Mus	Integr8
RAS	Q8R367	RERG_MOUSE	Mus	Integr8
RAS	Q5PR73	DIRA2_MOUSE	Mus	Integr8
RAS	Q9JIW9	RALB_MOUSE	Mus	Integr8
RAS	Q6P716	Q6P716_MOUSE	Mus	Integr8
RAS	Q76LV5	Q76LV5_MOUSE	Mus	Integr8
RAS	Q9CR56	KBRS2_MOUSE	Mus	Integr8
RAS	Q4FJP3	Q4FJP3_MOUSE	Mus	Integr8
RAS	P32883-1	RASK_MOUSE	Mus	Integr8
RAS	Q91Z61	DIRA1_MOUSE	Mus	Integr8
RAS	Q8CEC5	KBRS1_MOUSE	Mus	Integr8
RAS	P32883-2	RASK_MOUSE	Mus	Integr8
RAS	P62835	RAP1A_MOUSE	Mus	Integr8
RAS	Q99JI6	RAP1B_MOUSE	Mus	Integr8
RAS	P61226	RAP2B_MOUSE	Mus	Integr8
RAS	Q80ZJ1-1	RAP2A_MOUSE	Mus	Integr8
RAS	Q8BU31	RAP2C_MOUSE	Mus	Integr8
RAS	Q921J2	RHEB_MOUSE	Mus	Integr8
RAS	Q7TN89	RASE_MOUSE	Mus	Integr8
RAS	B2RVE2	B2RVE2_MOUSE	Mus	Integr8
RAS	Q9D8T3	REBL1_MOUSE	Mus	Integr8
RAS	P11233	RALA_HUMAN	Hsa	Integr8
RAS	P11234	RALB_HUMAN	Hsa	Integr8
RAS	P01111	RASN_HUMAN	Hsa	Integr8
RAS	P01116-2	RASK_HUMAN	Hsa	Integr8
RAS	P01116-1	RASK_HUMAN	Hsa	Integr8
RAS	P01112	RASH_HUMAN	Hsa	Integr8
RAS	Q9BR65	Q9BR65_HUMAN	Hsa	Integr8

RAS	Q7Z444	RASE_HUMAN	Hsa	Integr8
RAS	Q99578-1	RIT2_HUMAN	Hsa	Integr8
RAS	Q92963	RIT1_HUMAN	Hsa	Integr8
RAS	P10301	RRAS_HUMAN	Hsa	Integr8
RAS	B7Z7H6	B7Z7H6_HUMAN	Hsa	Integr8
RAS	O14807	RASM_HUMAN	Hsa	Integr8
RAS	P62834	RAP1A_HUMAN	Hsa	Integr8
RAS	P61224	RAP1B_HUMAN	Hsa	Integr8
RAS	P61225	RAP2B_HUMAN	Hsa	Integr8
RAS	P10114	RAP2A_HUMAN	Hsa	Integr8
RAS	Q9Y3L5	RAP2C_HUMAN	Hsa	Integr8
RAS	Q8IYK8	REM2_HUMAN	Hsa	Integr8
RAS	P55042	RAD_HUMAN	Hsa	Integr8
RAS	P55040	GEM_HUMAN	Hsa	Integr8
RAS	O75628	REM1_HUMAN	Hsa	Integr8
RAS	Q9NYN1	RASLC_HUMAN	Hsa	Integr8
RAS	Q96A58	RERG_HUMAN	Hsa	Integr8
RAS	Q9BPW5	RSLBB_HUMAN	Hsa	Integr8
RAS	Q6T310	RSLBA_HUMAN	Hsa	Integr8
RAS	Q9H628	RERGL_HUMAN	Hsa	Integr8
RAS	O95661	DIRA3_HUMAN	Hsa	Integr8
RAS	Q96HU8	DIRA2_HUMAN	Hsa	Integr8
RAS	O95057	DIRA1_HUMAN	Hsa	Integr8
RAS	Q92737-1	RSLAA_HUMAN	Hsa	Integr8
RAS	Q92737-2	RSLAA_HUMAN	Hsa	Integr8
RAS	Q96S79	RSLAB_HUMAN	Hsa	Integr8
RAS	Q96D21	RHES_HUMAN	Hsa	Integr8
RAS	Q9Y272	RASD1_HUMAN	Hsa	Integr8
RAS	Q15382	RHEB_HUMAN	Hsa	Integr8
RAS	Q8TAI7-1	REBL1_HUMAN	Hsa	Integr8
RAS	Q8TAI7-2	REBL1_HUMAN	Hsa	Integr8
RAS	Q9NYR9-1	KBRS2_HUMAN	Hsa	Integr8
RAS	Q9NYS0	KBRS1_HUMAN	Hsa	Integr8
RAS	-	216182	Cin	JGI
RAS	-	284756	Cin	JGI
RAS	-	206457	Cin	JGI
RAS	-	265878	Cin	JGI
RAS	-	239024	Cin	JGI
RAS	-	296857	Cin	JGI
RAS	-	242347	Cin	JGI
RAS	-	266139	Cin	JGI
RAS	-	377593	Cin	JGI
RAS	-	295097	Cin	JGI
RAS	-	276591	Cin	JGI
RAS	-	452052	Xtr	JGI
RAS	-	476175	Xtr	JGI
RAS	-	293522	Xtr	JGI
RAS	-	295805	Xtr	JGI
RAS	-	152487	Xtr	JGI
RAS	-	472582	Xtr	JGI
RAS	-	461693	Xtr	JGI
RAS	-	172581	Xtr	JGI
RAS	-	177765	Xtr	JGI
RAS	-	272610	Xtr	JGI
RAS	-	153186	Xtr	JGI
RAS	-	453667	Xtr	JGI
RAS	-	152589	Xtr	JGI
RAS	-	147240	Xtr	JGI
RAS	-	151104	Xtr	JGI
RAS	-	147382	Xtr	JGI
RAS	-	450587	Xtr	JGI
RAS	-	287738	Xtr	JGI
RAS	-	291007	Xtr	JGI
RAS	-	205398	Xtr	JGI
RAS	-	151479	Xtr	JGI
RAS	-	311892	Xtr	JGI

RAS	-	428032	Xtr	JGI
RAS	-	323794	Xtr	JGI
RAS	-	452957	Xtr	JGI
RAS	-	188498	Xtr	JGI
RAS	-	156708	Xtr	JGI
RHO	-	113475	Nve	JGI
RHO	-	153415	Xtr	JGI
RHO	-	297748	Cin	JGI
RHO	-	472713	Xtr	JGI
RHO	-	93126	Bfl	JGI
RHO	-	93126	Bfl	JGI
RHO	Q8RXF8	Q8RXF8_ARATH	Ath	Integr8
RHO	Q93Z33	Q93Z33_ARATH	Ath	Integr8
RHO	Q9LYA8	Q9LYA8_ARATH	Ath	Integr8
RHO	Q9MA88	Q9MA88_ARATH	Ath	Integr8
RHO	Q8BG51-2	MIRO1_MOUSE	Mus	Integr8
RHO	Q8BG51-4	MIRO1_MOUSE	Mus	Integr8
RHO	Q8IXI1-1	MIRO2_HUMAN	Hsa	Integr8
RHO	Q8IXI2-2	MIRO1_HUMAN	Hsa	Integr8
RHO	Q8IXI2-3	MIRO1_HUMAN	Hsa	Integr8
RHO	Q8JZN7	MIRO2_MOUSE	Mus	Integr8
RHO	Q94263	MIRO_CAEEL	Cel	Integr8
RHO	Q8IMX7-1	MIRO_DROME	Dme	Integr8
RHO	Q8IMX7-2	MIRO_DROME	Dme	Integr8
RHO	O59781	GEM1_SCHPO	Spo	Integr8
RHO	P39722	GEM1_YEAST	Sce	Integr8
RHO	Q9BW83-2	RAYL_HUMAN	Hsa	Integr8
RHO	Q9D0P8	RAYL_MOUSE	Mus	Integr8
RHO	-	238332	Bfl	JGI
RHO	-	245244	Nve	JGI
RHO	-	451804	Xtr	JGI
RHO	-	286273	Cin	JGI
RHO	P40792	RAC1_DROME	Dme	Integr8
RHO	Q05062	CDC42_CAEEL	Cel	Integr8
RHO	Q03206-1	RAC1_CAEEL	Cel	Integr8
RHO	Q94124	RAC2_CAEEL	Cel	Integr8
RHO	Q22038	RHO1_CAEEL	Cel	Integr8
RHO	Q01112	CDC42_SCHPO	Spo	Integr8
RHO	Q9HE04	RHO5_SCHPO	Spo	Integr8
RHO	Q09914	RHO1_SCHPO	Spo	Integr8
RHO	P48554	RAC2_DROME	Dme	Integr8
RHO	P40793	CDC42_DROME	Dme	Integr8
RHO	P19073	CDC42_YEAST	Sce	Integr8
RHO	P06780	RHO1_YEAST	Sce	Integr8
RHO	-	107964	Bfl	JGI
RHO	-	115215	Bfl	JGI
RHO	-	122664	Bfl	JGI
RHO	-	126918	Bfl	JGI
RHO	-	146871	Xtr	JGI
RHO	-	149865	Xtr	JGI
RHO	-	151814	Xtr	JGI
RHO	-	160649	Xtr	JGI
RHO	-	166147	Xtr	JGI
RHO	-	180355	Xtr	JGI
RHO	-	189251	Nve	JGI
RHO	-	19549712	Dme	JGI
RHO	-	212034	Nve	JGI
RHO	-	216617	Bfl	JGI
RHO	-	223842	Bfl	JGI
RHO	-	223854	Bfl	JGI
RHO	-	243859	Nve	JGI
RHO	-	244319	Nve	JGI
RHO	-	268273	Bfl	JGI
RHO	-	278135	Xtr	JGI
RHO	-	281984	Xtr	JGI
RHO	-	28574635	Dme	JGI

RHO	-	298064	Xtr	JGI
RHO	-	356222	Xtr	JGI
RHO	-	452134	Xtr	JGI
RHO	-	452673	Xtr	JGI
RHO	-	454855	Xtr	JGI
RHO	-	456173	Xtr	JGI
RHO	-	60502	Bfl	JGI
RHO	-	73115	Bfl	JGI
RHO	-	93088	Bfl	JGI
RHO	-	206104	Cin	JGI
RHO	-	207874	Cin	JGI
RHO	-	244400	Cin	JGI
RHO	-	294356	Cin	JGI
RHO	O00212	RHOD_HUMAN	Hsa	Integr8
RHO	O82480	RAC7_ARATH	Ath	Integr8
RHO	O82481	RAC10_ARATH	Ath	Integr8
RHO	O94844	RHBT1_HUMAN	Hsa	Integr8
RHO	P08134	RHOC_HUMAN	Hsa	Integr8
RHO	P15153	RAC2_HUMAN	Hsa	Integr8
RHO	P17081	RHOQ_HUMAN	Hsa	Integr8
RHO	P52198	RND2_HUMAN	Hsa	Integr8
RHO	P60763	RAC3_HUMAN	Hsa	Integr8
RHO	P60764	RAC3_MOUSE	Mus	Integr8
RHO	P60766-1	CDC42_MOUSE	Mus	Integr8
RHO	P60766-2	CDC42_MOUSE	Mus	Integr8
RHO	P60953-1	CDC42_HUMAN	Hsa	Integr8
RHO	P60953-2	CDC42_HUMAN	Hsa	Integr8
RHO	P61586	RHOA_HUMAN	Hsa	Integr8
RHO	P61587	RND3_HUMAN	Hsa	Integr8
RHO	P61588	RND3_MOUSE	Mus	Integr8
RHO	P62745	RHOB_HUMAN	Hsa	Integr8
RHO	P62746	RHOB_MOUSE	Mus	Integr8
RHO	P63000-1	RAC1_HUMAN	Hsa	Integr8
RHO	P63000-2	RAC1_HUMAN	Hsa	Integr8
RHO	P63001	RAC1_MOUSE	Mus	Integr8
RHO	P84095	RHOG_HUMAN	Hsa	Integr8
RHO	P84096	RHOG_MOUSE	Mus	Integr8
RHO	P92978	RAC11_ARATH	Ath	Integr8
RHO	P97348	RHOD_MOUSE	Mus	Integr8
RHO	Q05144	RAC2_MOUSE	Mus	Integr8
RHO	Q15669	RHOH_HUMAN	Hsa	Integr8
RHO	Q38902	RAC1_ARATH	Ath	Integr8
RHO	Q38903	RAC2_ARATH	Ath	Integr8
RHO	Q38912	RAC3_ARATH	Ath	Integr8
RHO	Q38919	RAC4_ARATH	Ath	Integr8
RHO	Q38937	RAC5_ARATH	Ath	Integr8
RHO	Q62159	RHOC_MOUSE	Mus	Integr8
RHO	Q7L0Q8-1	RHOU_HUMAN	Hsa	Integr8
RHO	Q8BLR7-1	RND1_MOUSE	Mus	Integr8
RHO	Q8BYP3	RHOF_MOUSE	Mus	Integr8
RHO	Q8R527	RHOQ_MOUSE	Mus	Integr8
RHO	Q8VDU1	RHOV_MOUSE	Mus	Integr8
RHO	Q92730	RND1_HUMAN	Hsa	Integr8
RHO	Q96L33	RHOV_HUMAN	Hsa	Integr8
RHO	Q9BYZ6	RHBT2_HUMAN	Hsa	Integr8
RHO	Q9D3G9	RHOH_MOUSE	Mus	Integr8
RHO	Q9EQT3	RHOU_MOUSE	Mus	Integr8
RHO	Q9ER71-1	RHOJ_MOUSE	Mus	Integr8
RHO	Q9H4E5-1	RHOJ_HUMAN	Hsa	Integr8
RHO	Q9HBH0-1	RHOF_HUMAN	Hsa	Integr8
RHO	Q9HBH0-2	RHOF_HUMAN	Hsa	Integr8
RHO	Q9QUI0	RHOA_MOUSE	Mus	Integr8
RHO	Q9QYM5	RND2_MOUSE	Mus	Integr8
RHO	Q9SBJ6	RAC6_ARATH	Ath	Integr8
RHO	Q9SU67	RAC8_ARATH	Ath	Integr8
RHO	Q9XGU0	RAC9_ARATH	Ath	Integr8

RHO	B2RPX3	B2RPX3_MOUSE	Mus	Integr8
RHO	Q3TLP8	Q3TLP8_MOUSE	Mus	Integr8
RHO	Q8BV20	Q8BV20_MOUSE	Mus	Integr8
RAB	Q7PLE8	Q7PLE8_DROME	Dme	Integr8
RAB	Q8I274	Q8I274_PLAF7	Pfa	Integr8
RAB	Q7K6A8	Q7K6A8_PLAF7	Pfa	Integr8
RAB	Q7K6B0	Q7K6B0_PLAF7	Pfa	Integr8
RAB	Q76NM4	Q76NM4_PLAF7	Pfa	Integr8
RAB	Q8IHR8	Q8IHR8_PLAF7	Pfa	Integr8
RAB	Q8I5A9	Q8I5A9_PLAF7	Pfa	Integr8
RAB	P01123	YPT1_YEAST	Sce	Integr8
RAB	P07560	SEC4_YEAST	Sce	Integr8
RAB	O18333	O18333_DROME	Dme	Integr8
RAB	O18336	O18336_DROME	Dme	Integr8
RAB	O18334	O18334_DROME	Dme	Integr8
RAB	P91857	P91857_CAEEL	Cel	Integr8
RAB	O01577	O01577_CAEEL	Cel	Integr8
RAB	O01803	O01803_CAEEL	Cel	Integr8
RAB	Q94148	Q94148_CAEEL	Cel	Integr8
RAB	Q9NA29	Q9NA29_CAEEL	Cel	Integr8
RAB	Q22045	Q22045_CAEEL	Cel	Integr8
RAB	Q23146	Q23146_CAEEL	Cel	Integr8
RAB	Q9XWR6	Q9XWR6_CAEEL	Cel	Integr8
RAB	Q9U1W9	Q9U1W9_CAEEL	Cel	Integr8
RAB	Q22908	RASEF_CAEEL	Cel	Integr8
RAB	Q20365	RAB33_CAEEL	Cel	Integr8
RAB	Q9XWZ3	Q9XWZ3_CAEEL	Cel	Integr8
RAB	Q9U2C3	Q9U2C3_CAEEL	Cel	Integr8
RAB	Q9UAQ6	Q9UAQ6_CAEEL	Cel	Integr8
RAB	Q93874	Q93874_CAEEL	Cel	Integr8
RAB	Q22782	RAB6B_CAEEL	Cel	Integr8
RAB	O02046	O02046_CAEEL	Cel	Integr8
RAB	O15971	O15971_DROME	Dme	Integr8
RAB	P25228	RAB3_DROME	Dme	Integr8
RAB	O18339	O18339_DROME	Dme	Integr8
RAB	O18338	O18338_DROME	Dme	Integr8
RAB	O76742	O76742_DROME	Dme	Integr8
RAB	P11620	YPT1_SCHPO	Spo	Integr8
RAB	O94655	YPT7_SCHPO	Spo	Integr8
RAB	P17608	RYH1_SCHPO	Spo	Integr8
RAB	P17610	YPT3_SCHPO	Spo	Integr8
RAB	P36586	YPT5_SCHPO	Spo	Integr8
RAB	P17609	YPT2_SCHPO	Spo	Integr8
RAB	O13876	YPT4_SCHPO	Spo	Integr8
RAB	O18335	O18335_DROME	Dme	Integr8
RAB	Q9VM50	Q9VM50_DROME	Dme	Integr8
RAB	Q95RH7	Q95RH7_DROME	Dme	Integr8
RAB	Q9VNG6	Q9VNG6_DROME	Dme	Integr8
RAB	Q9V3I2	Q9V3I2_DROME	Dme	Integr8
RAB	O76901	O76901_DROME	Dme	Integr8
RAB	O18337	O18337_DROME	Dme	Integr8
RAB	Q8IR80	Q8IR80_DROME	Dme	Integr8
RAB	O18332	O18332_DROME	Dme	Integr8
RAB	A1Z7S1	A1Z7S1_DROME	Dme	Integr8
RAB	Q7KY04	Q7KY04_DROME	Dme	Integr8
RAB	Q9VP48	RAB26_DROME	Dme	Integr8
RAB	Q9TYS2	Q9TYS2_CAEEL	Cel	Integr8
RAB	Q8MXS1-1	RAB18_CAEEL	Cel	Integr8
RAB	Q18969	Q18969_CAEEL	Cel	Integr8
RAB	Q9W0A7	Q9W0A7_DROME	Dme	Integr8
RAB	Q8IPT6	Q8IPT6_DROME	Dme	Integr8
RAB	D3DLT0	D3DLT0_YEAST	Sce	Integr8
RAB	P51996	YPT32_YEAST	Sce	Integr8
RAB	Q99260	YPT6_YEAST	Sce	Integr8
RAB	P32939	YPT7_YEAST	Sce	Integr8
RAB	P36019	YPT53_YEAST	Sce	Integr8

RAB	P36017	VPS21_YEAST	Sce	Integr8
RAB	Q94986	RAB3_CAEEL	Cel	Integr8
RAB	Q7YWU5	Q7YWU5_CAEEL	Cel	Integr8
RAB	Q8MXS1-2	RAB18_CAEEL	Cel	Integr8
RAB	-	111641	Nve	JGI
RAB	-	124506617	Pfa	JGI
RAB	-	146948	Xtr	JGI
RAB	-	148251	Nve	JGI
RAB	-	148553	Xtr	JGI
RAB	-	148766	Xtr	JGI
RAB	-	148831	Xtr	JGI
RAB	-	149669	Xtr	JGI
RAB	-	150533	Xtr	JGI
RAB	-	151005	Xtr	JGI
RAB	-	151299	Xtr	JGI
RAB	-	152461	Xtr	JGI
RAB	-	157201	Xtr	JGI
RAB	-	157367	Xtr	JGI
RAB	-	158216	Nve	JGI
RAB	-	159319	Xtr	JGI
RAB	-	159569	Xtr	JGI
RAB	-	160457	Nve	JGI
RAB	-	164354	Nve	JGI
RAB	-	164553	Nve	JGI
RAB	-	165056	Xtr	JGI
RAB	-	166681	Nve	JGI
RAB	-	167582	Nve	JGI
RAB	-	172228	Nve	JGI
RAB	-	176370	Nve	JGI
RAB	-	179212	Xtr	JGI
RAB	-	181611	Nve	JGI
RAB	-	182353	Nve	JGI
RAB	-	184492	Nve	JGI
RAB	-	18543235	Dme	JGI
RAB	-	187579	Xtr	JGI
RAB	-	187673	Xtr	JGI
RAB	-	188235	Xtr	JGI
RAB	-	188543	Xtr	JGI
RAB	-	189983	Nve	JGI
RAB	-	191466	Nve	JGI
RAB	-	191733	Nve	JGI
RAB	-	193205	Nve	JGI
RAB	-	200891	Nve	JGI
RAB	-	204447	Xtr	JGI
RAB	-	227824	Nve	JGI
RAB	-	230545	Nve	JGI
RAB	-	232494	Nve	JGI
RAB	-	233657	Nve	JGI
RAB	-	234148	Nve	JGI
RAB	-	236786	Nve	JGI
RAB	-	238931	Nve	JGI
RAB	-	243307	Nve	JGI
RAB	-	24640395	Dme	JGI
RAB	-	24641533	Dme	JGI
RAB	-	24652026	Dme	JGI
RAB	-	24652028	Dme	JGI
RAB	-	25310	Nve	JGI
RAB	-	25811	Nve	JGI
RAB	-	281426	Xtr	JGI
RAB	-	285527	Xtr	JGI
RAB	-	291702	Xtr	JGI
RAB	-	291819	Xtr	JGI
RAB	-	293977	Xtr	JGI
RAB	-	297830	Xtr	JGI
RAB	-	323671	Xtr	JGI
RAB	-	330989	Xtr	JGI

RAB	-	348601	Xtr	JGI
RAB	-	351109	Xtr	JGI
RAB	-	360474	Xtr	JGI
RAB	-	36550	Nve	JGI
RAB	-	37059	Nve	JGI
RAB	-	401284	Xtr	JGI
RAB	-	448193	Xtr	JGI
RAB	-	448685	Xtr	JGI
RAB	-	452754	Xtr	JGI
RAB	-	456069	Xtr	JGI
RAB	-	457553	Xtr	JGI
RAB	-	457682	Xtr	JGI
RAB	-	458661	Xtr	JGI
RAB	-	459207	Xtr	JGI
RAB	-	468345	Xtr	JGI
RAB	-	474919	Xtr	JGI
RAB	-	477031	Xtr	JGI
RAB	-	478676	Xtr	JGI
RAB	-	84449	Nve	JGI
RAB	-	96019	Nve	JGI
RAB	-	203641	Cin	JGI
RAB	-	205518	Cin	JGI
RAB	-	206725	Cin	JGI
RAB	-	209755	Cin	JGI
RAB	-	212080	Cin	JGI
RAB	-	219863	Cin	JGI
RAB	-	220378	Cin	JGI
RAB	-	231855	Cin	JGI
RAB	-	239482	Cin	JGI
RAB	-	241799	Cin	JGI
RAB	-	253369	Cin	JGI
RAB	-	254960	Cin	JGI
RAB	-	257462	Cin	JGI
RAB	-	276517	Cin	JGI
RAB	-	283618	Cin	JGI
RAB	-	290037	Cin	JGI
RAB	-	291258	Cin	JGI
RAB	-	294372	Cin	JGI
RAB	-	296479	Cin	JGI
RAB	-	297442	Cin	JGI
RAB	-	298006	Cin	JGI
RAB	-	298731	Cin	JGI
RAB	-	299204	Cin	JGI
RAB	-	381722	Cin	JGI
RAB	-	399628	Cin	JGI
RAB	A4D1S5-1	RAB19_HUMAN	Hsa	Integr8
RAB	O00194	RB27B_HUMAN	Hsa	Integr8
RAB	O04157	RAB7_ARATH	Ath	Integr8
RAB	O14966	RAB7L_HUMAN	Hsa	Integr8
RAB	O35963	RB33B_MOUSE	Mus	Integr8
RAB	O80501	RBH1B_ARATH	Ath	Integr8
RAB	O95716	RAB3D_HUMAN	Hsa	Integr8
RAB	O95755-1	RAB36_HUMAN	Hsa	Integr8
RAB	O95755-2	RAB36_HUMAN	Hsa	Integr8
RAB	P20336	RAB3A_HUMAN	Hsa	Integr8
RAB	P20337	RAB3B_HUMAN	Hsa	Integr8
RAB	P20339	RAB5A_HUMAN	Hsa	Integr8
RAB	P20340-1	RAB6A_HUMAN	Hsa	Integr8
RAB	P20340-2	RAB6A_HUMAN	Hsa	Integr8
RAB	P28185	RAA1A_ARATH	Ath	Integr8
RAB	P28186	ARA3_ARATH	Ath	Integr8
RAB	P28188	RBD2A_ARATH	Ath	Integr8
RAB	P31582	RHA1_ARATH	Ath	Integr8
RAB	P35276	RAB3D_MOUSE	Mus	Integr8
RAB	P35278	RAB5C_MOUSE	Mus	Integr8
RAB	P35279-1	RAB6A_MOUSE	Mus	Integr8

RAB	P35279-2	RAB6A_MOUSE	Mus	Integr8
RAB	P35282	RAB21_MOUSE	Mus	Integr8
RAB	P35285	RB22A_MOUSE	Mus	Integr8
RAB	P35288	RAB23_MOUSE	Mus	Integr8
RAB	P35290	RAB24_MOUSE	Mus	Integr8
RAB	P35292	RAB17_MOUSE	Mus	Integr8
RAB	P35293	RAB18_MOUSE	Mus	Integr8
RAB	P35294	RAB19_MOUSE	Mus	Integr8
RAB	P46638	RB11B_MOUSE	Mus	Integr8
RAB	P51148	RAB5C_HUMAN	Hsa	Integr8
RAB	P51149	RAB7A_HUMAN	Hsa	Integr8
RAB	P51150	RAB7A_MOUSE	Mus	Integr8
RAB	P51151	RAB9A_HUMAN	Hsa	Integr8
RAB	P51153	RAB13_HUMAN	Hsa	Integr8
RAB	P51157-1	RAB28_HUMAN	Hsa	Integr8
RAB	P51157-2	RAB28_HUMAN	Hsa	Integr8
RAB	P51159-1	RB27A_HUMAN	Hsa	Integr8
RAB	P53994	RAB2A_MOUSE	Mus	Integr8
RAB	P55258	RAB8A_MOUSE	Mus	Integr8
RAB	P57735	RAB25_HUMAN	Hsa	Integr8
RAB	P59190-1	RAB15_HUMAN	Hsa	Integr8
RAB	P59190-2	RAB15_HUMAN	Hsa	Integr8
RAB	P59279	RAB2B_MOUSE	Mus	Integr8
RAB	P61006	RAB8A_HUMAN	Hsa	Integr8
RAB	P61018-1	RAB4B_HUMAN	Hsa	Integr8
RAB	P61018-2	RAB4B_HUMAN	Hsa	Integr8
RAB	P61019	RAB2A_HUMAN	Hsa	Integr8
RAB	P61020	RAB5B_HUMAN	Hsa	Integr8
RAB	P61026	RAB10_HUMAN	Hsa	Integr8
RAB	P61027	RAB10_MOUSE	Mus	Integr8
RAB	P61028	RAB8B_MOUSE	Mus	Integr8
RAB	P61106	RAB14_HUMAN	Hsa	Integr8
RAB	P61294	RAB6B_MOUSE	Mus	Integr8
RAB	P62491	RB11A_HUMAN	Hsa	Integr8
RAB	P62492	RB11A_MOUSE	Mus	Integr8
RAB	P62820-1	RAB1A_HUMAN	Hsa	Integr8
RAB	P62821	RAB1A_MOUSE	Mus	Integr8
RAB	P62823	RAB3C_MOUSE	Mus	Integr8
RAB	P63011	RAB3A_MOUSE	Mus	Integr8
RAB	P97950	RB33A_MOUSE	Mus	Integr8
RAB	Q12829	RB40B_HUMAN	Hsa	Integr8
RAB	Q13637	RAB32_HUMAN	Hsa	Integr8
RAB	Q14088	RB33A_HUMAN	Hsa	Integr8
RAB	Q14964	RB39A_HUMAN	Hsa	Integr8
RAB	Q15286	RAB35_HUMAN	Hsa	Integr8
RAB	Q15771	RAB30_HUMAN	Hsa	Integr8
RAB	Q15907	RB11B_HUMAN	Hsa	Integr8
RAB	Q39222	RAA1B_ARATH	Ath	Integr8
RAB	Q504M8	RAB26_MOUSE	Mus	Integr8
RAB	Q5RI75-1	RASEF_MOUSE	Mus	Integr8
RAB	Q6IQ22	RAB12_HUMAN	Hsa	Integr8
RAB	Q6PHN9	RAB35_MOUSE	Mus	Integr8
RAB	Q86YS6	RAB43_HUMAN	Hsa	Integr8
RAB	Q8BHC1	RB39B_MOUSE	Mus	Integr8
RAB	Q8BHD0	RB39A_MOUSE	Mus	Integr8
RAB	Q8BHH2	RAB9B_MOUSE	Mus	Integr8
RAB	Q8CAM5	RAB36_MOUSE	Mus	Integr8
RAB	Q8CG50	RAB43_MOUSE	Mus	Integr8
RAB	Q8IZ41-1	RASEF_HUMAN	Hsa	Integr8
RAB	Q8K386	RAB15_MOUSE	Mus	Integr8
RAB	Q8QZZ8	RAB38_MOUSE	Mus	Integr8
RAB	Q8VEA8-1	RAB7B_MOUSE	Mus	Integr8
RAB	Q8VHP8	RB40B_MOUSE	Mus	Integr8
RAB	Q8VHQ4	RB40C_MOUSE	Mus	Integr8
RAB	Q8WUD1	RAB2B_HUMAN	Hsa	Integr8
RAB	Q8WXH6	RB40A_HUMAN	Hsa	Integr8

RAB	Q91V41	RAB14_MOUSE	Mus	Integr8
RAB	Q91YQ1	RAB7L_MOUSE	Mus	Integr8
RAB	Q91ZR1	RAB4B_MOUSE	Mus	Integr8
RAB	Q923S9	RAB30_MOUSE	Mus	Integr8
RAB	Q92930	RAB8B_HUMAN	Hsa	Integr8
RAB	Q969Q5	RAB24_HUMAN	Hsa	Integr8
RAB	Q96AH8	RAB7B_HUMAN	Hsa	Integr8
RAB	Q96DA2	RB39B_HUMAN	Hsa	Integr8
RAB	Q96E17	RAB3C_HUMAN	Hsa	Integr8
RAB	Q96S21	RB40C_HUMAN	Hsa	Integr8
RAB	Q99KL7	RAB28_MOUSE	Mus	Integr8
RAB	Q99P58	RB27B_MOUSE	Mus	Integr8
RAB	Q9BZG1-1	RAB34_HUMAN	Hsa	Integr8
RAB	Q9CQD1	RAB5A_MOUSE	Mus	Integr8
RAB	Q9CZE3	RAB32_MOUSE	Mus	Integr8
RAB	Q9CZT8	RAB3B_MOUSE	Mus	Integr8
RAB	Q9D1G1	RAB1B_MOUSE	Mus	Integr8
RAB	Q9DD03	RAB13_MOUSE	Mus	Integr8
RAB	Q9ERI2	RB27A_MOUSE	Mus	Integr8
RAB	Q9FK68	RAA1C_ARATH	Ath	Integr8
RAB	Q9H082	RB33B_HUMAN	Hsa	Integr8
RAB	Q9H0N0	RAB6C_HUMAN	Hsa	Integr8
RAB	Q9H0T7	RAB17_HUMAN	Hsa	Integr8
RAB	Q9H0U4	RAB1B_HUMAN	Hsa	Integr8
RAB	Q9NP72	RAB18_HUMAN	Hsa	Integr8
RAB	Q9NP90	RAB9B_HUMAN	Hsa	Integr8
RAB	Q9NRW1	RAB6B_HUMAN	Hsa	Integr8
RAB	Q9R0M6	RAB9A_MOUSE	Mus	Integr8
RAB	Q9SMR4	RBH1C_ARATH	Ath	Integr8
RAB	Q9UL25	RAB21_HUMAN	Hsa	Integr8
RAB	Q9UL26	RB22A_HUMAN	Hsa	Integr8
RAB	Q9ULC3	RAB23_HUMAN	Hsa	Integr8
RAB	Q9ULW5	RAB26_HUMAN	Hsa	Integr8
RAB	Q9WTL2	RAB25_MOUSE	Mus	Integr8
RAB	A2CG35	A2CG35_MOUSE	Mus	Integr8
RAB	B1ATT4	B1ATT4_MOUSE	Mus	Integr8
RAB	O23594	O23594_ARATH	Ath	Integr8
RAB	O23657	O23657_ARATH	Ath	Integr8
RAB	O24466	O24466_ARATH	Ath	Integr8
RAB	O49513	O49513_ARATH	Ath	Integr8
RAB	O49841	O49841_ARATH	Ath	Integr8
RAB	P92963	P92963_ARATH	Ath	Integr8
RAB	P93020	P93020_ARATH	Ath	Integr8
RAB	Q0PD20	Q0PD20_MOUSE	Mus	Integr8
RAB	Q0PD56	Q0PD56_MOUSE	Mus	Integr8
RAB	Q2V3A4	Q2V3A4_ARATH	Ath	Integr8
RAB	Q38922	Q38922_ARATH	Ath	Integr8
RAB	Q3TQ93	Q3TQ93_MOUSE	Mus	Integr8
RAB	Q3TSQ6	Q3TSQ6_MOUSE	Mus	Integr8
RAB	Q3TXV4	Q3TXV4_MOUSE	Mus	Integr8
RAB	Q53EY4	Rab22B-Q53EY4_HUMAN	Hsa	Integr8
RAB	Q53GC2	Rab4A-Q53GC2_HUMAN	Hsa	Integr8
RAB	Q7Z4W7	Rab38-Q7Z4W7_HUMAN	Hsa	Integr8
RAB	Q9C820	Q9C820_ARATH	Ath	Integr8
RAB	Q9FJF1	Q9FJF1_ARATH	Ath	Integr8
RAB	Q9FJH0	Q9FJH0_ARATH	Ath	Integr8
RAB	Q9FPJ4	Q9FPJ4_ARATH	Ath	Integr8
RAB	Q9LFT9	Q9LFT9_ARATH	Ath	Integr8
RAB	Q9LK99	Q9LK99_ARATH	Ath	Integr8
RAB	Q9LP15	Q9LP15_ARATH	Ath	Integr8
RAB	Q9LS94	Q9LS94_ARATH	Ath	Integr8
RAB	Q9LW76	Q9LW76_ARATH	Ath	Integr8
RAB	Q9LZD4	Q9LZD4_ARATH	Ath	Integr8
RAB	Q9S810	Q9S810_ARATH	Ath	Integr8
RAB	Q9SF91	Q9SF91_ARATH	Ath	Integr8
RAB	Q9SF92	Q9SF92_ARATH	Ath	Integr8

RAB	Q9SID8	Q9SID8_ARATH	Ath	Integr8
RAB	Q9SN35	Q9SN35_ARATH	Ath	Integr8
RAB	Q9SN68	Q9SN68_ARATH	Ath	Integr8
RAB	Q9SZ88	Q9SZ88_ARATH	Ath	Integr8
RAB	Q9XI98	Q9XI98_ARATH	Ath	Integr8
RAB	-	228748	Nve	JGI
RAB	-	475516	Xtr	JGI
RAB	P35295	RAB20_MOUSE	Mus	Integr8
RAB	Q9NX57	RAB20_HUMAN	Hsa	Integr8
RAB	-	297126	Cin	JGI
RAB	-	301191	Xtr	JGI
RAB	-	163982	Nve	JGI
RAB	Q8K2P9	Q8K2P9_MOUSE	Mus	Integr8
RAB	Q9UBK7-1	RBL2A_HUMAN	Hsa	Integr8
RAB	Q9UNT1-1	RBL2B_HUMAN	Hsa	Integr8
RAB	Q9UNT1-2	RBL2B_HUMAN	Hsa	Integr8
RAB	-	100555	Bfl	JGI
RAB	-	113929	Bfl	JGI
RAB	-	114333	Bfl	JGI
RAB	-	114662	Bfl	JGI
RAB	-	116143	Bfl	JGI
RAB	-	116379	Bfl	JGI
RAB	-	118354	Bfl	JGI
RAB	-	118838	Bfl	JGI
RAB	-	121119	Bfl	JGI
RAB	-	122037	Bfl	JGI
RAB	-	122387	Bfl	JGI
RAB	-	126112	Bfl	JGI
RAB	-	129905	Bfl	JGI
RAB	-	131227	Bfl	JGI
RAB	-	149126	Bfl	JGI
RAB	-	168899	Bfl	JGI
RAB	-	202673	Bfl	JGI
RAB	-	204961	Bfl	JGI
RAB	-	212674	Bfl	JGI
RAB	-	232668	Bfl	JGI
RAB	-	245828	Bfl	JGI
RAB	-	248199	Bfl	JGI
RAB	-	253798	Bfl	JGI
RAB	-	255436	Bfl	JGI
RAB	-	263879	Bfl	JGI
RAB	-	266781	Bfl	JGI
RAB	-	281466	Bfl	JGI
RAB	-	281741	Bfl	JGI
RAB	-	283834	Bfl	JGI
RAB	-	287065	Bfl	JGI
RAB	-	287190	Bfl	JGI
RAB	-	287780	Bfl	JGI
RAB	-	289556	Bfl	JGI
RAB	-	57441	Bfl	JGI
RAB	-	58617	Bfl	JGI
RAB	-	61011	Bfl	JGI
RAB	-	62225	Bfl	JGI
RAB	-	62895	Bfl	JGI
RAB	-	67302	Bfl	JGI
RAB	-	68105	Bfl	JGI
RAB	-	69112	Bfl	JGI
RAB	-	69124	Bfl	JGI
RAB	-	91085	Bfl	JGI
RAB	-	92958	Bfl	JGI
RAB	-	95080	Bfl	JGI
RAB	-	57602	Bfl	JGI
RAB	-	246042	Bfl	JGI
RAN	P62826	RAN_HUMAN	Hsa	Integr8
RAN	P41917	RAN2_ARATH	Ath	Integr8
RAN	Q8H156	RAN3_ARATH	Ath	Integr8

RAN	P41916	RAN1_ARATH	Ath	Integr8
RAN	-	282949	Bfl	JGI
RAN	-	132195	Bfl	JGI
RAN	O17915	RAN_CAEEL	Cel	Integr8
RAN	-	201001	Cin	JGI
RAN	Q9VZ23	RAN_DROME	Dme	Integr8
RAN	P62827	RAN_MOUSE	Mus	Integr8
RAN	Q7KQK6	Q7KQK6_PLAF7	Pfa	Integr8
RAN	P32835	GSP1_YEAST	Sce	Integr8
RAN	P32836	GSP2_YEAST	Sce	Integr8
RAN	P28748	SPI1_SCHPO	Spo	Integr8
RAN	-	152138	Xtr	JGI
RAN	-	170199	Nve	JGI

Source: JGI, sequences obtained from DOE Joint Genome Institute (ftp://ftp.jgi-psf.org/pub/JGI_data); Integr8, sequences obtained EBI, http://www.ebi.ac.uk/integr8/EBI-Integr8-HomePage.do. *Xenopus tropicalis*: draft assembly 4.1 3 feb 2010; *Nematostella vectensis*: draft assembly 1.0, Feb 8, 2010; *Ciona intestinalis*, draft assembly 2.0, 9 Feb 2010; *Branchiostoma floridae*, draft assembly 1.0, 9 Feb 2010. Orthologues were obtained using Inparanoid version 4.0. (Ostlund et al., 2010). Organisms: Cin, *Ciona intestinalis*; Bfl, *Branchiostoma floridae*; Has, *Homo sapiens*; Mus, *Mus musculus*; Sce, *Saccharomyces cerevisiae*; Spo, *Schizosaccharomyces pombe*; Ath, *Arabidopsis thaliana*; Dme, *Drosophila melanogaster*; Cel, *Caenorhabditis elegans*; Pfa, *Plasmodium falciparum*; Nve, *Nematostella vectensis*; Xtr, *Xenopus tropicalis* (for cross-identifiers between JGI and Uniprot see Table S4).

Table S4. **Cross-identifiers between JGI and Uniprot accessions in JGI species with entries in Uniprot (see Table S2)**

JGI identifiers|organism	Uniprot identifiers
71998726|Cel	sp|Q09654|ARD1_CAEEL
17551730|Cel	sp|Q10943|ARF12_CAEEL
17543766|Cel	tr|O18237|O18237_CAEEL
17538186|Cel	tr|Q9U2S4|Q9U2S4_CAEEL
17538184|Cel	tr|O45099|O45099_CAEEL
17544540|Cel	sp|Q23445|SAR1_CAEEL
17531197|Cel	sp|Q20758|ARL1_CAEEL
17532861|Cel	sp|Q19705|ARL2_CAEEL
17531201|Cel	sp|O45379|ARL3_CAEEL
17551732|Cel	sp|P34212|ARL5_CAEEL
17551734|Cel	sp|Q18510|ARL6_CAEEL
17510341|Cel	tr|Q9N3C8|Q9N3C8_CAEEL
86561524|Cel	tr|Q2V076|Q2V076_CAEEL
86561526|Cel	tr|Q2V075|Q2V075_CAEEL
17136866|Dme	sp|P61209|ARF1_DROME
24668777|Dme	sp|P61209|ARF1_DROME
24668769|Dme	sp|P61209|ARF1_DROME
161085839|Dme	sp|P61209|ARF1_DROME
24668773|Dme	sp|P61209|ARF1_DROME
221513662|Dme	sp|P61209|ARF1_DROME
24668762|Dme	sp|P61209|ARF1_DROME
24653829|Dme	sp|P40946|ARF3_DROME
24653831|Dme	sp|P40946|ARF3_DROME
24653827|Dme	sp|P40946|ARF3_DROME
24653835|Dme	sp|P40946|ARF3_DROME
24653833|Dme	sp|P40946|ARF3_DROME
21355085|Dme	sp|Q9VHV5|ARL8_DROME
17864182|Dme	sp|P40945|ARF2_DROME
17136754|Dme	sp|Q06849|ARL2_DROME
24648950|Dme	tr|Q95SY7|Q95SY7_DROME
24648948|Dme	tr|Q95SY7|Q95SY7_DROME
45553457|Dme	tr|Q95SY7|Q95SY7_DROME
24648946|Dme	tr|Q95SY7|Q95SY7_DROME
21355813|Dme	tr|Q95SY7|Q95SY7_DROME
24660781|Dme	tr|Q9VSG8|Q9VSG8_DROME
24664933|Dme	sp|P25160|ARL1_DROME
18858177|Dme	tr|Q9W389|Q9W389_DROME
24638544|Dme	tr|Q9V4B2|Q9V4B2_DROME
21355879|Dme	tr|Q9VD64|Q9VD64_DROME
24655721|Dme	tr|A1ZBK9|A1ZBK9_DROME
124802497|Pfa	tr|Q7KQL3|Q7KQL3_PLAF7
124802873|Pfa	tr|Q8IJ63|Q8IJ63_PLAF7
124505467|Pfa	tr|Q8I1S0|Q8I1S0_PLAF7
124809432|Pfa	tr|Q8IL50|Q8IL50_PLAF7
6320064|Sce	sp|P19146|ARF2_YEAST
6320009|Sce	sp|P11076|ARF1_YEAST
6319641|Sce	sp|P38116|ARL1_YEAST
6325038|Sce	sp|P20606|SAR1_YEAST
6325206|Sce	sp|Q02804|ARL3_YEAST
19112910|Spo	sp|P36579|ARF1_SCHPO
19113614|Spo	sp|Q9Y7Z2|ARF2_SCHPO
19113360|Spo	sp|Q01475|SAR1_SCHPO
19113948|Spo	sp|Q09767|ARL_SCHPO
17542026|Cel	tr|Q18246|Q18246_CAEEL
71999796|Cel	sp|P22981|LET60_CAEEL
17556130|Cel	tr|Q9N3F8|Q9N3F8_CAEEL
71984917|Cel	tr|O17599|O17599_CAEEL
17532559|Cel	tr|Q09930|Q09930_CAEEL
17535679|Cel	sp|P22981|LET60_CAEEL
71984056|Cel	sp|P22981|LET60_CAEEL

17554726|Cel	tr|Q19524|Q19524_CAEEL
17553566|Cel	sp|P34443|RHEB1_CAEEL
17507497|Cel	sp|Q19143-2|KBRAS_CAEEL
17507497|Cel	sp|Q19143-1|KBRAS_CAEEL
17507497|Cel	sp|Q19143-3|KBRAS_CAEEL
17510501|Cel	tr|A4UZ34|A4UZ34_CAEEL
17136706|Dme	sp|P08645|RAS3_DROME
17933550|Dme	sp|P48555|RALA_DROME
24639552|Dme	sp|P48555|RALA_DROME
17136430|Dme	sp|P08646|RAS1_DROME
24645521|Dme	tr|Q9VH66|Q9VH66_DROME
17137620|Dme	tr|O96692|O96692_DROME
281363483|Dme	tr|Q7JMZ0|Q7JMZ0_DROME
17137290|Dme	tr|Q7JMZ0|Q7JMZ0_DROME
28571525|Dme	sp|Q9VND8|RHEB_DROME
28571523|Dme	sp|Q9VND8|RHEB_DROME
24659726|Dme	tr|Q9VS10|Q9VS10_DROME
221330026|Dme	sp|Q9V4L4-1|KBRAS_DROME
19921732|Dme	tr|B7YZS7|B7YZS7_DROME
19921732|Dme	sp|Q9V4L4-1|KBRAS_DROME
281360089|Dme	tr|Q9VNB7|Q9VNB7_DROME
6324675|Sce	sp|P01119|RAS1_YEAST
6321591|Sce	sp|P13856|RSR1_YEAST
6324231|Sce	sp|P01120|RAS2_YEAST
10383790|Sce	sp|P25378|RHEB_YEAST
19114491|Spo	sp|P08647|RAS_SCHPO
19111986|Spo	sp|O94363|RHB1_SCHPO
17532607|Cel	sp|Q05062|CDC42_CAEEL
17541992|Cel	sp|Q22038|RHO1_CAEEL
17539474|Cel	sp|Q03206-1|RAC1_CAEEL
17541972|Cel	sp|Q94124|RAC2_CAEEL
28574635|Dme	not found
17136856|Dme	sp|P40792|RAC1_DROME
21356563|Dme	sp|P48554|RAC2_DROME
24643363|Dme	sp|P40793|CDC42_DROME
17647249|Dme	sp|P40793|CDC42_DROME
19549712|Dme	sp|P48148|RHO1_DROME
24654021|Dme	sp|P48148|RHO1_DROME
45552653|Dme	sp|P48148|RHO1_DROME
45552651|Dme	sp|P48148|RHO1_DROME
45552649|Dme	sp|P48148|RHO1_DROME
17137100|Dme	sp|P48148|RHO1_DROME
19549710|Dme	sp|P48148|RHO1_DROME
6323259|Sce	sp|P19073|CDC42_YEAST
6325423|Sce	sp|P06780|RHO1_YEAST
6323259|Sce	sp|P19073|CDC42_YEAST
6325423|Sce	sp|P06780|RHO1_YEAST
19114448|Spo	sp|Q01112|CDC42_SCHPO
19115402|Spo	sp|Q09914|RHO1_SCHPO
19114543|Spo	sp|Q9HE04|RHO5_SCHPO
17507539|Cel	tr|O01577|O01577_CAEEL
17568765|Cel	tr|Q93874|Q93874_CAEEL
17507543|Cel	tr|O01803|O01803_CAEEL
71982447|Cel	sp|Q94986|RAB3_CAEEL
71982452|Cel	sp|Q94986|RAB3_CAEEL
17558550|Cel	tr|Q9UAQ6|Q9UAQ6_CAEEL
17570073|Cel	sp|Q22782|RAB6B_CAEEL
17506899|Cel	tr|P91857|P91857_CAEEL
25150215|Cel	tr|Q9TYS2|Q9TYS2_CAEEL
17536699|Cel	tr|Q23146|Q23146_CAEEL
17509233|Cel	tr|Q94148|Q94148_CAEEL
25151658|Cel	sp|Q8MXS1-1|RAB18_CAEEL
71996496|Cel	sp|Q8MXS1-2|RAB18_CAEEL

17510659|Cel	tr|Q9NA29|Q9NA29_CAEEL
17555956|Cel	tr|Q9U2C3|Q9U2C3_CAEEL
17555898|Cel	tr|Q9XWZ3|Q9XWZ3_CAEEL
17550768|Cel	sp|Q22908|RASEF_CAEEL
17553424|Cel	sp|Q20365|RAB33_CAEEL
25153277|Cel	tr|Q18969|Q18969_CAEEL
17543864|Cel	tr|Q9U1W9|Q9U1W9_CAEEL
17542952|Cel	tr|Q9XWR6|Q9XWR6_CAEEL
17535871|Cel	tr|Q22045|Q22045_CAEEL
17570221|Cel	tr|O02046|O02046_CAEEL
71994817|Cel	tr|Q7YWU5|Q7YWU5_CAEEL
17137088|Dme	tr|O18333|O18333_DROME
28574177|Dme	tr|O18336|O18336_DROME
28574179|Dme	tr|O18336|O18336_DROME
17137218|Dme	tr|O18336|O18336_DROME
19549675|Dme	tr|O18335|O18335_DROME
17137216|Dme	tr|O18335|O18335_DROME
17137220|Dme	tr|O18334|O18334_DROME
17737457|Dme	sp|P25228|RAB3_DROME
24648682|Dme	tr|O18332|O18332_DROME
17865835|Dme	tr|O76742|O76742_DROME
24654467|Dme	tr|Q7KY04|Q7KY04_DROME
45552705|Dme	tr|Q7KY04|Q7KY04_DROME
17647849|Dme	tr|Q7KY04|Q7KY04_DROME
17737663|Dme	tr|O18338|O18338_DROME
24641533|Dme	not found
24641535|Dme	tr|Q8IR80|Q8IR80_DROME
17737369|Dme	tr|O15971|O15971_DROME
24581103|Dme	tr|Q9V3I2|Q9V3I2_DROME
24581110|Dme	tr|Q9V3I2|Q9V3I2_DROME
24581107|Dme	tr|Q9V3I2|Q9V3I2_DROME
24581105|Dme	tr|Q9V3I2|Q9V3I2_DROME
17736973|Dme	tr|Q9V3I2|Q9V3I2_DROME
24581101|Dme	tr|Q9V3I2|Q9V3I2_DROME
24652026|Dme	not found
24652028|Dme	not found
24652024|Dme	tr|A1Z7S1|A1Z7S1_DROME
45551040|Dme	tr|A1Z7S1|A1Z7S1_DROME
20129057|Dme	tr|Q95RH7|Q95RH7_DROME
24668006|Dme	sp|Q9VP48|RAB26_DROME
281366559|Dme	tr|Q8IPT6|Q8IPT6_DROME
161085488|Dme	tr|Q8IPT6|Q8IPT6_DROME
19920864|Dme	tr|Q9VM50|Q9VM50_DROME
24582410|Dme	tr|Q9VM50|Q9VM50_DROME
24582407|Dme	tr|Q9VM50|Q9VM50_DROME
21357169|Dme	tr|Q9VNG6|Q9VNG6_DROME
18543235|Dme	not found
24639106|Dme	tr|O76901|O76901_DROME
24640395|Dme	not found
17737545|Dme	tr|O18339|O18339_DROME
221500833|Dme	tr|Q7PLE8|Q7PLE8_DROME
116007254|Dme	tr|Q7PLE8|Q7PLE8_DROME
281365477|Dme	tr|Q9W0A7|Q9W0A7_DROME
24639915|Dme	not found
124806378|Pfa	tr|Q8I5A9|Q8I5A9_PLAF7
124513178|Pfa	tr|Q76NM4|Q76NM4_PLAF7
124506171|Pfa	tr|Q7K6A8|Q7K6A8_PLAF7
124804843|Pfa	tr|Q8IHR8|Q8IHR8_PLAF7
124505771|Pfa	tr|Q8I274|Q8I274_PLAF7
124506617|Pfa	not found
124512632|Pfa	tr|Q7K6B0|Q7K6B0_PLAF7
14318480|Sce	sp|P01123|YPT1_YEAST
6320869|Sce	tr|D3DLT0|D3DLT0_YEAST

6321228|Sce	sp|P51996|YPT32_YEAST
6323291|Sce	sp|Q99260|YPT6_YEAST
6323642|Sce	sp|P32939|YPT7_YEAST
14318517|Sce	sp|P07560|SEC4_YEAST
6324663|Sce	sp|P36017|VPS21_YEAST
6324236|Sce	sp|P36019|YPT53_YEAST
19112997|Spo	sp|P11620|YPT1_SCHPO
19114161|Spo	sp|P17608|RYH1_SCHPO
19114579|Spo	sp|P17610|YPT3_SCHPO
19113099|Spo	sp|O94655|YPT7_SCHPO
19115492|Spo	sp|P17609|YPT2_SCHPO
19114819|Spo	sp|P36586|YPT5_SCHPO
19115708|Spo	sp|O13876|YPT4_SCHPO
17553976|Cel	sp|O17915|RAN_CAEEL
21356159|Dme	sp|Q9VZ23|RAN_DROME
24641219|Dme	sp|Q9VZ23|RAN_DROME
124803934|Pfa	tr|Q7KQK6|Q7KQK6_PLAF7
6323324|Sce	sp|P32835|GSP1_YEAST
6324759|Sce	sp|P32836|GSP2_YEAST
19113619|Spo	sp|P28748|SPI1_SCHPO
17541392|Cel	sp|Q94263|MIRO_CAEEL
17510041|Cel	tr|Q9BL82|Q9BL82_CAEEL
17563220|Cel	tr|Q22013|Q22013_CAEEL
17542612|Cel	tr|Q9XUC2|Q9XUC2_CAEEL
24649497|Dme	sp|Q8IMX7-1|MIRO_DROME
24649499|Dme	sp|Q8IMX7-2|MIRO_DROME
18921187|Dme	tr|Q9VXA9|Q9VXA9_DROME
28574941|Dme	tr|Q9VSN9|Q9VSN9_DROME
124806868|Pfa	tr|Q8I4W4|Q8I4W4_PLAF7
6319268|Sce	sp|P39722|GEM1_YEAST
6322695|Sce	sp|P36057|SRPB_YEAST
19075225|Spo	sp|O59781|GEM1_SCHPO
19114311|Spo	sp|O13950|SRPB_SCHPO

When possible, Uniprot identifiers have been used. Here we show the correspondence between Uniprot entries and JGI entries for genomes with annotations in Uniprot. Cin, *C. intestinalis*; Bfl, *B. floridae*; Sce, *S. cerevisiae*; Spo, *S. pombe*; Dme, *D. melanogaster*; Cel, *C. elegans*; Pfa, *P. falciparum*.

Table S5. **Crystal structures used in this study**

Ras protein	Partner	Partner type	Nucleotide	PDB	Ref
HRas	Hs-SOS1	GEF	none	1bkd	{9690470}
	Hs-p120GAP	GAP	GDP.AlF3	1wq1	{9219684}
	SP-protein kinase byr2	effector (RBD)	GNP	1k8r	{11709168}
	Hs-PI3 kinase γ	effector (RBD)	GNP	1he8	{11136978}
	Rt-RalGDS	effector (RA)	GNP	1lfd	{9628477}
	PLCe1	effetor (RA)	GTP	2c5l	{16483931}
Raps	Hs-cRaf	effector (RBD)	GNP	1gua	{8756332}
RalA	CBDP-Exoenzyme C3	effector	GDP	2bov	{15809419}
	Rat-rSec5	effector	GNP	1uad	{12839989}
RhoA	Mm-Dbs	GEF	none	1lb1	{12006984}
	Hs-Rho guanine nucleotide exchange factor 12	RhoGEF		1x86	{15331592}
	Hs-Rho guanine nucleotide exchange factor 11	RhoGEF		1xcg	{15530360}
	Hs-P50-RhoGAP	GAP	GDP.AlF3	1tx4	{9338791}
	Hs-RhoGDI	GDI	GDP	1cc0	{10489445}
	Hs-PKN	effector	GSP	1cxz	{10619026}
RhoC	Mm-p140mDIA	Effector	GNP	1z2c	{15864301}
Rac1	Mm-Tiam	GEF	none	1foe	{11130063}
	Hs-PTPRF–interacting protein	GEF		2nz8	{17391702}
	Pa-Exos	Bacterial GAP	GDP.AlF3	1he1	{11135665}
	Hs-RhoGDI1	GDI	GDP	1hh4	{11513578}
	Hs-P67-Phox	Effector	GTP	1e 96	{11090627}
	Hs-Arfaptin2	Effector	GNP	1i4t	{11346801}
	Hs-PLC-β-2	Effector	GSP	2fju	{17115053}
Rac3	St-Sptp	Bacterial GAP	GDP.AlF3	1g4u	{11163217}
	Hs-PAK4	Effector (CRIB)	GCP	2ov2	To be published
Rac2	Hs-Rho GDI 2	GDI	GDP	1ds6	{10655614}
Cdc42	Mm-Dbs	GEF	none	1kz7	{11889037}
	St-SopE	Bacterial GEF	none	1gzs	{12093730}
	Rat-Collybistin	GEF	GOL	2dfk	{16616186}
	Hs-Intersectin-1	RhoGEF		1ki1	{12006984}
	Hs-Cdc42GAP	GAP	GDP.AlF3	1grn	{9846874}
	Bovin-RhoGDI1	GDI	GDP	1doa	{10676816}
	Mm-Par6	Effector (CRIB)	GNP	1nf3	{12606577}
	Hs-PAK6	Effector (CRIB)	GCP	2odb	To be published
	Mm-PAK3	Effector (CRIB)	none	1ees	{10747784}
	Rat-PAK1	Effector (CRIB)	GNP	1e0a	{10802735}
	Hs-ACK-1	Effector (CRIB)	GNP	1cf4	{10360579}
	Hs-WASp	Effector (CRIB)	GCP	1cee	{10360578}
Rab4A	Hs-Rabenosyn5	Effector	GTP	1z0k	{16034420}
Rab7	Hs-RILP	Effector	GTP	1yhn	{15933719}
Rab8A	Hs-MSS4	GEF	BME		{16541104}
Rab11A	Hs-Rab11-FIP3	Effector (RBD)	GTP	2hv8	{17007872}
	Hs-Nrip11	Effector	GTP	2gzh	{16905101}
	Hs-Rab11-FIP3	Effector (FIP-RBD)	GTP	2d7c	{17030804}
Rab22A	Hs-Rabenosyn-5	Effector	GTP	1z0j	{16034420}
Arf1	Hs-ARNO-BFA	GEF	GDP	1r8q	{14654833}

	Hs-Cytohesin-2	Arf exchange factor	GDP	1s9d	{14654833}
Arf2	Hs-GGA1	Effector	GTP	1j2j	{12679809}
Arf6	Vi-Cholera enterotoxin	Effector	GTP	2a5g	{16099990}
Arl1	Hs-golgin-245 grip domain	Effector	GTP	1upt	{14580338}
Arl2	Hs-GMP-PDE delta	Effector	GTP-GDP	1ksj	{11980706}
Ran	Hs-RCC1	GEF	none	1i2m	{11336674}
	Sp-RNA1	GAP	GNP		{11832950}
	Hs-karyopherin β2	Effector	GNP	1qbk	{10353245}
	Hs-importin β	Effector	GNP	1ibr	{10367892}
	Hs-RanBP2	Effector (RanBD)	GNP	1rrp	{10078529}
	Hs-RanBP1	Effector (RanBD)	GNP	1k5d	{11832950}

Ref column indicates PubMed identifiers.

Table S6. **SDPs detected by the multivariate analyses**

Column in the initial alignment of 919 sequences	Position in the corresponding PDB chain					
	ARF	RAS	RHO	RAB	RAN	Subfamily
	P84077	P01112	P61586	P62820	P62826	UniprotAC
	1HUR	121P	1A2B	2FOL	1I2M	PDB
	A & B	A	A	A	A	CHAIN
7	25	11	13	16	18	
10	28	14	16	19	21	
16	34	20	22	25	27	
85	47	34	36	39	41	
94	51	37	39	43	45	
156	66	56	58	62	64	
161	68	58	60	64	66	
164	69	59	61	65	67	
204	75	65	67	71	73	
219	78	68	70	74	76	
261	85	75	77	81	83	
269	91	81	83	87	89	
272	93	83	85	89	91	
361	131	121	122	126	127	

The SDPs detected in the multivariate analysis (see main text) are numbered according to the columns in the initial alignment of 919 sequences (available upon request) and their corresponding positions in the PDB structures.

References

Aspenstrom, P., A. Ruusala, and D. Pacholsky. 2007. Taking Rho GTPases to the next level: the cellular functions of atypical Rho GTPases. *Exp. Cell Res.* 313:3673–3679. http://dx.doi.org/10.1016/j.yexcr.2007.07.022

Li, Y., W.G. Kelly, J.M. Logsdon Jr., A.M. Schurko, B.D. Harfe, K.L. Hill-Harfe, and R.A. Kahn. 2004. Functional genomic analysis of the ADP-ribosylation factor family of GTPases: phylogeny among diverse eukaryotes and function in *C. elegans*. *FASEB J.* 18:1834–1850. http://dx.doi.org/10.1096/fj.04-2273com

Ostlund, G., T. Schmitt, K. Forslund, T. Köstler, D.N. Messina, S. Roopra, O. Frings, and E.L. Sonnhammer. 2010. InParanoid 7: new algorithms and tools for eukaryotic orthology analysis. *Nucleic Acids Res.* 38(Database issue):D196–D203. http://dx.doi.org/10.1093/nar/gkp931

Rausell, A., D. Juan, F. Pazos, and A. Valencia. 2010. Protein interactions and ligand binding: from protein subfamilies to functional specificity. *Proc. Natl. Acad. Sci. USA*. 107:1995–2000. http://dx.doi.org/10.1073/pnas.0908044107

Schwartz, S.L., C. Cao, O. Pylypenko, A. Rak, and A. Wandinger-Ness. 2007. Rab GTPases at a glance. *J. Cell Sci.* 120:3905–3910. http://dx.doi.org/10.1242/jcs.015909

Stenmark, H. 2009. Rab GTPases as coordinators of vesicle traffic. *Nat. Rev. Mol. Cell Biol.* 10:513–525. http://dx.doi.org/10.1038/nrm2728